INVESTIGATING THE EFFECTS OF RADIATION EXPOSURE ON LUNG CARCINOGENESIS

APPROVED BY SUPERVISORY COMMITTEE

_____

Jerry W. Shay, Ph.D.
Professor of Cell Biology

_____

Pier Paolo Scaglioni, M.D.
Associate Professor, Internal Medicine

_____

Michael Story, Ph.D.
Associate Professor of Radiation Oncology

_____

Carole Mendelson, Ph.D.
Professor of Biochemistry

Dedicated to

Mom, Dad, Grandpa, Grandma, Mehreen and Nida for all their love and support

INVESTIGATING THE EFFECTS OF RADIATION EXPOSURE ON LUNG CARCINOGENESIS

By

AADIL A. KAISANI

DISSERTATION/THESIS

Presented to the Faculty of the Graduate School of Biomedical Sciences

The University of Texas Southwestern Medical Center at Dallas

In Partial Fulfillment of the Requirements

For the Degree of

DOCTOR OF PHILOSOPHY

The University of Texas Southwestern Medical Center

Dallas, Texas

August, 2014

Acknowledgement

I would like to express my gratitude to several people who have been instrumental in my success during graduate work here at UTSW. First and foremost, I would like to thank my mentors Dr. Jerry Shay and Dr. Woodring Wright for accepting me into their laboratory and guiding me through the intricacies of graduate school. Your encouragement, support and mentorship have allowed me become an independent thinker and develop as a young scientist. I would also like to thank my thesis committee members Dr. Story, Dr. Scaglioni and Dr. Mendelson for their valuable input, ideas and suggestions during my research.

I would like to thank all past and present Shay/Wright lab members that have assisted me throughout my research over the last six years. In particular I would like to thank Dr. Sang Kim, Summer Barron, Richard McDonnell, Tracy Chow, Gail Marian, Jonathan Gooden, Dr. Peter Ly, Kimberly Batten and Mariam El-Ashmawy for their expertise and support with various projects. I would especially like to thank Dr. Oliver Delgado for helping me lay the groundwork for my thesis project and for his valuable advice and input all through my graduate work.

Thank you to the entire support team at Brookhaven National Laboratory for helping us organize experiments at their facilities. I would also like to thank the UTSW NSCOR team especially Dr. James Richardson for training and helping me understand lung cancer pathology.

A special thank you to my better half Nida Sajan for being my support system throughout my graduate studies. Without your love, patience and understating I would have been lost. Thank you for always being there for me no matter what.

Lastly, I would like to thank my family who has been the most positive influences in my life; my parents Akberali and Mumtaz Kaisani, my sister Mehreen and my grandpa and grandma. Mom and Dad, I am who I am today because of the sacrifices you have made for me throughout these years. My success and achievements in life would not have been possible without you.

INVESTIGATING THE EFFECTS OF RADIATION EXPOSURE ON LUNG CANCER CARCINOGENESIS

Aadil A. Kaisani, Ph.D.

University of Texas Southwestern Medical Center at Dallas, 2014.

Jerry W. Shay, Ph.D.

Although it is the second most diagnosed cancer in both males and females, lung cancer accounts for the most cancer-related deaths worldwide. Radiation-induced carcinogenesis is a major concern for therapeutic radiation oncology as well as for astronauts on long-term missions. The large surface area of the lung makes it a prominent target for radiation exposure. From analysis of several human populations such as atomic bomb survivors, it is evident that the lung is remarkably susceptible to radiation-induced cancer. However, this data cannot be extrapolated to assess the risk in astronauts because of differences between terrestrial and space radiation. Due to lack of

understanding of how the ionizing space radiation affects cellular functions and carcinogenesis, there is a need to develop *in vitro* and *in vivo* systems.

Using immortalized human bronchial epithelial cells (HBECs) we have developed a novel three-dimensional (3D) culture system. When cultured on top of reconstituted basement membrane with lung fetal fibroblasts cultured below, HBECs form budding and branching structures resembling branching morphogenesis during lung development. HBECs in this culture system maintain markers of multiple cell types in the airway epithelium indicative of their multipotent potential. Studies to determine the effects of radiation on HBECs in 3D cultures are ongoing.

Radiation-induced carcinogenesis may require changes to the immune system and tumor microenvironment therefore we utilized the LA1 K-ras mouse model to analyze the effects of terrestrial and space radiation. Mice irradiated with simulated solar particle events (SPE) and silicon particle radiation (types of radiation in space) had a significantly shorter lifespan in contrast to unirradiated cohorts or mice irradiated with equivalent terrestrial radiation. A significant increase in invasive carcinoma was also observed in mice irradiated with SPE and silicon particle radiation but not with terrestrial radiation. Analysis of mice 70 days post-irradiation suggests that chronic inflammation is a likely contributor to tumor progression. CDDO-EA an anti-oxidant/anti-inflammatory modulator was tested as a potential radio-protector. A significant decrease in carcinoma was observed in mice fed a CDDO-EA countermeasure diet. These observations suggest

that the lung is highly susceptible to carcinogenesis upon irradiation and countermeasure compounds may mitigate this outcome.

TABLE OF CONTENTS

PRIOR PUBLICATIONS

Kaisani A, Kim SB, Delgado O, Barron S, Minna JD, Wright WE, Shay JW. Irradiation with simulated SPE increases lung invasive carcinoma incidence in LA1 K-ras mouse model. (In preparation).

Kaisani A, Delgado O, Fasciani G, Kim SB, Wright WE, Minna JD, Shay JW. Branching morphogenesis of immortalized human bronchial epithelial cells in three-dimensional culture. (2014) *Differentiation*, In press

Delgado O, Batten KG, Richardson JA, Xie XJ, Gazdar AF, **Kaisani A**, Girard L, Behrens C, Suraokar M, Fasciani G, Wright WE, Story MD, Wistuba II, Minna JD, Shay JW. Radiation-enhanced lung cancer progression in a transgenic mouse model of lung cancer is predictive of outcomes in human lung and breast cancer. (2014), *Clin Cancer Res*, 20(6):1610-22

Kim SB, Ly P, **Kaisani A**, Zhang L, Wright WE, Shay JW. Mitigation of radiation-induced damage by targeting EGFR in noncancerous human epithelial cells. (2013), *Radiat Res*, 180(3):259-67

Kim SB, Pandita RK, Eskiocak U, Ly P, **Kaisani A**, Kumar R, Cornelius C, Wright WE, Pandita TK, Shay JW. Targeting of Nrf2 induces DNA damage signaling and protects colonic epithelial cells from ionizing radiation. (2012), *Proc Natl Acad Sci U S A*, 109(43):E2949-5

Ly P, Kim SB, **Kaisani A**, Marian G, Wright WE, Shay JW. Aneuploid human colonic epithelial cells are sensitive to AICAR-induced growth inhibition through EGFR degradation. (2013), *Oncogene*, 32(26):3139-46

Delgado O, **Kaisani A**, Spinola M, Xie XJ, Batten KG, Minna JD, Wright WE, Shay JW. Multipotent capacity of immortalized human bronchial epithelial cells. (2011), *PLoS One*, 6(7):e22023

LIST OF FIGURES

LIST OF TABLES

LIST OF ABBREVIATION

2D - two-dimensional

3D - three-dimensional

ACA - American Cancer Association

ALI -Air-Liquid Interface

AQP5 - Aquaporin 5

BADJ - Bronchioalveolar Duct Junction

BASCs - Bronchioalveolar Stem Cells

BrdU - Bromodeoxyuridin

BMP - Bone Morphogenetic Protein

CC10 or CCSP - Clara Secretory Protein

CDK4 (K) - Cyclin-Dependent Kinase 4

Cyp2f2 - Cytochrome P4502F2

DAPI - 4', 6-diamidino-2-phenylindole

DNA - Deoxyribonucleic Acid

DSBs - Double Strand Break

ECM - Extracellular Matrix

EGFR - Epidermal Growth Factor Receptor

EM - Electron Microscopy

ERR - Excess Relative Risk

ETS - Environmental Tobacco Smoke

Fe- Iron

FGF - Fibroblast Growth Factor

FOXA2 - Forkhead Box Protein A2

GAB1 - GRB2-Associated-Binding Protein 1

GCR - Galactic Cosmic Radiation

H&E - Hematoxylin and Eosin

HBECs - Human Bronchial Epithelial Cells

HGF - Hepatocyte Growth Factor

hTERT (T) - Human Telomerase Reverse Transcriptase

HUVECs - Human Umbilical Vein Endothelial Cells

HZE - High Charge and Energy

IACUC - Institution of Animal Care and Use Committee

K14 - Keratin 14

K5 - Keratin 5

Keap1 - Kelch-like ECH-associated protein 1

KSFM - Keratinocyte Serum Free media

LET - Linear Energy Transfer

LSS - Life Span Study

MAPK - Mitogenic-Activated Protein Kinase

NASA - National Aeronautic and Space Association

NCI - National Cancer Institute

NCRP - National Council of Radiation Protection and Measurement

NFkB - Nuclear Factor Kappa-Light-Chain-Enhancer of Activated B Cells

NO_2 - Nitric Oxide

NSCLC - Non-Small Cell Lung Cancer

P63 - Transformation-Related Protein 63

PNECs - Pulmonary Neuroendocrine Cells

REID - Radiation Induced Death

SCC - Squamous Cell Carcinoma

SCLCs - Small Cell Lung Cancer

Si - Silicon

SP-A - Surfactant Protein-A

SP-C - Surfactant Protein C

SP-D - Surfactant Protein D

SPE - Solar Particle Events

SPF - Specific Pathogen Free

SPRY 2 - Sprouty Family Members

SSBs - Single Strand Breaks

STAT - Signal Transducer and Activator of Transcription

TA - Transient Amplifying Cells

TGFβ - Transforming Growth Factor-Beta

TKI - Tyrosine Kinase Inhibitors

TTF1 - Thyroid Transcription Factor

TP53 - Tumor Suppressor p53

US - United States

UTSW - University of Texas Southwestern Medical Cen

Chapter One:

Introduction

1.1 The Respiratory System

The vertebrate respiratory system mediates the vital exchange of gases between the circulatory system and the exogenous environment. To achieve this goal, the lung consists of two-intertwined and highly branched tubular structures; one conducting blood and the other air (Morrisey and Hogan, 2010). The basic design of the respiratory system comprises of a tree of epithelial tubules in which air is cleaned, humidified and channeled towards numerous alveolar units where the circulating blood is oxygenated (Cardoso and Lu, 2006). Besides its primary function of respiration, the highly specialized epithelial cell layer lining the airways also plays a critical role in defense against airborne pathogens from the outside environment. The lung has evolved various strategies such as using innate immunity, secretion of mucus for clearing the

airways, and maintaining suitable surface tension for defense against the external environment (Herriges and Morrisey, 2014). The complex three dimensional architecture and cellular composition of the lung allows it to perform these functions fluently.

The respiratory system can be divided into two functional and structural constituents: the conducting airway (central) and the respiratory zone (peripheral) **(Figure 1.1)**. The central airway comprises of the trachea and bronchi while the peripheral region includes terminal bronchioles, respiratory bronchioles and the alveolar sacs (Treuting et al., 2012). The trachea is the largest conducting airway and is supported by 15-20 U-shaped cartilaginous rings connected by fibro-muscular membrane. Air enters the trachea after passing through the upper respiratory system which encompasses the nasal passage, pharynx and larynx. The cartilaginous rings provide rigidity and support to the airway keeping it from collapsing. As the trachea transitions, the cartilaginous rings become less organized and the airway bifurcates into the right and left main bronchi (Treuting et al., 2012). The trachea is lined by pseudostratified columnar epithelial cells containing three primary cell types; basal cells, ciliated cells and goblet cells **(Figure 1.2)**. Epithelial cells in the central airways humidify and clean the inspired air efficiently. The goblet cells produce a protective layer that moisturizes the inhaled air and trap foreign airborne matter (Treuting et al., 2012). The ciliated columnar epithelial cells use the motile cilia on their apical surface to impel foreign matter towards the upper respiratory system. The basal cells, so-named for their vicinity to the basal lamina help anchor the pseudostratified epithelium to the matrix and protect the stroma from the exogenous environment (Rock et al., 2010).

Columnar pulmonary neuroendocrine cells (PNECs) are also found in the central airway, with a higher abundance near the site where the trachea bifurcates. These cells are either found individually or in cluster called neuroepithelial bodies (Rock and Hogan, 2011; Van Lommel, 2001). PNECs perform the function of sensing stimuli such as hypoxia within the airway and transmitting them to the central nervous system (Rock and Hogan, 2011; Van Lommel et al., 1998). The molecular mechanisms of PNECs are still not well understood.

The right bronchus in the human lung subdivides further into three lobular bronchi while the left bronchus subdivides into two lobular bronchi (Treuting et al., 2012). This disparity of division between the left and the right leads to the right lung dividing into three lobes and the left lung dividing into two, each functioning independently (Treuting et al., 2012).

Each lobular bronchus further subdivides into various segmented and tertiary bronchi (Treuting et al., 2012). This division of the airway is also followed by changes in the surrounding connective tissue. As the lobular bronchi subdivide, the cartilaginous rings become sporadic and eventually disappear at the primary bronchioles. The rings are replaced by smooth muscle tissue and an increased density of elastic fibers which help with lung recoil (Treuting et al., 2012). The successive divisions also bring about a gradual histological change along the airway epithelium. The epithelium diminishes in height eventually transitioning into a simple columnar morphology and the number of goblet cells decline in comparison to the trachea.

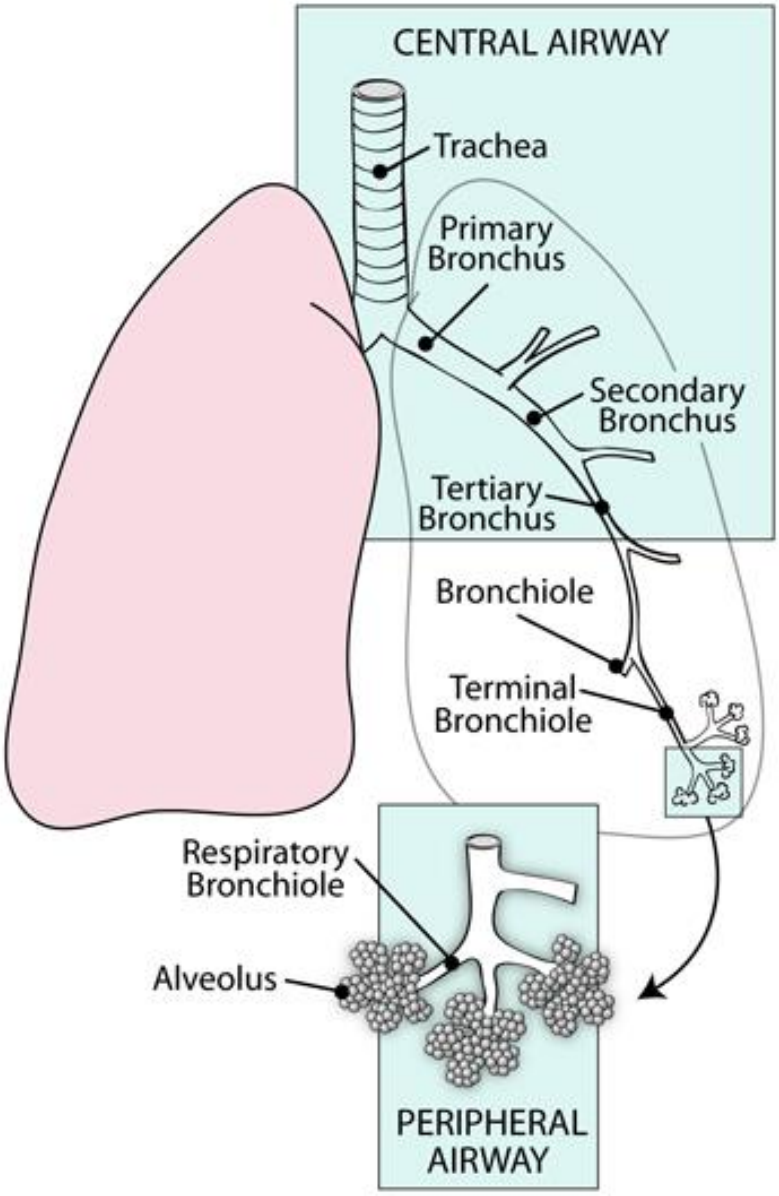

Figure 1.1 Central and peripheral regions of the adult lung.
The central lung comprises of trachea, primary and the secondary bronchus. The central airway primarily functions to humidify and filter the inhaled air from airborne particles. The peripheral lung consists of the terminal bronchioles, respiratory bronchioles and the septated alveolar sacs. Alveoli are the functioning unit of the respiratory system where the final gas exchange takes place with the cardiovascular system (Adapted from Delgado Dissertation 2010).

As the airway transitions into the primary bronchioles and further subdivides into terminal bronchioles, the airway epithelium shifts into a simple cuboidal morphology. The number of ciliated cells decreases in density in comparison to the central airway and the density of Clara cells (also referred to as club cells) increases in the airway epithelium (Treuting et al., 2012). Clara cells make up the majority of the airway epithelium in the peripheral respiratory system. These dome-shaped secretory cells contribute in the degradation of the mucus produced in the central airway and play a detoxifying role. The terminal bronchioles transition into respiratory bronchioles eventually leading to the final site of gas exchange, the alveoli (Treuting et al., 2012).

Respiratory bronchioles run through the thin alveolar duct wall and transition into the alveoli. Each respiratory bronchiole is estimated to give rise to 2-11 alveolar ducts in the human lung (Treuting et al., 2012). Alveoli are septated saccular structures that form a network by connecting to neighboring alveolar ducts. Two primary epithelial cell types found in the alveoli are the Type I and Type II pneumocytes. Type I pneumocytes are squamous in morphology and interspersed by Type II pneumocytes which are cuboidal **(Figure 1.2)**. Type I pneumocytes are directly involved in gas exchange, where Type II pneumocytes produce surfactant. Secreted pulmonary surfactant and other lipids decrease alveolar surface tension and also contribute to host defense (Rock and Hogan, 2011). Alveolar macrophages are also present in the alveolar sacs, where they scavenge airborne foreign particle that made it through the central respiratory airway. The alveoli are surrounded by a rich capillary network with loose connective tissue containing other cell types such as fibroblasts, pericytes, lymphocytes and mast cells. The close proximity to the capillaries allow for efficient gas exchange (Treuting et al., 2012). Overall, the

complex three dimensional design and specialized airway epithelium of the lung allows the organ to carry out its functions proficiently.

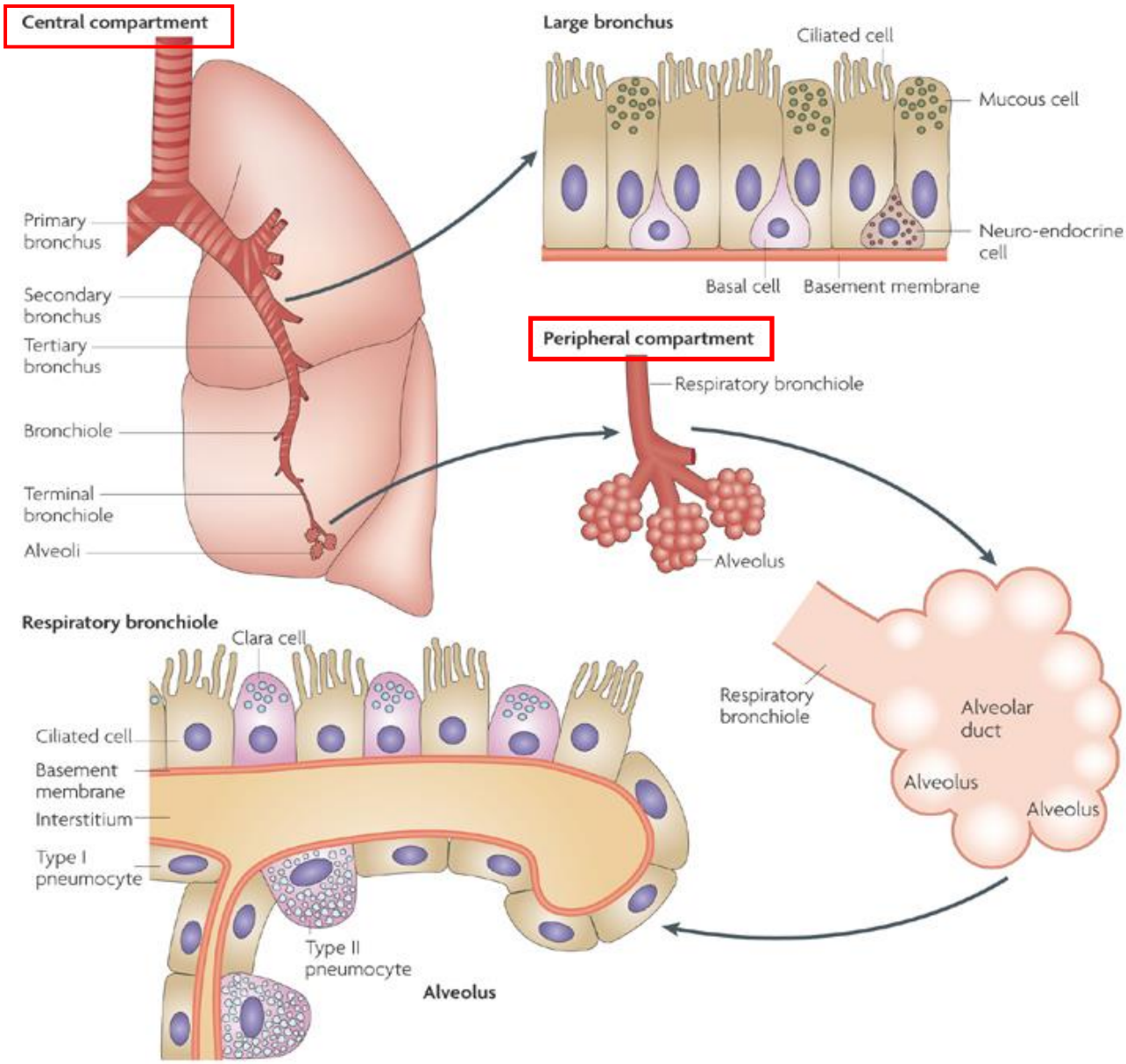

Figure 1.2 Respective cell types of the central and peripheral airways.
The central airway consists primarily of basal cells, goblet cells and ciliated maintaining a pseudostratified epithelium. Sporadic PNECs are also found along the epithelium lining of the central airway. The peripheral compartment comprises of secretory Clara cells with a few ciliated cells. Type I and II pneumocytes line the alveoli with Type I cells covering the majority of the surface area. (Adapted from Schiller et al. Nature Cancer Review 2007).

1.2 Development of the Adult Lung

Lung morphogenesis is a dynamic process requiring integration of multiple regulatory factors. The respiratory tract composed of airway epithelial cells is derived from the endoderm, surrounded by mesenchymal cells derived from the mesoderm (Kimura and Deutsch, 2007). Signaling between the epithelial and mesenchymal tissue compartments plays a crucial role in formation and differentiation of the lung. Cells direct their response to these dynamic signaling through transcription factors. This coordinated regulation of transcription factors also determines epithelial cell fate (Kimura and Deutsch, 2007). The lung development can be delineated into five stages based on anatomical and histological features. The embryonic and pseudoglandular stages elaborate the conducting airway; the later stages canalicular, saccular and alveolar stages are responsible for vascularization, modification of the mesenchyme and differentiation of the airway epithelium **(Figure 1.3)**. Understanding of human lung development mechanisms have largely been studied using model organism since the process is conserved through many species.

The embryonic stage of lung development begins with the separation of the interior foregut endoderm forming two tubes; one developing into trachea and the other into esophagus (Que et al., 2006). The respiratory domain where the budding initiates is designated by the expression of Thyroid transcription factor 1(TTF1) and Forkhead box protein A2 (FOXA2) (Cardoso and Lu, 2006; Rock and Hogan, 2011). Wnt/β-catenin and bone morphogenetic protein (BMP) from the surrounding developing mesenchyme also play a role in specifying TTF1 positive region in the interior endoderm (Domyan et al., 2011; Herriges and Morrisey, 2014).

The pseudoglandular stage is defined by the growth of the primary airway through the process of branching morphogenesis and it continues until the development of terminal bronchioles. After the early budding of the main bronchi, the lung buds extend into the surrounding mesenchyme and develop rapidly (Herriges and Morrisey, 2014). The process of branching morphogenesis is essential both for the formation of the central airway as well as the terminal alveolar compartments. Signaling between the simultaneously developing airway epithelial and connective mesenchyme is key for initiating new branching in the emerging airway (Morrisey and Hogan, 2010). Fibroblast growth factor signaling (FGF) in particular FGF10 secreted by the neighboring mesenchyme is essential for the branching process. Secreted FGF10 binds to Fgfr2 receptor in the endoderm guiding the developing airway. Loss of this pathway leads to a complete abrogation of branching (Ohuchi et al., 2000; Sekine et al., 1999). FGF10 secretion is further regulated by other signaling pathways including BMP4, sonic hedgehog (SHH) and retinoic acid (Pepicelli et al., 1998; Weaver et al., 1999). Transforming growth factor-beta (TGFβ) subfamily also positively regulates this process

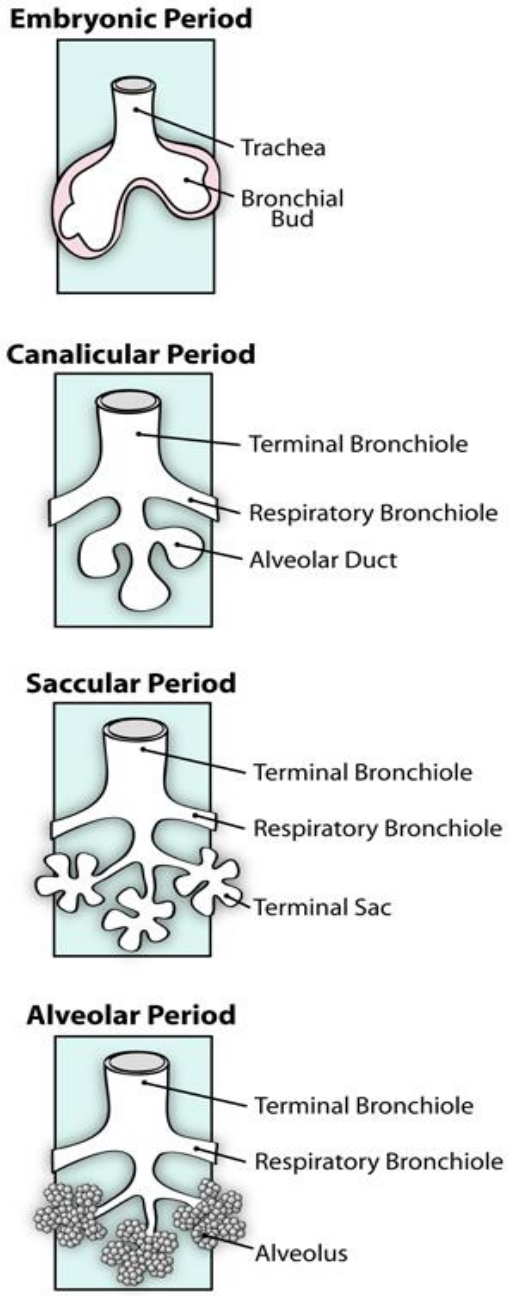

Figure 1.3: Developmental stages of the adult lung.
Lung development can be divided into five distinct stages. The lung bud emerges from the foregut endoderm in the embryonic stage followed by branching morphogenesis in the pseudglandular stage (not shown). These stages primarily are responsible for giving the airways their initial architecture. The last three stages canalicular, saccular and alveolar are where the epithelial cells differentiate into specialized airway cells based on their location along the proximal-distal airway. (Adapted from Delgado Dissertation 2010).

by specifically regulating epithelial cell proliferation and extracellular matrix (ECM) deposition (Heine et al., 1990; Kimura and Deutsch, 2007). Sprouty family members in particular (Spry2) plays the role of antagonist in branching by inducing negative regulators of FGF signaling (Mahlapuu et al., 2001; Tefft et al., 2002; Weaver et al., 2000). Spry2 controls the size of the lung buds by limiting their outgrowth. ECM interactions also play an important role in generating airway epithelial structure. For example, fibronectin accumulates at sites of branch point constriction, directing new branch points and guiding its formation (Sakai et al., 2003). The airway epithelium in the central airway starts differentiating towards the conclusion of the pseudoglandular stage. This complex interplay between signaling pathways regulate branching in a temporal-spatial way.

The canalicular stage marks the end of branching morphogenesis, and development of respiratory bronchioles and alveolar ducts commences (Maeda et al., 2007). Airway epithelium differentiates into cell types originating from the peripheral airway such as Clara cells (Maeda et al., 2007). Type II pneumocytes which can differentiate into squamous Type I pneumocytes also begin to appear at the alveolar duct. Along the airway, an invasion of capillaries in to the mesenchyme also occurs; endothelial cells begin to differentiate in close proximity to the developing airway epithelium. These capillaries will eventually carry deoxygenated blood to the alveoli.

Alveolar sacs begin to develop from the alveolar duct leading to the formation of alveoli in the saccular stage of lung development. This stage also marks the transition of a fluid-filled to an air-filled lung (Maeda et al., 2007). Pulmonary capillaries continue to differentiate and

develop in close vicinity to the epithelium. Type I and II pneumocytes line the alveolar sac and secrete surfactant into the alveoli by the end of this stage (Maeda et al., 2007). The septa in between Type I and capillaries remains thick, not allowing efficient gas exchange. Birth signifies the end of saccular stage where the lungs start to perform its respiratory function.

The alveolar stage, the last stage of lung development continues into the postnatal period. Type II pneumocytes continue to expand, secrete surfactant and differentiate into type I cells. The septa between the airways and capillaries also shrinks and the vasculature continue to modify in order to allow efficient gas exchange. The alveolar stage continues several years past birth (Maeda et al., 2007).

This complex process involving cross talk amongst multiple cell types from endoderm and the mesoderm eventually leads to development of this intricate organ. This signaling not only helps guide the branching epithelium, but also regulates the differentiation of the lung into specific cell types. These evolutionary conserved processes help assure that the lungs can perform its functions efficiently.

1.3 Progenitor Cells of the Adult Lung

Multicellular organisms are required to produce new cells to maintain the structural integrity and function of their tissues. Cells in the body are constantly exposed to potential toxic agents and pathogens in the environment, and must therefore be able to respond promptly to cellular damage. Since the process of lung development and function has been broadly conserved throughout evolution, model organisms have been extensively used over the last decade to understand lung biology. Using model organism and rodents in particular, cells responsible for repair and maintenance of the lung epithelial lining have been identified.

The classical hierarchal stem cell model does not apply to the adult lung (Rawlins and Hogan, 2006). Organs such as hair follicles, blood and colon constantly renew themselves and have a high turnover rate (Fuchs et al., 2004). These organs contain stem cells that are morphologically unspecialized, with low rate of divisions. These cells are also restricted to a localized region known as ‘niche’ that tightly regulates their behavior (Fuchs et al., 2004; Rawlins and Hogan, 2006). These dedicated stem cells undergo long term self-renewal and are capable of producing daughter cells known as transient amplifying cells (TA). In organ systems with high renewal/turnover rate, these transient amplifying cells serve as precursors for many differentiated cells. Since organs with high turnover rate require constant replenishment, these transient amplifying cells can also self-renew and display a high proliferation rates for a short period of time (Rawlins and Hogan, 2006).

For tissues with low turnover rate such as lung, liver and pancreas, the classical hierarchal model does not hold true (Raff, 2003). In these organs, the hierarchy is not always rigid and is reversible. In contrast to rapidly renewing organs such as blood and skin, these organs are capable of maintaining themselves without the aid of an undifferentiated stem cell population. Recent experiments have elucidated this concept where labeled insulin producing β-cells of the adult pancreas were able to regenerate after a partial pancreatectomy (Dor et al., 2004). Conversely, the turnover and differentiation after a hepatectomy involves the division of differentiated hepatocyte population (Alison et al., 2004). These observations provide evidence for the concept of 'facultative' stem cells, where a quiescent differentiated/specialized cell is capable of acting as a stem cell in an event of injury.

Lack of in vitro models using human airway epithelial cells have meant that a majority of our understanding of lung repair, regeneration and homeostasis comes from rodents. Murine in vitro and in vivo models have been extensively utilized over the last decade to deduce the cells and mechanism responsible for repair and regeneration within the adult lung.

The earliest studies to understand the steady-state maintenance and turnover of the adult lung involved pulse/chase experiments using tritiated thymidine or bromodeoxyuridine (BrdU) (Rawlins and Hogan, 2006). The technique involves continuous administration of the pulse compound to the test subject allowing it to bind deoxyribonucleic acid (DNA). After introducing the pulse, the tissue of interest is followed to determine the strength of the signal. Frequently dividing cells start diluting their signal as the DNA content in replicated and transferred to the daughter cells. By identifying cell that are dividing frequently or staying quiescent, cells

responsible for maintaining the tissues can be identified. The earliest studies using this technique determined that the turnover time of the tracheal-bronchial epithelium of adult rodent is more than 100 days (Blenkinsopp, 1967; Wells, 1970). Recent studies have further elaborated on these earlier studies by determining turnover over rate for specific cell types such as ciliated cells of the trachea and bronchi that have half-lives of 6 months and 17 months respectively (Rawlins and Hogan, 2006; Rock and Hogan, 2011).

Although the pulse/chase experiments provided valuable insight into turnover rate of the adult lung, it failed to identify specific cell types responsible for repair and regeneration; BrdU or tritiated thymidine cannot selectively label certain cell types. The most promising way to identify lineage relationships has been though the use of Cre/lox genetic labeling of specific cell types in mice and following their descendants. This technique relies upon cell-type specific markers that can be used to identify different cell types and then determine progeny-progenitor relationships. Cell types of both central and peripheral lung in adult can be identified using specific markers described in **Table 1.1**. Since the proliferation under steady-state conditions is relative infrequent within the lung, it is necessary to induce epithelial injury in these in vivo models to test the cell types that potentially contribute to the maintenance and repair (Kauffman, 1980; Rawlins and Hogan, 2006). After the ablation of certain cell types using chemical and oxidizing agents, the lung can be inspected to analyze cells responsible for regeneration based on their specific marker.

Cell Type	Location and Function	Molecular Markers
Basal cells	Stem cells of the pseudostratified epithelium lining the central airway. Also anchor the epithelium to the basement membrane.	P63, Keratin 5, Keratin 14
Goblet cells	Secrete mucin which forms protective barrier and traps airborne particles in the inhaled air.	Mucin 5 subtype AC
Ciliated cells	Mutlicialted cells containing cilia. The rythmic movement of ciala helps prevent airbone particles form entering the peripheral airway	Forkhead box protein J1, apical acetylated tubulin
PNECs	Found sporadically in the central airway. Largely unknown function	Calcitonin gene related peptide (CGRP)
Clara cells	Non-ciliated dome-shaped cells in the peripheral airway. Contain secretory granules.	TTF1, CC10, SP-A, SP-D, CypP450 family members
Clara^{v} cells	Non-ciliated secretory found in the adult rodent peripheral airways. Resistant to naphthalene injury.	TTF1, CC10
Type I Pneumocytes	Squamous cells in the alveoli covering majority of the surface area. In close proximity to endothelial cells.	TTF1, CC10, SP-A, SP-C, SP-D
Type II Pneumocytes	Large cuboidal cells in the alveoli. Secrete surfactant to lower the surface tension for efficient gas exchange.	Aquaporin-5, Podoplanin precursor

Table 1.1: Markers, location and functions of adult lung epithelial cell types.

The adult lung contains region specific epithelial cell types (Wansleeben et al., 2013). Cell types serving as progenitor cells only repair injury based on their location within the airway. The central airway which includes the trachea and the primary bronchi, is comprised of basal cells, goblet cells and ciliated cells. There is strong evidence from recent studies that basal cells in the central airway function as multipotent stem cells within that region. They can both self-

renew and give rise to ciliated and goblet cells during postnatal growth, in steady-state conditions and during repair following injury to the epithelium (Wansleeben et al., 2013). *In vitro* evidence for this claim comes from both air-liquid interface (ALI) and three-dimensional culture studies (Rock et al., 2009; Schoch et al., 2004). Purified basal cells from both human and rodents by flow cytometry are able to differentiate into ciliated and goblet cells when seeded into decellularized tracheal scaffold and cultured at the air liquid interface (Engelhardt et al., 1995; Hackett et al., 2008; Liu et al., 1994; Randell et al., 1991). These cells also give rise to the same progeny when cultured in reconstituted basement membrane at single cell density (Schoch et al., 2004). Such *in vitro* models have been proposed to understand the molecular signaling responsible for regulating self-renewal and differentiation since these mechanisms remain undetermined.

The first in vivo evidence for basal cells being the progenitor cells in the central airway comes from experiments with labeled DNA precursors. Upon inhalation of nitric oxide (NO) which ablates ciliated cells, basal cells proliferated in response to this injury in the rodents's trachea-bronchial region (Breuer et al., 1990; Evans et al., 1986). This *in vivo* evidence was still not definitive because of DNA precursors being a non-selective marker. The most relevant evidence comes from studies using Keratin 14(K14)-CreER transgenic mouse to lineage label cells in the adult epithelium (Hong et al., 2004a, b). Under steady-state conditions with no injury to the epithelium, only a small subset of basal cells expresses K14 (Cole et al., 2010; Rock et al., 2010). Upon administrating naphthalene to cause injury, the basal cells expressing K14 proliferate, self-renew and are able to repopulated the central airway with ciliated and goblet

cells (Hong et al., 2004a, b). Although these experiments provided further evidence, they did not analyze the role of basal cells in a steady-state environment with no injury.

Recent experiments with Keratin 5 (another basal cell marker) (K5)-CreER, transgenic mice demonstrate that basal cells also function as progenitor cells during postnatal growth and in a steady-state environment (Rock et al., 2009). Without any injury to the epithelium, the basal cells still function as the progenitor cells indicating that their role as stem cell is not restricted to events after injury. The question of basal cell heterogeneity still remains unclear and further studies are needed to address this question. It is probable that certain K14 and K5 positive cells are programmed only to differentiate into goblet or ciliated cells or self-renew (Borthwick et al., 2001). Another important aspect that remains unclear regarding basal cells is their "niche'. Currently there is no evidence that the niche of basal cells is required as in other fast turnover tissue such as hair follicles or intestinal crypts. There is some evidence from long-term lineage tracing studies that there are quiescent and label retaining cells residing in higher densities near submucosal gland but further studies are required (Borthwick et al., 2001; Wansleeben et al., 2013).

The current working model for how basal cells in the central airway respond to injury is that the surviving basal cells spread and cover the basal lamina. Their first task is to form apical intercellular junctions to restore a barrier between the airway and the underlying mesenchyme. The basal cells then proliferate and differentiate into ciliated and goblets cells (Rock et al., 2011). While restoring the epithelium, there may be a population of undifferentiated basal cells (similar to transient –amplifying cells) that eventually regenerate the central airway but further

studies are needed to test this hypothesis. The process of completely restoring the central airway epithelium after injury takes between 2 and 3 weeks (Borthwick et al., 2001; Wansleeben et al., 2013). Although the transgenic murine models have offered critical insight into the progenitor cells of the central airway, a lot remains unknown. The finding from the rodent lung may also not hold true for human respiratory system due to anatomical differences between the two species (discussed in the next section).

The columnar epithelial cells lining the intralobular airways (peripheral lung; terminal bronchioles) are mainly composed by secretory Clara cells and ciliated epithelial cells. Clusters of PNECs are also found in the peripheral lung. Similar to studies utilized to identify basal cells as the progenitor cells of the trachea and primary bronchi, lineage tracing experiments using cell type specific markers have been used to analyze the peripheral airways. The injury model using aromatic hydrocarbon naphthalene is the most popular model used to identify progenitor cell population of the peripheral lung (Rawlins and Hogan, 2006). Naphthalene is administered through intraperitoneal injection, where it reaches the lung through the bloodstream. Naphthalene kills only a selected population of Clara cells; specifically Clara cells expressing cytochrome P4502F2 (*Cyp2f2*) are killed when the compound is converted to toxic epoxides (Lawson et al., 2002; Plopper et al., 1992). After naphthalene treatment, the remaining population of Clara cells is known as ‘variant’ Clara cells (Clara^{v}) which are located in clusters near PNECs and bronchioalveolar duct junction (BADJ). BADJ is defined as the transition zone between the smallest respiratory bronchiole and the beginning of the alveoli (9). Clara secretory protein (CC10 or CCSP) a secretoglobin found specifically in Clara cells is used as a marker to identify Clara cells. Upon ablation of Clara cells using a CC10-CreER mouse model, the

surviving Clara^{v} cells proliferate and are able to regenerate the epithelium, including differentiating into ciliated epithelial cells (Giangreco et al., 2002; Reynolds et al., 2000; Wansleeben et al., 2013). Lineage tracing studies have also demonstrated that the ciliated cells in the peripheral lung are not able to self-renew or differentiate in an injury (Rawlins et al., 2007). Long term lineage tracing (up to a year) studies to analyze the behavior of Clara cells under steady-state environmental conditions have also revealed that these cells serve as the progenitor cells (Perl et al., 2011). Although the lineage tracing studies have helped identify the stem cells in the peripheral lung, the signaling events and mechanisms involved in Clara cells renewal and regeneration after an injury are still unclear. There is also no concrete evidence present regarding if a specific niche of these cells is important.

The BADJ zone in rodents are composed of Clara and ciliated epithelial cells however, the human resident cell types are poorly defined. There is considerable controversy regarding the behavior of ciliated epithelial cells in response to injury in this peripheral region of the lung and further studies are required. The Clara^{v} cells also play the role of progenitor cells in this region of the lung in response to naphthalene injury and are able to self-renew and repopulate the BADJ (Giangreco et al., 2002; Rawlins et al., 2009). However, these CC10+ Clara^{v} cells do not give rise to Type I or Type II pneumocyte descendants which are present in the alveoli. Interestingly, studies from the last decade have also identified a cell type in the BADJ (about 1-2 cells per duct) that co-expresses CC10 and Surfactant protein C (SP-C). SP-C is strongly expressed in Type II pnemocytes present in the alveoli. It has been proposed that these dual positive cells in the BADJ are resident stem cell and are named bronchioalveolar stem cells (BASCs) (Kim et al., 2005; Wansleeben et al., 2013). These claims for BASCs are largely based on *in vitro* studies

where cell isolated through flow cytometry are able to give rise to bronchiolar and alveolar cell types. However no lineage tracing analysis on these dual positive cells have been performed. These studies are further complicated by the fact that about 10% of Type II pneumocytes in the alveoli normally express low level of CC10 beside SP-C (Rawlins et al., 2009). As a result there is no certainty if the BASCs can repair and regenerate both bronchiolar and alveolar cell types.

Experimental injuries used to induce damage in the alveoli to understand regenerative potential of cell types involve hyperoxia (exposing the lungs to high concentration of oxygen over several days), inhalation of ozone or nitric oxide and systemic administration with bleomycin (Wansleeben et al., 2013). None of these agents selectively injure specific cell types in the alveoli therefore lineage tracing using cell specific markers is required. Early studies using pulse chase methodology estimate that the turnover in the alveolar region of an adult mouse lung is about 28 to 35 days (Bowden et al., 1968; Kauffman, 1980). Using a SP-C-CreER (Type II pneumocyte specific marker) it has been demonstrated that Type II cells can self-renew and differentiate into Type I cells in response to injury and under steady-state conditions (Chapman et al., 2011; Wansleeben et al., 2013). Type I cells in the alveoli have no regenerative potential and rely entirely on Type II cells. There have been speculations regarding the niche of Type II pneumocytes being in close proximity to fibroblast-like cells but further experimental analyses are required to confirm this claim. A summary of progenitor cells of the adult lung is described in **Figure 1.4**

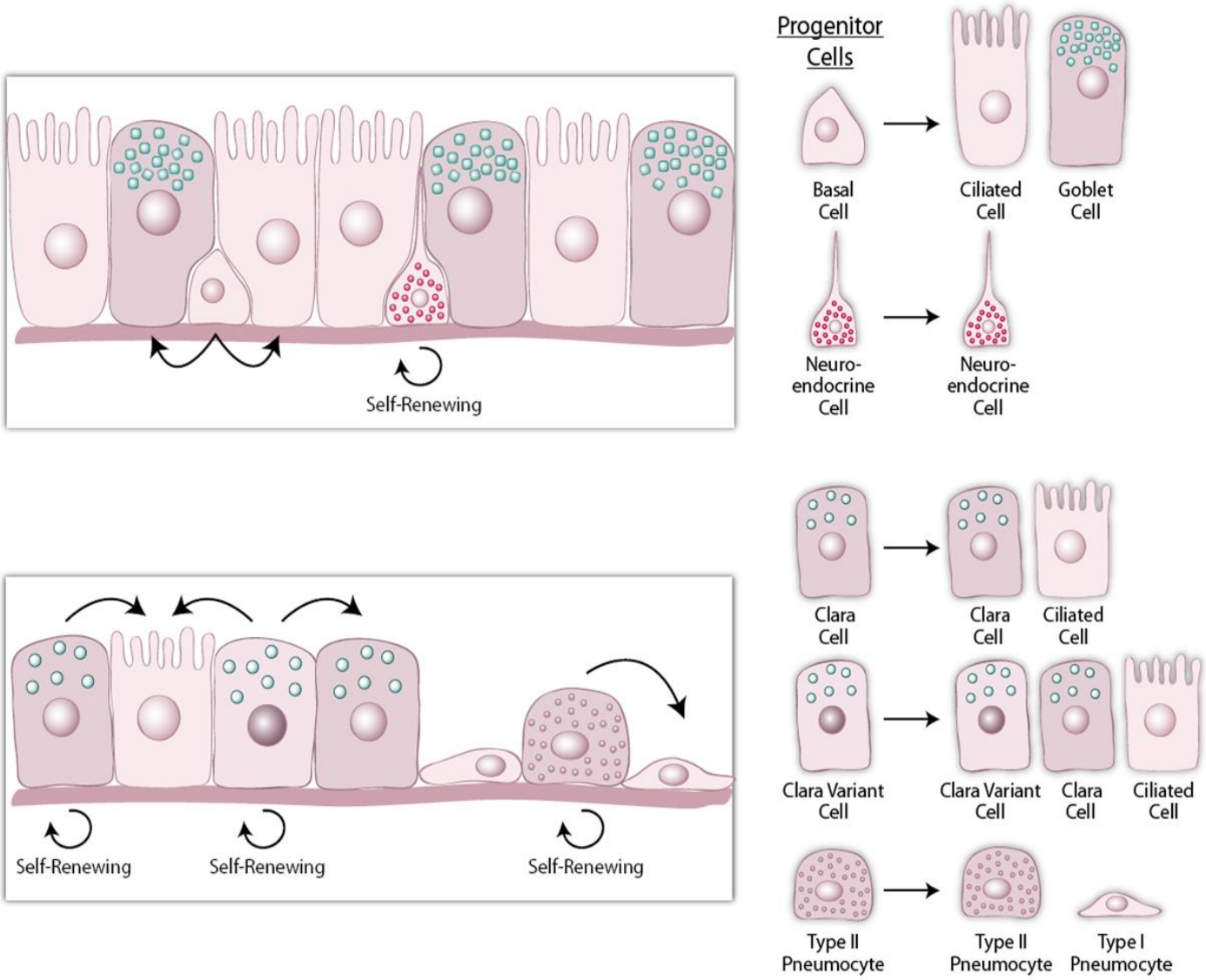

Figure 1.4: Stem cells in the central and peripheral airways of the adult lung.
In the central airway, the basal cells are capable of self-renewing and regenerating goblet and ciliated cells. Neuroendocrine (PNECs) cells only possess the capacity to self-renew.
In the peripheral airway Clara cells can self-renew and differentiate into ciliated cells. In an event of injury where Clara cells are ablated (naphthalene injury), Clara-variant cells are able to regenerate Clara cells. These cells can also self-renew and differentiate into ciliated cells. Type II pneumocytes in the alveoli are capable of self-renewing and differentiating into Type I cells. (Adapted from Delgado Dissertation, 2010).

The lung with its dynamic 3D architecture and specialized airway epithelial cell types have evolved mechanisms that allow for repair and regeneration. The use of facultative stem cells in different compartments of the lung allows the airways to effectively deal with injuries. Although the rodent models have been vital in understanding lung homeostasis, repair and regeneration, a lot still remains unknown. New *in vivo* and *in vitro* model systems are required to understand key molecular mechanisms of how these stem cells function and communicate with their environment.

1.4 Anatomical Variation Between the Rodent and Human Adult Lung

There are key anatomical differences between the adult rodent and human airways, even though the basic design of the lung has been conserved between the two species. In mice, the largest airway, the trachea has an internal diameter of ~1.5 mm, equivalent to the smallest peripheral airway in the human lung (Rock et al., 2010). The cartilaginous structure supporting the trachea only extends till the primary airway bifurcates in mice while, it is present in the bronchial region of the human lung. The major difference between the two airways is in the distribution of certain cell types along the epithelium. In mice, basal cells (the progenitor cells of the central airway) are restricted to the proximal trachea but penetrate deep into the human lung. Basal cells can be found in terminal bronchioles of the human airway although their density is significant lower compared to the trachea. In human, mucin secreting goblets cells are relatively abundant but in adult mice, these cells are rare. Conversely, Clara cells which generally reside in the bronchioles of the human airway extend and populate the mouse trachea. Clara^{v} cells which

through lineage tracing studies are determined to be stem cells in the peripheral airways do not exist in the human airway. Currently there is no experimental evidence for these cells in the human lung. These differences between the two airways indicate the need to develop novel systems which may better resemble the human airway.

1.5 Cancer; a Growing Worldwide Pandemic

Cancer is responsible for 1 in 8 deaths worldwide and is rapidly becoming a global pandemic (ACA, 2014). There are estimated 12.7 million new cancers cases annually and if these rates do not change, the global cancer burden is expected to nearly double by year 2030. Increases in pollution in major cities, decline in physical activity, tobacco use, diets high in fats and general increase in life expectancy are a few factors amongst many for this dramatic increase in cancer rates. Besides, the hefty death toll, the economic toll is equally alarming; in 2008, cancer accounted for nearly $1 trillion in economic losses from disability and premature death (ACA, 2014).

Cancer simply defined is unregulated cell growth, where cells divide and grow without misregulated intrinsic controls, eventually forming a malignant tumor that invades secondary tissues in a process named metastasis. Decades of research has contributed to our understanding of cancer as a multi-step disease involving multiple genetic and epigenetic alterations, through which resulting DNA damage transforms normal cells. The multistep process of tumor pathogenesis where cancer cells acquire traits to become malignant has been defined by the six

core hallmarks and several emerging hallmarks of cancer (Hanahan and Weinberg, 2000). The core of hallmarks are the tumor cells ability to sustain proliferative signaling, evade growth suppression, resist cell death, enable replicative immortality, induce angiogenesis and activating tumor invasion and metastasis. These core hallmarks define the basic requirements for a normal cell to develop and transform into a malignant tumor. The other emerging hallmarks take in account the notion that cancer is a systemic disease and that tumor progression requires changes to the immune system and microenvironment of the tumor (Hanahan and Weinberg, 2011).

1.6 Lung Cancer Statistics

Lung cancer is the second most common cancer in both men and women in US. Even though prostate cancer in men and breast cancer in women account for a majority of the new cases, lung cancer accounts for the most deaths **(Table 1.2)**. More people in the US die of lung cancer than of colon, breast and prostate combined. The American Cancer Society (ACA) estimates that about 224,210 new cases of lung cancer will be discovered in 2014 accounting for 13% of all new cancers. An estimated 159,260 deaths from lung cancer will account for 27% of all cancer deaths in 2014 (ACA, 2014). About 2 out of 3 people diagnosed with lung cancer are 65 or older and only 2% of all cases are found in people younger than 45. Currently, the average age of diagnosis is about 70 years. Men in general have a higher susceptibility to lung cancer compare to females. The chance of a man developing lung cancer in his lifetime is 1 in13; the risk for women is 1 in 16 (Sun et al., 2007)

The overall combined 5-year survival rate for lung cancer at various stages combined is 17% (ACA, 2014). The survival for localized disease where the tumor is limited to the primary tissue is 54% whereas if the disease has metastasized, the rate dramatically decreases to 4% **(Table 1.3)**. Only 15% of lung cancers are diagnosed at a localized stage due to lack of early detection methods. Unlike breast, colon and prostate cancers, there are no standard early detection methods although recent clinical trials have focused on using early CT/X-ray for early detection in highly susceptible populations. Cigarette smoking still remains the most important risk factor with smokers accounting for a majority of the new cases. A person smoking less than 100 cigarettes (lifetime) or exposed only to environmental tobacco smoke (ETS) is considered a non-smoker. Smokers have a 10-20 fold higher risk of developing lung cancer compared to non-smokers and never smokers still account for the 7th leading cause of cancer realted deaths in the U.S. (Brownson et al., 1998; Sun et al., 2007).

1.7 Lung Cancer Pathology

Lung cancer can be divided into two broad categories, small cell lung cancer (SCLC) and non-small cell lung cancer (NSCLC) based on their histo-pathology (Brambilla et al., 2001; Sun et al., 2007). SCLCs are identified by neuroendocrine characteristics and all tumors that are not classified as SCLCs fall in the category of NSCLCs. NSCLC can further be divided into three major sub-types; squamous cell carcinoma (SCC), adenocarcinoma and large cell carcinoma. Many tumors are not well differentiated or are defined by mixed histological types (eg. adenosquamous carcinoma) and also fall in the category of NSCLC (Gazdar, 2010). These

differences and subtype classification of lung cancer tumors have allowed for targeted therapy towards certain tumor types and have helped improved patient outcomes.

NSCLCs account for 80-85% of new lung cancer cases while SCLCs account for 15-20% cases (Blot et al., 2011). Although smoking risk is highly associated with all lung cancer histological types, smoking association is strongest with SCLCs. Over the last decade, there has been a decline in SCLCs in smokers and an increase in adenocarcinomas, which have been attributed to lower tar and nicotine content in cigarettes (Saccone et al., 2007). By comparison, adenocarcinoma is the most common form of lung cancer in never-smokers. About 25% of new lung cancer cases worldwide are not attributed to smoking and presents a gender bias towards Asian female population (Sun et al., 2007). SCLCs tend to occur in the central lung airway and are known to originate from pulmonary neuroendocrine cells PNECs lining the airway epithelium. Adenocarcinomas prevalent in the peripheral airways are known to arise from secretory Type II pneumocytes and express a transcription factor termed TTF1 (thyroid transcription factor1). SCCs arise from multilayered squamous cells and even though the human airway epithelium does not comprise of squamous cells, metaplastic changes to secretory cells may give rise to these tumors. Expression of p63 (a basal cell marker) is prevalent in SCC subtypes in human lung cancers (Sun et al., 2007).

1.8 Molecular Changes in Lung Cancer

Three most commonly mutated pathways that contribute to lung pathogenesis are epidermal growth factor receptor (EGFR), KRAS and tumor suppressor p53 pathway. Oncogene activation occurs in all lung cancers and is typically associated with gene amplification, over-expression, point mutations or DNA rearrangements. These changes result in persistent upregulation of growth signals that induce cell growth as well as 'oncogene addiction' where cells become dependent on an aberrant signaling pathways to survive (Larsen and Minna, 2011; Lynch et al., 2004; Merlino et al., 1984). The EGFR protein belongs to ErbB family of tyrosine kinase receptors and is overexpressed or aberrant in 50 to 90% NSCLCs (Hirsch et al., 2003). Upon binding of the ligand, EGFR forms homodimers and heterodimers with other family members initiating a cascade of downstream signaling that trigger anti-apoptotic signaling, proliferation, angiogenesis, invasion and metastasis (Ishihara and Hirano, 2002). These numerous downstream effects are activated by three major pathways; the AKT pathway, mitogenic-activated protein kinase pathway (MAPK) and STAT (signaling transducer and activator of transcription).. AKT signaling (the mammalian homologue of retroviral oncogene v-akt encoding a serine/threonine protein kinase) leads to increased cell survival by inhibition of apoptosis and MAPK signaling leads to increased cell proliferation. EGFR mutations are most prevalent in adenocarcinoma with a strong correlation with non-smoker female patients (Kosaka et al., 2004; Pham et al., 2006).

Activation of RAS/RAF (proto-oncogene) pathway occurs frequently in lung cancer and is most commonly via the activation of KRAS in about 20% of cancers. KRAS (homolog of the

Kirsten rat sarcoma viral oncogene) activation almost exclusively occurs in adenocarcinomas of smokers and is rare in SCLCs (Downward, 2003; Karnoub and Weinberg, 2008). Mutation in other subfamily members *HRAS* and *NRAS* are also not very frequent compared to *KRAS.* Mutation in *KRAS* results in loss of intrinsic GTPase activity that is required to return KRAS protein to its inactive form. Loss of this negative feedback control results in constitutively active downstream KRAS signaling (Downward, 2003). Both *KRAS* and *EGFR* signaling pathways are redundant in lung tumorgenesis and occur exclusively.

The tumor suppressor p53 has multiple functions and acts as a transcription factor for a large number of target genes. In response to cellular stress, p53 induces cyclin dependent kinase (CDK) inhibitors, which regulate cell cycle checkpoints. These checkpoints allow the cells to undergo G1 arrest and regulate DNA damage and apoptosis (Breuer et al., 2005). Mutations in the *p53* gene are common throughout all cancers and typically affect the DNA binding region of the protein. Mutations in *p53* occurs both in cancers arising from smokers and never smokers (about 80% of lung cancers) although, less frequent in never smokers (Le Calvez et al., 2005; Vahakangas et al., 2001).

1.9 Treatment Options for Lung Cancer

Treatment plans for lung cancer patients are determined by progression of the disease. Disease stage is determined by the size, histology and confinement of the tumor. Patients presenting with stage I and II lung cancer generally undergo surgical resection or radiation therapy if they are not candidates for surgery (Gadgeel et al., 2012). Stage I and II disease is

referred to as tumors confined at the primary site with no invasion within the surrounding tissue or lymph nodes. Distant relapse is the prime cause for deaths in patients after surgical resection since micrometastases cannot be removed at the time of surgery. Therefore stage I and II patients often undergo adjuvant chemotherapy after surgery (Gadgeel et al., 2012). Patients presenting disease in stage III or IV receive standard chemotherapy care followed by radiation therapy or palliative care (Gadgeel et al., 2012). In stage III and IV disease, the initial tumor mass has escaped the primary site and metastasized into the local lymph nodes or distant secondary sites. For NSCLC treatments, the commonly used chemotherapy agents include platinum based cispatin and carboplatin combined with paclitaxel, docetaxel pemetrexed, vinorelbine or gemcitabine (Gadgeel et al., 2012).

Targeted treatments of lung cancer based on oncogene addiction have been successful over the past decade although these targeted therapies are only available for a few commonly known mutations. Target therapy treatment is still based on the confines of staging of the tumor. Patients are given selected chemotherapeutic agents based on the genotype of their tumor for instance, gefitnib, erlotinib are tyrosine kinase inhibitors (TKI) used in patients with EGFR mutations. Patients with these known mutations respond well to the target/personalized treatment however, after the patient relapses these therapies become less effective. The relapsed tumor bypasses the signaling pathway being targeted by the drug (Kris et al., 2003; Shepherd et al., 2005). Despite advances in the field of targeted therapy, the 5-year survival rate has not dramatically improved for patients with lung cancer.

1.10 Radiation and Lung Cancer

Although the adult lung has adequate strategies to regenerate and repair from damage caused by external hazardous agents, constant insults overtime inevitably leads to permanent damage with long term consequences. Despite considerable benefits obtained from radiation use such as cancer therapy, energy production and other industrial uses, it is clear that there are significant health risks to humans exposed to radiation. Even though there is strong evidence that radiation exposure increases susceptibility to lung cancer, our understating of mechanisms and signaling pathways involved in this process remains poorly understood. With the increased use of radiation it is important to understand the effects of radiation on lung repair, regeneration and disease progression. Primary analysis of lung cancer risk associated with radiation exposure comes from atomic bomb survivors, underground miners exposed to radon gas and patients receiving radiotherapy (Hall and Giaccia, 2006). While the incidence of cancer increases in most tissues with exposure to moderate and high doses of radiation, the lung including several other tissues have been demonstrated to be also susceptible to low dose radiation (Little, 2009; Newhauser and Durante, 2011; Ron, 2003). A Life Span Study (LSS) cohort of over 150,000 Hiroshima and Nagasaki atomic bomb survivors indicated that the excess relative risk (ERR) of cancer/Gy of radiation for all solid tumors is 0.47. ERR quantifies to what extent the risk for an individual with a given level of exposure exceeds in contrast to that of a non-exposed individual. Lung cancer is the second most common solid cancer in the LSS cohort at 10% behind stomach cancer with a ERR of 0.81 Gy (Little, 2009; Preston et al., 2007). These studies indicate the high susceptibility of lung cancer after radiation exposure.

Radiation is the emission and propagation of energy through matter or space by means of electromagnetic disturbances (e.g. X-ray) or particles (photons). The absorption of radiation with sufficient energy in biological material may lead to the ejection of one or more electrons from the atom. This process is known as ionization and the radiation responsible is called ionizing radiation. Ionizing radiation can be sub-divided into two categories, electromagnetic radiation and particle radiation. Electromagnetic radiation consists of waves with higher energies such as X-rays and gamma-rays (γ) in the electromagnetic spectrum. Particulate radiation consists of electron, proton, neutrons, alpha particles and high atomic number (Z), high energy (E) (high charge and energy [HZE]) particles (Hall and Giaccia, 2006). To determine increased carcinogenic risk from exposure to radiation, it is important to elucidate how different types of radiation interact with biological matter.

The biological effects of ionizing radiation result principally from damage to the DNA within the exposed material. The action of ionizing radiation interacting with matter can be divided into two classes; direct and indirect (Michaels and Hunt, 1978). The primary difference between the two subclasses depends upon whether radiation directly ionizes the target atom or uses intermediary molecules to ionize the target. In cells, the indirect method involves radiolysis of water. Water is the major constituent (~80%) of the cell and interaction with ionization radiation results in creation of oxygen free radical species which in turn interact with DNA (Leach et al., 2001; Li et al., 2014). The scheme of action utilized by the radiation depends upon the amount of energy deposited per unit length of track defined as linear energy transfer (LET) (Hall and Giaccia, 2006). Electromagnetic radiation such as (γ) and X-ray have low LET values and ionize their targets largely using the indirect method **(Figure 1.5)**. It is estimated that about

two-thirds of X-ray damage to DNA in mammalian cells is caused by hydroxyl radicals and not by direct interaction (Hall and Giaccia, 2006). In contrast, HZE particles typically have high-LET values ionize their target atoms predominantly by direct action.

The spatial distribution of ionizing events produced by different types of radiation and how the energy is deposited varies considerably and thus results in different biological effects. Electromagnetic radiation such as X-ray produces ionizing event which are well spaced out and randomly distributed therefore X-rays and other low-LET radiations are known as sparsely ionizing (Hall and Giaccia, 2006)(Neyman and Puri, 1976). Particle radiation however, is highly localized and densely ionizing when it impacts matter. High amount of energy is densely deposited per unit track resulting in a dense cluster of ionization events. These differences in distribution of ionization events hold important consequences in terms of biological effectiveness. The complexity of radiation damage also increases with LET and these LET based effects are critical in determining biological effects (Ward, 1994).

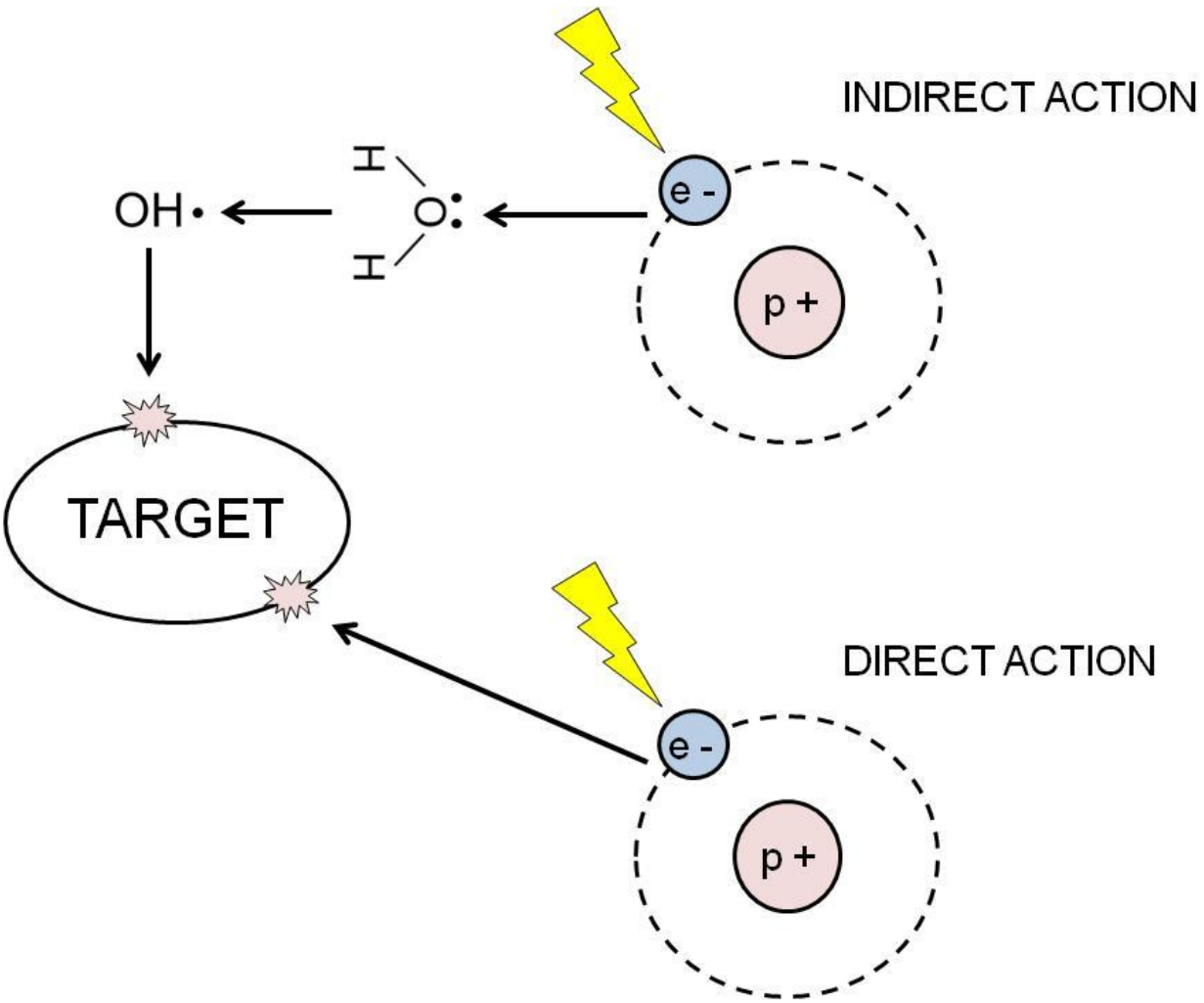

Figure 1.5: Direct and indirect actions of ionizing radiation.
In direct action, a secondary electron emitted as a result of absorption of radiation energy directly interacts with the target. Indirect action involves the secondary electron interacting with other molecules (e.g. water molecules) resulting in the formation of free radical species. These free radicals then proceed to ionize the target molecule.

The distribution of energy deposited in biological tissue matter also varies with tissue depth. For low LET ionizing electromagnetic radiation, the energy deposited exponentially decrease as a function of depth in the target tissue (Li et al., 2014). By contrast high-LET charged particle radiation has a well-defined depth of range in matter depending on particle size and energy. The energy deposited by particles is relatively low, even at the entrance of the target material with a pronounced sharp maximum near the end of its range. This maximum spike in energy deposited is known as the Bragg peak (Katz and Cucinotta, 1999; Raju et al., 1978). At the Bragg peak, extremely high LET values can be reached especially with HZE particle radiation. This characteristic of charged particle radiation energy deposition is also exploited in proton therapy for cancer where the peak is focused inside the tumor mass. These differences in the way energy is deposited across tissue depth between low and high LET radiation may have important biological consequences.

Another characteristic of charged particle radiation is the generation of secondary ionizing events along the track of the primary particle. As the particle traverses through the target, a large amount of energy is deposited along the track resulting in ionization and emission of electrons, recoiling away from the primary track. These electrons have enough energy to form ionizing tracks of their own and are called delta (δ) rays (Cucinotta et al., 1996; Dingfelder, 2012). The primary particles track consists of a dense core of ionization events as well as a concentric region known as the ‘penumbra’ formed by the δ-rays surrounding the core **(Figure 1.6)** (Li et al., 2014). The δ-rays are capable of causing ionization and producing biochemical changes in cells that are adjacent to the primary track. The range of δ-rays depends on the velocity and mass of the particle (Cucinotta et al., 1998; Finkel and Holbrook, 2000). The δ-rays

can have important consequences in terms of assessing risk of radiation induced cancer due to the increased propensity of non-targeted effects. High-LET charged particle radiations more prominently produce secondary radiation in comparison to Low-LET electromagnetic radiation.

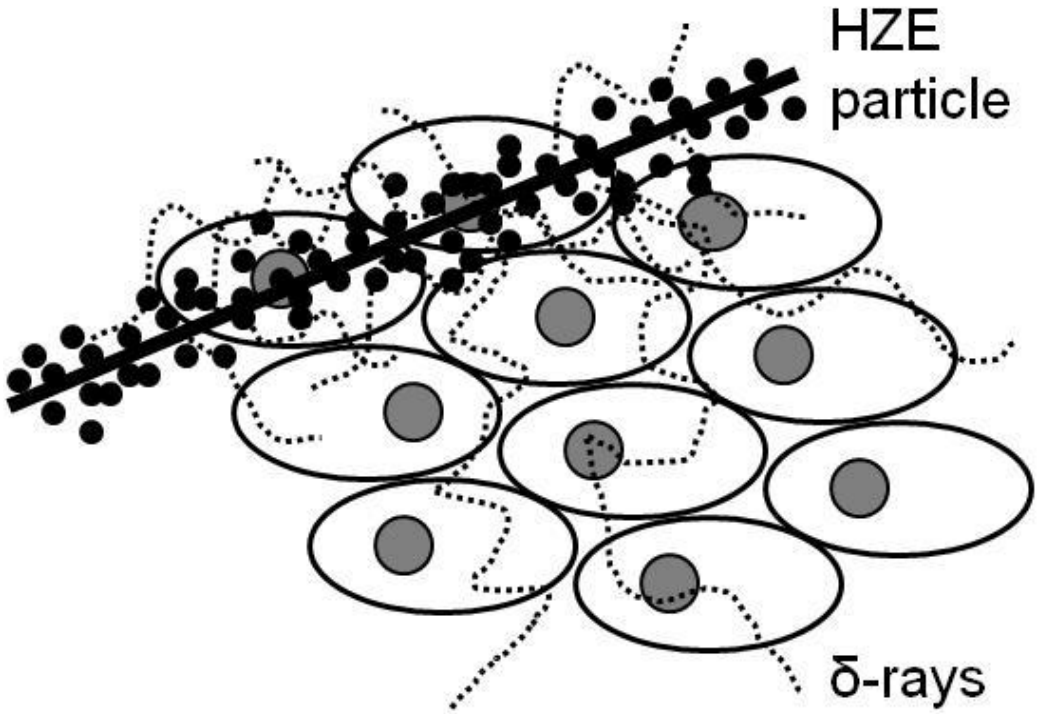

Figure 1.6: δ-rays emitted from the primary track of particle radiation can target cells not traversed by the primary radiation
Cells not affected by primary radiation can be ionized by secondary electrons defined as δ-rays. Secondary ionizing events with δ-rays are more prominent with high-LET charged particle radiation.

Damage to the DNA is the principal target for biological effects, including cell killing, carcinogenesis and mutations. Several different types of DNA damage can occur as a result of exposure to ionizing radiation. Single strand breaks (SSBs) are the most common and easily repaired break in the DNA (Hall and Giaccia, 2006). SSBs are repaired by using the opposite strand as the template and therefore have minimal biological consequences. By contrast, if the break occurs in two DNA strands opposite to one another, or separated by a few bases, the break is known as double strand break (DSB). This cleavage of the chromatin into two pieces is considered the most important lesion in terms of biological effects. DSBs are less prominent with low-LET exposure and if present are repaired quickly in comparison to high-LET exposure(Rydberg et al., 2005). Repair of DSBs is also more complicated and error prone and these inaccuracies may have important biological consequences in the targeted cell (Asaithamby and Chen, 2011). Severity of the biological outcome as a result of radiation exposure can be classified based on whether it is directly correlated with radiation dose. If the severity of the biological outcome worsens with increased dose, the effect is known as deterministic effect. Diseases such as tissue fibrosis and cataracts fall under this category (Hall and Giaccia, 2006). If the severity of the outcome is independent of the dose, the effect is known as stochastic effect. Carcinogenesis is a stochastic effect where an exposure to increased dose of radiation does not dictate the severity of cancer. A cancer induced by a dose of 1 Gy is no worse than induced by 0.1 Gy in terms of grade although, there is higher probability of induction of cancer with a 1 Gy dose (Hall and Giaccia, 2006).

Overall, there is clear evidence of association between radiation exposure and increased risk of carcinogenesis. With the increasing use of particle radiation in radiation oncology, further

investigations are needed into how biological outcomes may differ in contrast to low-LET radiation. Since cancer is a systemic disease, further investigation is also needed to understand bystander and non-target effects of radiation exposure which currently are not well understood. The cell microenvironment and immune system of the body play crucial role in cancer progression and it is important to determine how radiation exposure may affect these systems.

Chapter Two:

Characterization of Immortalized Human Bronchial Epithelial Cells in Three-Dimensional Culture

2.1 Introduction

Due to lack of good *in vitro* models, our understanding of development and stem cell biology of the human lung remains limited. Important aspects of human lung development, repair and regeneration have been studied through the use of mouse models (Morrisey and Hogan, 2010). Although these murine models have provided valuable insights into lung homeostasis and regeneration, there are intrinsic differences between the human and mouse airway epithelia (Rock and Hogan, 2011; Rock et al., 2010). Basal cells are limited to the trachea in mice while they are present throughout the human airways (Boers et al., 1998; Evans et al., 2001). Clara cells (also referred to as club cells) are found throughout the murine airways but are enriched only in the distal bronchioles of the human lung (Boers et al., 1999; Rawlins et al., 2009). Conversely, variant Clara cells have been demonstrated in the murine lung to self-renew

and give rise to differentiated progeny in an event of injury, but there is no evidence of these cells in the human lung (Hong et al., 2001; Rackley and Stripp, 2012).These differences support the importance of developing *in vitro* model systems using human airway epithelial cells.

In an effort to recapitulate the native airway architecture and differentiation, different *in vitro* model systems using human bronchial epithelial cells (HBECs) have previously been established (Bals et al., 2004; Fessart et al., 2013; Franzdottir et al., 2010; Pageau et al., 2011). When primary HBECs are cultured on a contracted fibroblast matrix and raised to air-liquid interface (ALI), the HBECs are able to differentiate into ciliated and goblet cells (Vaughan et al., 2006). Although the ALI culture system demonstrates the ability of HBECs to differentiate into lung epithelial cells lining the central lung, it does not address differentiation in the distal airways. Recent studies have also described culturing HBECs in reconstituted basement membrane (Matrigel®) to reproduce a more physiologically relevant microenvironment for cell differentiation (McQualter et al., 2010; Rock et al., 2009). HBECs cultured in three-dimensional (3D) Matrigel® models differentiate into distinct lung epithelial lineages however, these studies did not address the importance of stromal epithelial interactions (Wu et al., 2011). Signaling from the mesenchyme plays a critical role in lung development. Cues from stromal cell types such as fibroblasts, endothelial cells and smooth muscle cells are important in determining epithelial cell fate (Kimura and Deutsch, 2007). These interactions also contribute to respiratory disease such as lung cancer where the stroma plays a critical role in cancer progression and metastasis (Mueller and Fusenig, 2004). Current *in vitro* models also fail to recapitulate phenotypic features such as branching morphogenesis of the distal lung airway during

development. These phenotypes have mostly been mimicked using primary tissues from embryonic human and mouse lungs (Miura and Shiota, 2000; Weaver et al., 2000).

Previously, it has also been suggested that ectopically introduced telomerase and cyclin-dependent kinase 4 immortalized HBECs display characteristics of multipotent stem cells of the lung (Delgado et al., 2011). These HBECs express markers indicative of several epithelial cell types from both central and distal airway lineages in two-dimensional culture (2D) **(Figure 2.1)**. When cultured in different types of 3D systems, subtle changes in the microenvironment result in the ability of HBECs to differentiate into multiple central and distal lung epithelial cell types. In ALI conditions, these HBECs can differentiate into ciliated and goblet cells (Vaughan et al., 2006). When embedded in Matrigel®, HBECs form cyst like structures resembling and expressing markers indicative of cells from the distal lung airways (Delgado et al., 2011) **(Figure 2.2)**. These observations are consistent with the hypothesis that the adult human lung may contain a multipotent stem-like cell capable of differentiating into multiple cell lineages in different microenvironments.

In the present study, we describe a novel HBEC 3D culture system that displays the phenotype reminiscent of lung branching morphogenesis during development. Branching of the lung buds terminating into alveoli, the site of gas exchange during lung development, signifies differentiation of lung epithelium into distal airway cell types such as Clara and Type II pneumocytes (Warburton et al., 2010). We demonstrate that when HBECs are seeded on top of Matrigel®, overlaying fetal lung fibroblasts (IMR90 cells), the HBECs form an aggregate structure that buds and branches (resembling the canalicular/saccular period of lung

development). HBECs in this culture system maintain markers of multiple cell types in the airway epithelium indicating their multipotent stem-like characteristics. We also describe how this new 3D system can be utilized to not only understand lung development, but also lung diseases such as lung cancer.

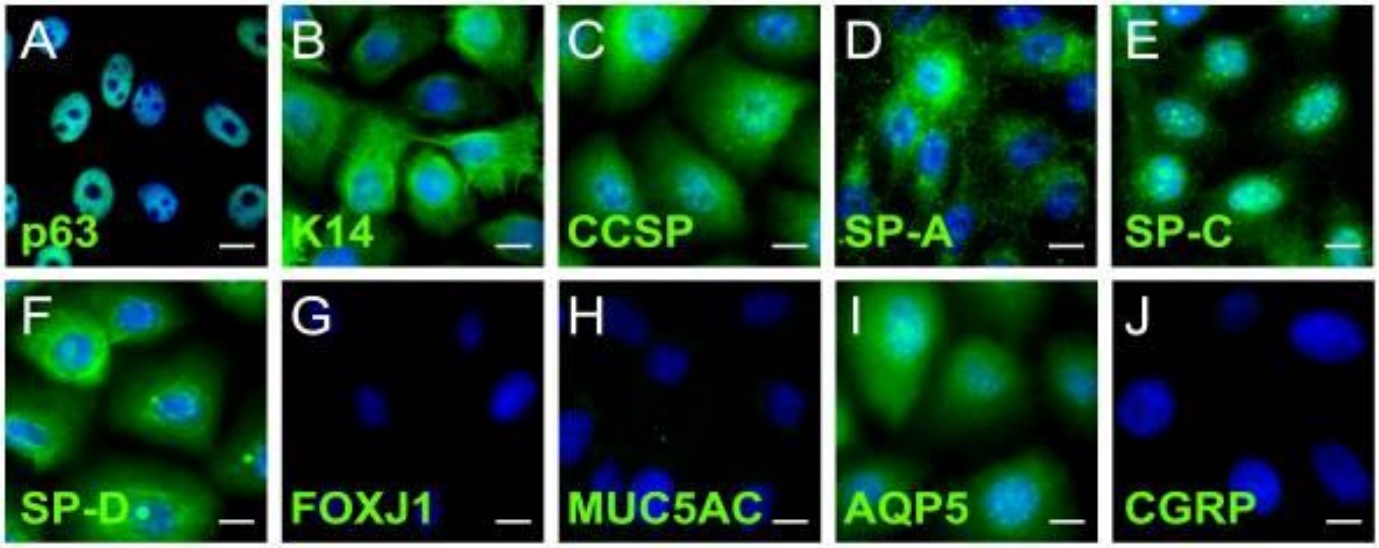

Figure 2.1: Immortalized HBEC 3s express markers of cell types present both in central and peripheral human airways.

Immunofluorescence analysis of HBEC 3KTs in two dimensional culture demonstrates their capacity to differentiate into central and peripheral lung cell lineages. (A) p63. (B) K14. (C) CCSP. (D) SP-A. (E) SP-C. (F) SP-D. (G) FOXJ1. (H) MUC5AC. (I) AQP5. (J) CGRP. DAPI stain in blue. Scale bars 10 µm.

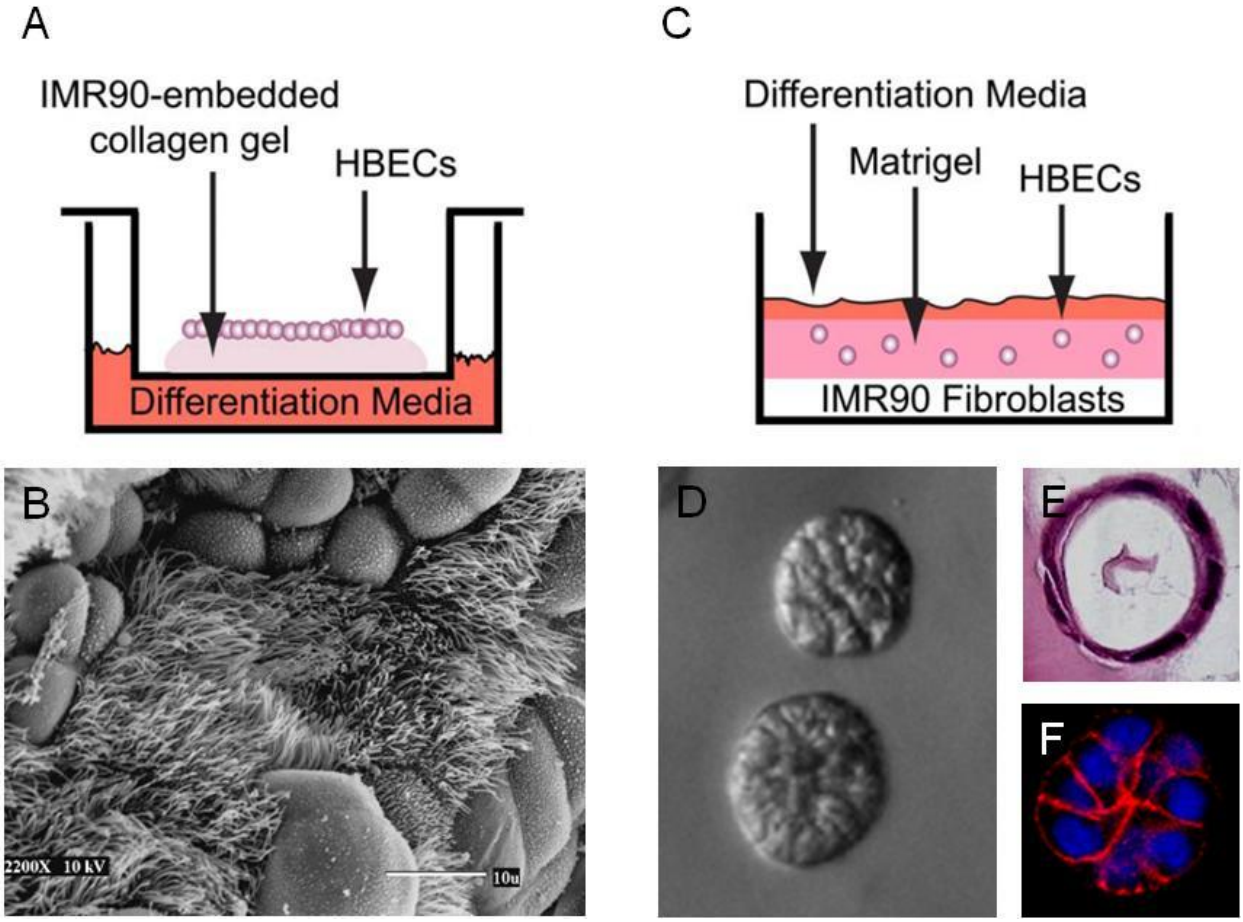

Figure 2.2: HBEC 3s demonstrate distinct phenotypes under different culture conditions.

HBEC 3s cultured on top of an IMR90-embedded collagen type 1 plug (A) result in differentiation into ciliated and goblet cells. (B) Scanning electron micrograph analysis of HBEC 3s seeded on top of the collagen plug after 13-weeks in culture; scale bar 10 µm. When embedded within Matrigel™ in the presence of IMR90 fibroblasts (C) HBEC 3s form cyst like structures. Phase contrast image, H&E section, and immunofluorescence staining for E-cadherin (red) in HBEC3 KT cyst-like structures after 5 days of culture (D, E, and F) (scale bar 20 µm; DAPI (blue)) .

2.2 Materials and Methods

2.2.1 Cell Culture

Immortalized HBEC3, HBEC13, and the experimentally transformed HBEC3 cells were cultured in Keratinocyte Serum Free media (KSFM) (Gibco) at 37°C and 5 % CO_2. The KSFM media contained 50 µg/mL of bovine pituitary extract and 5 µg/mL of epidermal growth factor. These cells were also cultured on porcine gelatin coated tissue culture dishes (Sigma Aldrich) as described previously (Ramirez et al., 2004). For 3D culture studies, HBECs were cultured in air liquid interface media (Vaughan et al., 2006). Air liquid interface media comprised of a 50:50 mixture of DMEM high glucose media (Thermo Scientific) and BEBM media (Lonza) with various differentiation factors added to the media **(Table 2.1)**. IMR90s and other primary fibroblasts derived from normal lung tissues were cultured in DMEM media (Thermo Scientific) supplemented with 10% Cosmic Calf Serum (Thermo Scientific) at 37°C in 5% CO_2 and 2% O_2.

	Final Concentration
Gentamicin	0
Amphotericin	0
Epidermal Growth Factor	0.50 ng/mL
CaCl2	1.0 mM
Insulin	0.87 μM
Hydrocortisone	0.21 μM
Transferrin	0.125 μM
Epinephrine	2.7 μM
Bovine Pituitary Extract	10 μg/mL
Retinoic Acid	5×10^{-8} M
Phosphorylethanolamine	0.5 μM
Ethanolamine	0.5 μM

Table 2.1: Various factors present in air-liquid interface medium and their respective concentrations

2.2.2 3D Matrigel® Culture

HBEC 3D cultures were performed as previously described with minor modifications (Lee et al., 2007). IMR90 fibroblasts were seeded as a feeder layer at a density of 1.25×10^5 cells/cm^2 48 hours prior to seeding HBECs. Pre-thawed growth factor reduced and phenol-red free Matrigel® (BD Biosciences) was layered on top of the fibroblasts (75 μL/cm^2) and then allowed to gel at 37°C for 15 minutes. The Matrigel® plated was at 100% concentration and was not diluted with medium. 1.0×10^5/cm^2 HBECs were suspended in ALI media and seeded on top of the Matrigel®. Approximately 24 hours after plating the HBECs, ALI medium was removed and replaced with ALI medium containing 10% Matrigel. There is no difference between the

phenotype of HBECs cultured on top of Matrigel® with or without the 10% overlay **(Figure 2.3)**. Adding 10% Matrigel aids in extending the integrity of the 3D culture. The 3D cultures were prepared in triplicates and repeated multiple times. Cultures were grown at 37°C and 5 % CO_2 for up to 15 days with media being changed every other day.

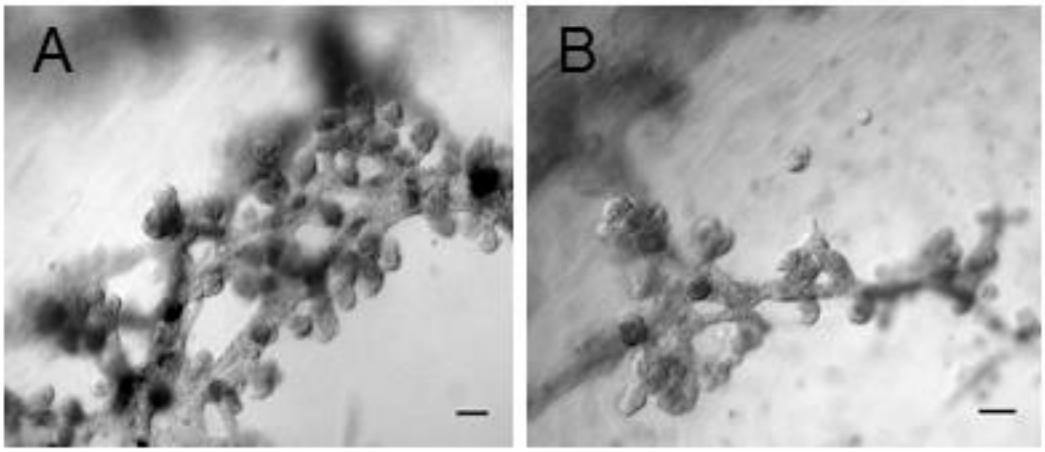

Figure 2.3: Adding Matrigel® to the ALI medium does not change the phenotype of HBEC3 KTs in 3D culture.

The branching phenotype of HBEC3 KTs is identical with (A) or without (B) 10% Matrigel® overlaid on top of the culture in ALI medium. Scale bar 100µm

2.2.3 Immunofluorescence Staining

For 3D immunofluorescence analysis of the HBEC Matrigel® cultures, the aggregated lung budding structures were washed twice with cold phosphate buffer saline (PBS) and fixed for 30 minutes at RT with 4% paraformaldehyde. Following fixation, the structures were washed twice with PBS and 2% agarose was poured directly into the well containing the 3D HBEC structures to create a plug. The agarose was allowed to cool down at RT and the plugs containing the 3D HBEC structures were placed in histology cassettes. The samples were then processed, embedded and 5μm thick sections were cut for immunofluorescence analysis. The sections were deparaffinized through three different xylenes, rehydrated in a series of ethanol and washed in de-ionized water for 5 minutes. Heat induced antigen-retrieval was performed in a microwave for 10 minutes in 10 mM sodium citrate buffer. Following antigen retrieval, sections were blocked at RT with 10% goat serum albumin (Zymed) in PBS containing 1% bovine serum albumin (Sigma Aldrich) and 0.025% Triton X-100 (Sigma Aldrich) for 2 hours. Sections were rinsed with PBS and incubated with primary antibodies overnight at 4°C in a humidified chamber. The following primary antibodies were used for 3D immunofluorescence analysis: mouse monoclonal anti-p63 (Millipore; clone 4A4), mouse monoclonal anti-Keratin 14 (Thermo Scientific; Cat. #MS-115-P), rabbit polyclonal anti-CCSP (Santa Cruz; sc-25554), rabbit polyclonal anti-SP-A (gift from Dr. Carole Mendelson, University of Texas Southwestern Medical Center, Dallas, TX)(Odom et al., 1987), mouse monoclonal anti-MUC5AC (Abcam; ab24070), and mouse monoclonal anti-TTF1 (Santa Cruz; 8G7G3/1). The antibodies used have been tested for immunofluorescence analysis of paraffin-embedded samples.

Sections were washed three times in PBS after overnight primary antibody incubation and stained with secondary antibodies. A secondary antibody deletion control to check the specificity was performed with each primary antibody. The sections were incubated at a dilution of 1:500 for an hour at RT in a dark humidified chamber (Alexa Fluor 488 goat anti-rabbit (Invitrogen; A-11008) or Alexa Fluor 488 goat anti-mouse (Invitrogen; A-11001)). Sections were then washed three times with PBS and mounted with Vecta Shield mounting medium with DAPI (Vector Labs) cover-slipped, and imaged. (Axiovert 200 M fluorescence microscope). Each staining was performed on multiple sections in triplicates.

2.2.4 Electron Microscopy:

3D structures were fixed in 2.5 % glutaraldehyde (in 0.1 M cacodylate) solution overnight at 4°C. The samples were then placed in a 2% agarose plug and processed according to standard electron microscopy procedures. The final samples were then imaged using a Tecnai G2 Spirit 120KV TEM.

2.3 Results

2.3.1 IMR90 Fibroblasts Stimulate Branching Morphogenesis of HBEC3s when Cultured on Reconstituted Basement Membrane Matrix

HBEC3s used in the current study were obtained from a central lung bronchus and immortalized using ectopic expression of human telomerase reverse transcriptase (hTERT; T) and cyclin-dependent kinase 4 (CDK4; K) as described previously (Ramirez et al., 2004). Immortalized HBEC3 KTs retain a normal/non-malignant phenotype in cell culture thus allowing the use of an isogenic human bronchial cell population to characterize aspects of lung development and differentiation *in vitro* (Ramirez et al., 2004; Sato et al., 2006). When cultured on gelatin-coated dishes, HBEC3 KTs proliferate into a two-dimensional confluent monolayer that has a cobblestone appearance **(Figure 2.4 A)**. However, when HBEC3 KTs are cultured on top of reconstituted basement (Matrigel®) in the presence of IMR90 fetal lung fibroblasts seeded as feeder layer underneath **(Figure 2.4 B)**, HBEC3 KTs form aggregate structures that develop into complex branching structures by ten days **(Figure 2.4 C)**. In the absence of an IMR90 monolayer, HBEC3 KTs fail to form any self-aggregating structures and do not further develop into any budding and branching structures **(Figure 2.4 D)**. The monolayer of IMR90 cells under the Matrigel® culture remains viable for the duration of the culture and does not form any structures **(Figure 2.4 E)**. HBEC3 KTs cultured with other lung fibroblast cell lines seeded as monolayer under Matrigel® also form branching structures **(Figure 2.4 F)**, indicating that the phenotype of HBEC3 KTs is not limited to one type of feeder layer.

To further investigate the formation of branching structures by HBEC3 KT cells on Matrigel®, the cultures were observed over multiple days. When HBEC3 KTs are seeded on top of Matrigel®, the cells self-aggregated into tubule-like structures after one day **(Figure 2.5 A)**. This phenotype is very similar to what is observed in endothelial cell organotypic cultures (Madri and Williams, 1983). Small bud-like structures emerge alongside of the tubules by the third day; as indicated by the arrows **(Figure 2.5 B)**. The budding structures form complex branching structures by the sixth day **(Figure 2.5 C)** and continue to increase in size and complexity by day ten **(Figure 2.5 D)**. The complex branching structures are reminiscent of bronchoalveolar units in the lung during the canalicular and saccular stages of development. Since the aggregation and formation of branching structures by HBEC3 KTs is dependent on the presence of IMR90s seeded under the Matrigel®, we tested the effects of varying IMR90 monolayer densities during the Matrigel® culture **(Figure 2.6)**. Significant differences are observed in the phenotype of HBEC3 KTs in 3D culture depending on the density of IMR90s. Lower densities of these fibroblasts are not able to induce complex branching in HBEC3 KTs. The fibroblasts also remain as a monolayer on the bottom of the culture dish and do not make direct contact with the HBEC3 KTs above the Matrigel® layer **(Figure 2.7)**. These observations emphasize the importance of cues from the microenvironment that are necessary for lung development and differentiation (Kimura and Deutsch, 2007; Warburton et al., 2010).

The branching structures that formed on top of Matrigel® are organized at the buds as indicated by the expression of E-cadherin at the cell-cell junctions **(Figure 2.5 E)**. Hematoxylin and eosin staining of the structures after eight days in culture also demonstrate polarity and

organization within the budding structures **(Figure 2.5 F)**. Cells within the buds display a cuboidal to low columnar morphology. HBEC3 KT cells along the tubular structure seem to form a cavity with cells organized along the edge **(Figure 2.5 G)**. This may signify the formation of a lumen within the aggregated budding structure.

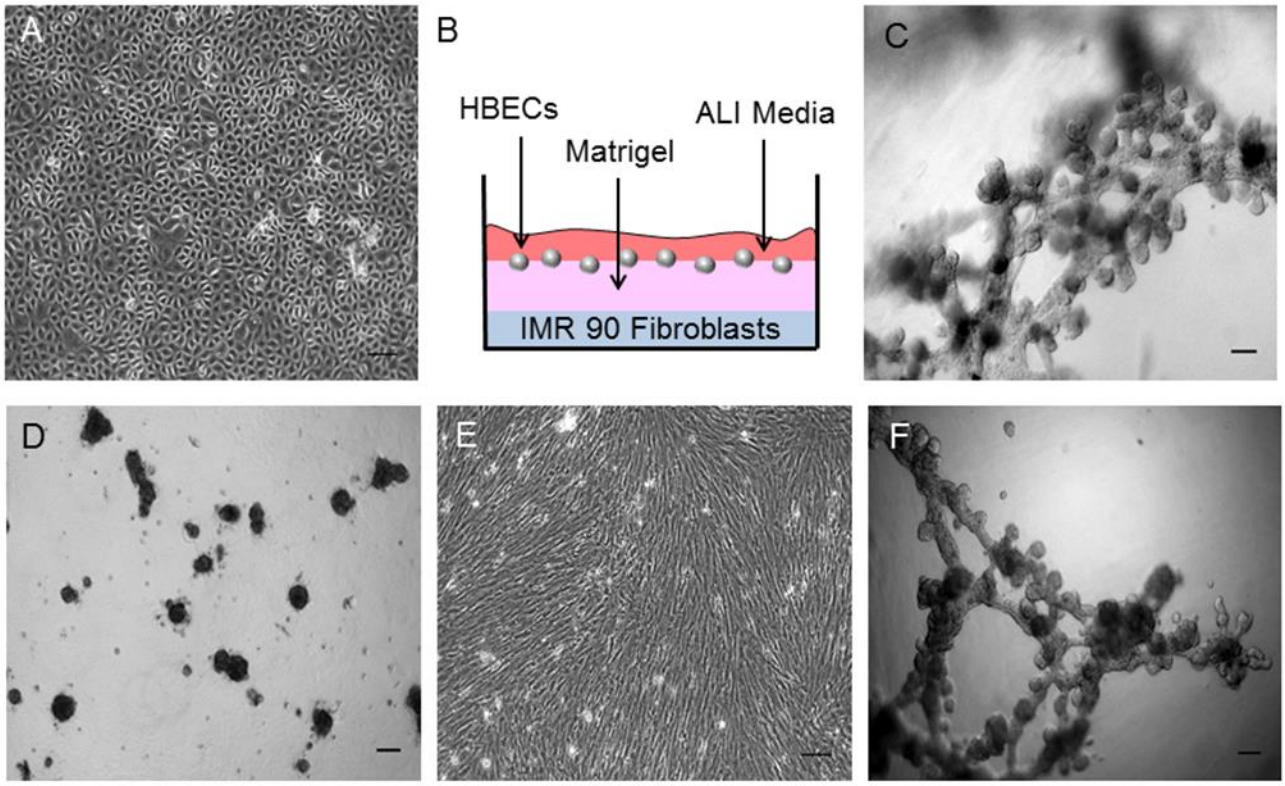

Figure 2.4: HBEC3 KT cells exhibit different morphologies under different culture conditions.

HBEC3 KT cells cultured in 2D and 3D conditions exhibit different morphologies. (A) Under 2D culture conditions on gelatin coated plates, HBEC3 KTs grow in a monolayer with a cobblestone appearance. (B) When seeded on top of Matrigel® in the presence of IMR90s seeded as a monolayer, (C) HBEC3 KT cells aggregate into tubular structures which bud and branch (Day 10). (D) In the absence of IMR90s, HBEC3 KTs fail to form complex branching structures when cultured on Matrigel®. (E) IMR90s seeded as a monolayer under the Matrigel® culture do not form any structures or invade the Matrigel®. (F) The phenotype of HBEC3 KTs on Matrigel® is not limited to IMR90s and can be recapitulated with other primary lung fibroblast cells. Scale bar 100 µm.

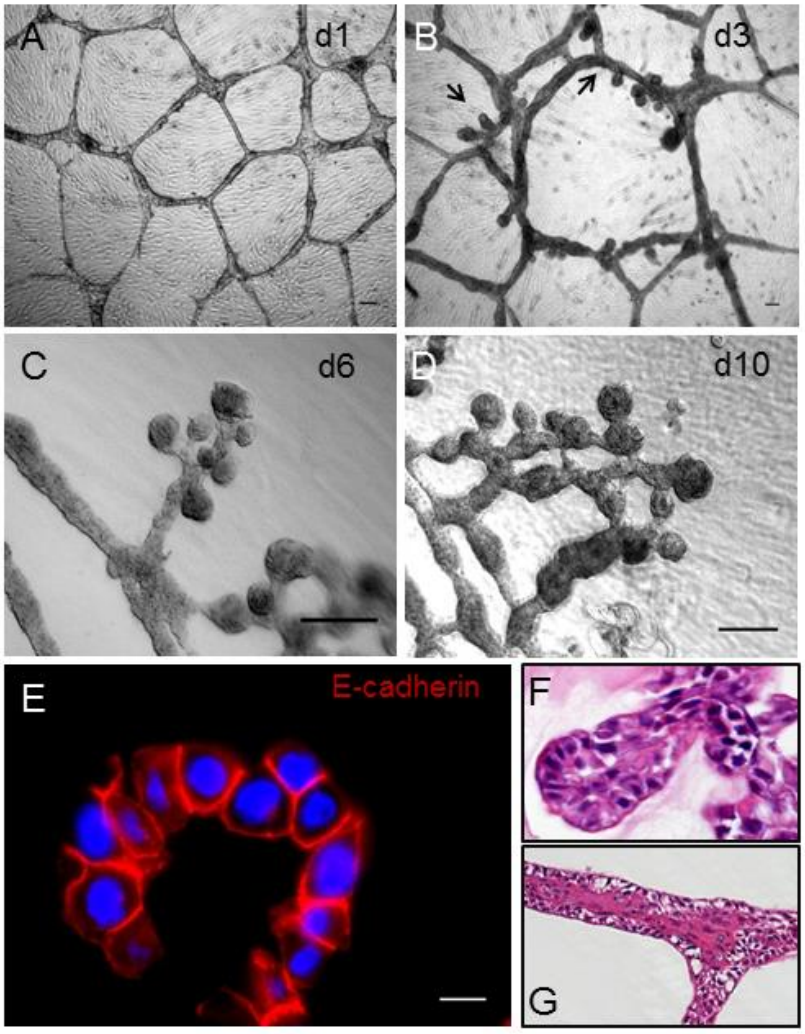

Figure 2.5: HBEC3 KT cells form complex branching structures when co-cultured with IMR90s on Matrigel®

When co-cultured with IMR90s on Matrigel®, (A) HBEC3 KTs aggregate and form tubule-like structures after 1 day. This phenotype is very similar to what is observed in 3D cultures of endothelial cells. (B) Small budding structures emerge from the initial tubule-like structure by day 3. (C) Initial budding structures start to branch by day 6. The aggregated structures continue to grow and (D) develop more complex branching by day 10. (E) E-cadherin immunostaining shows formation of cell-cell junctions and organization within the HBEC3 KT structures. (F) HBEC3 KT cells in the buds are organized and exhibit a columnar morphology by day 8 as indicated by the H&E stain. (G) Cells in the tubule part of the structure are also organized along the length of the structure by day 8. Scale bar 100µm (A-D, F, G), 10µm (E).

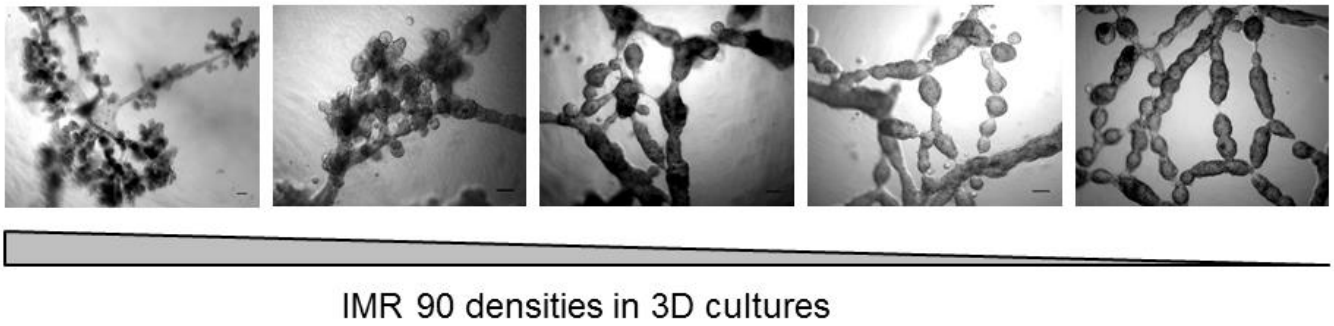

Figure 2.6: Varying Densities of IMR90s in 3D culture

The 3D phenotype of HBEC3 KTs on Matrigel® is dependent on signaling from fetal lung fibroblasts. At a high density (left panel) of IMR90 cells (2.5×10^5), HBEC3 KTs form complex branching structures. Reducing the number of IMR90s seeded under the culture changes the branching phenotype. At a lower density (right panel) of IMR90 cells (5.0×10^4), HBEC3 KTs form an aggregate structure but fail to branch and bud.

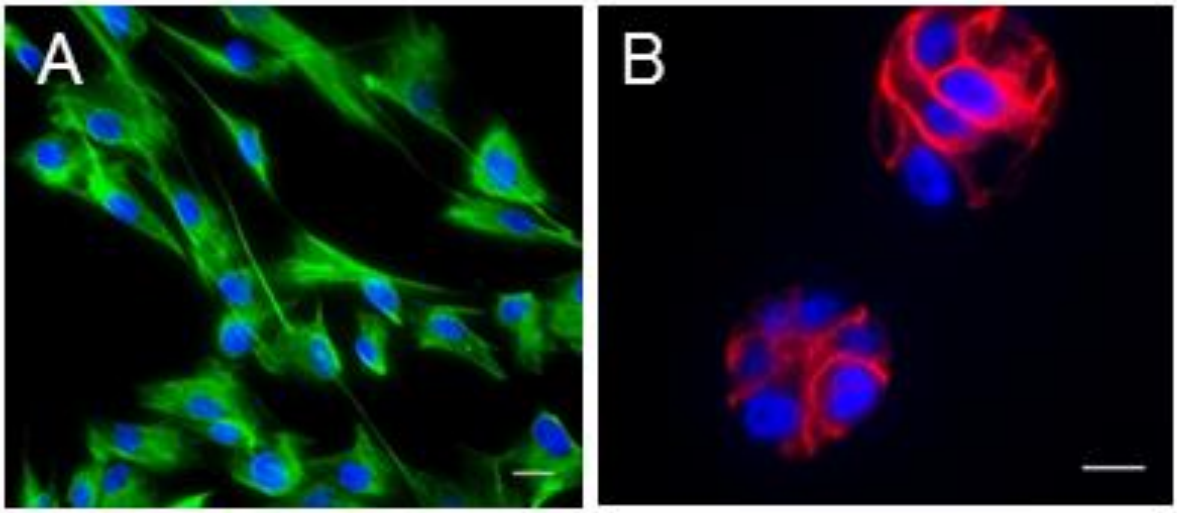

Figure 2.7: IMR90s do not invade the Matrigel® to make contact with the HBEC3 KTs in the 3D culture.

Vimentin (green) is expressed by IMR90s in 2D culture. No vimentin expression is observed in the HBEC3 KT structures (B) cultured on top of Matrigel ® indicating that IMR90s do not make contact with the HBECs. E-cadherin (red), DAPI (blue); Scale bar 10 µm

2.3.2 HBEC3 KTs Express Basal Cell Markers when Cultured in 3D

We analyzed the expression of several epithelial cell markers in the branching 3D structures on Matrigel®. Mature cell-types in the adult lung can be identified by the expression of unique differentiation markers or a combination of a few markers (Wuenschell et al., 1996). Previously, we have shown that HBEC3 KTs under 2D conditions express the basal cell marker p63 (Delgado et al., 2011). HBEC 3KTs retain expression of p63 in 3D culture by day 8 as observed by immunofluorescence analysis **(Figure 2.8 A)**. Both the buds and the tubules within the branching structures express p63 which is localized within the nuclei. HBEC3 KTs also express Keratin 14 (K14), another marker of basal cells in 3D culture **(Figure 2.8 B)** (Rock et al., 2010). K14 is expressed within the cytoplasm of the branching structures. Immunostaining for mature goblet cells with Muc5AC was negative (data not show). Basal cells in the human airways are present throughout but enriched in the central airways (Rackley and Stripp, 2012; Rock et al., 2010). Even though the branching phenotype of HBEC3 KTs resembles the morphology observed in the distal lung, all the cells retained basal cell expression. These observations suggest that further microenvironmental cues from the human lung stroma may be necessary to completely differentiate HBEC3 KTs into distal lung lineages.

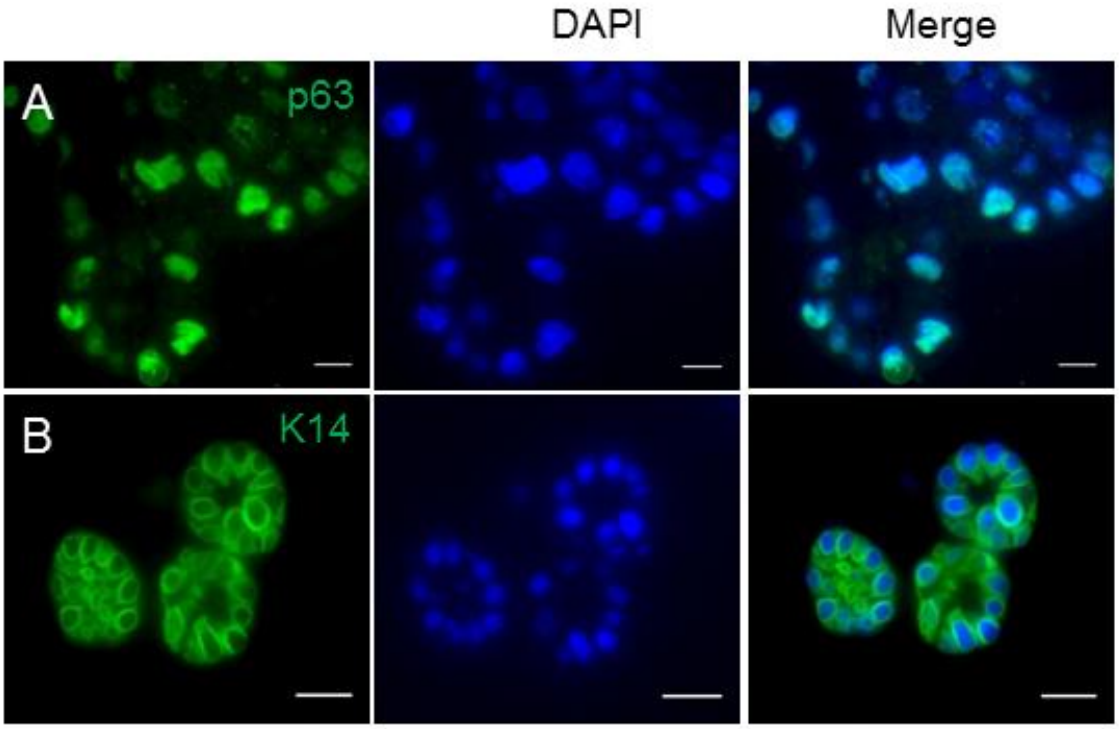

Figure 2.8: Branching HBEC3 KTs structures express basal cell markers

HBEC3 KT cells cultured on Matrigel® were immunostained for expression of basal cell markers (Day 8). (A) Nuclear staining with DAPI is shown in blue. p63 expression is seen in all the nuclei within the branching structures. (B) Keratin 14, another basal cell marker is expressed in the cytoplasm of all the cells within the branching structure. Scale bar 10µm

2.3.4 Differentiation Markers from Distal Lung Cell Types are Expressed by HBEC3 KTs in 3D Culture

Examining the expression of different cell type markers in 3D culture suggests HBEC3 KTs also retain the potential to differentiate into cell types originating in the distal lung. HBEC 3KTs express Clara cell secretory protein (CCSP) when cultured on Matrigel® **(Figure 2.9 A)**. CCSP is a marker of Clara cells with limited expression in Type II pneumocytes (Rawlins et al., 2009). CCSP was uniformly expressed in the cytoplasm of HBEC3 KT cells in 3D culture (Day 8). No difference in the expression is observed between cells that are present within the buds or tubules. CCSP expression has not been previously reported in cells from the central airways (e.g. basal cells) and is restricted to cell types in the distal airway (Rock et al., 2010). Expression of Surfactant Protein-A (SP-A) is observed in HBEC3 KTs (Day 8) cultured on Matrigel® **(Figure 2.9 B)** which is expressed in both Type II pneumocytes and Clara cells (Madsen et al., 2003). Although SP-A is expressed in HBEC3 KTs in 2D culture, expression of SP-A in 3D is more representative of its expression and secretion *in vivo.* SP-A expression is more prominent within the buds of the branching structures with more distinct expression towards the apical side of HBEC3 KTs. The expression of SP-A within the branching structure resembled its secretion into the alveolar space where it facilitates air exchange (Warburton et al., 2010). Transmission electron microscopy on HBEC3 KTs branching structures after 8 days of culture identified structures that resemble lamellar bodies within individual HBEC3 KT cells **(Figure 2.9 D-E)** SP-A is generally associated with lamellar bodies which are surrounded by lipid vesicles. Lamellar bodies secret surfactant to reduce surface area tension at the site of air-exchange within the alveolar sacs (Fehrenbach, 2001). HBEC 3KTs also express aquaporin 5 (AQP5), a marker of

alveolar type I cells that is potentially expressed in many other cell types of the lung including basal cells (Krane et al., 2001). HBEC 3KTs express AQP5 under both 2D (Delgado et al., 2011) and 3D culture conditions **(Figure 2.10)**.

Thyroid-transcription factor (TTF-1) is a multifunctional transcription factor expressed by the multipotent progenitor cells of the airway during development (Boggaram, 2009). TTF-1 is expressed in Clara cells and Type II pneumocytes in the adult lung. TTF-1 drives the transcription of CCSP and other surfactant protein expressed by Clara cells and Type II pneumocytes (Maeda et al., 2007). TTF-1 expression is observed in the HBEC3 KT branching structures on Matrigel® **(Figure 2.9 C)** by day 8. Although TTF-1 is a transcription factor, a majority of the protein is expressed within the cytoplasm. TTF-1 is variably detected in HBEC3 KTs under 2D conditions while it's constituently expressed in cells cultured on Matrigel®. These observations indicate that HBEC3 KTs when cultured on Matrigel® in the presence of IMR90 cells contain the capacity to differentiate into cell types originating in the distal lung.

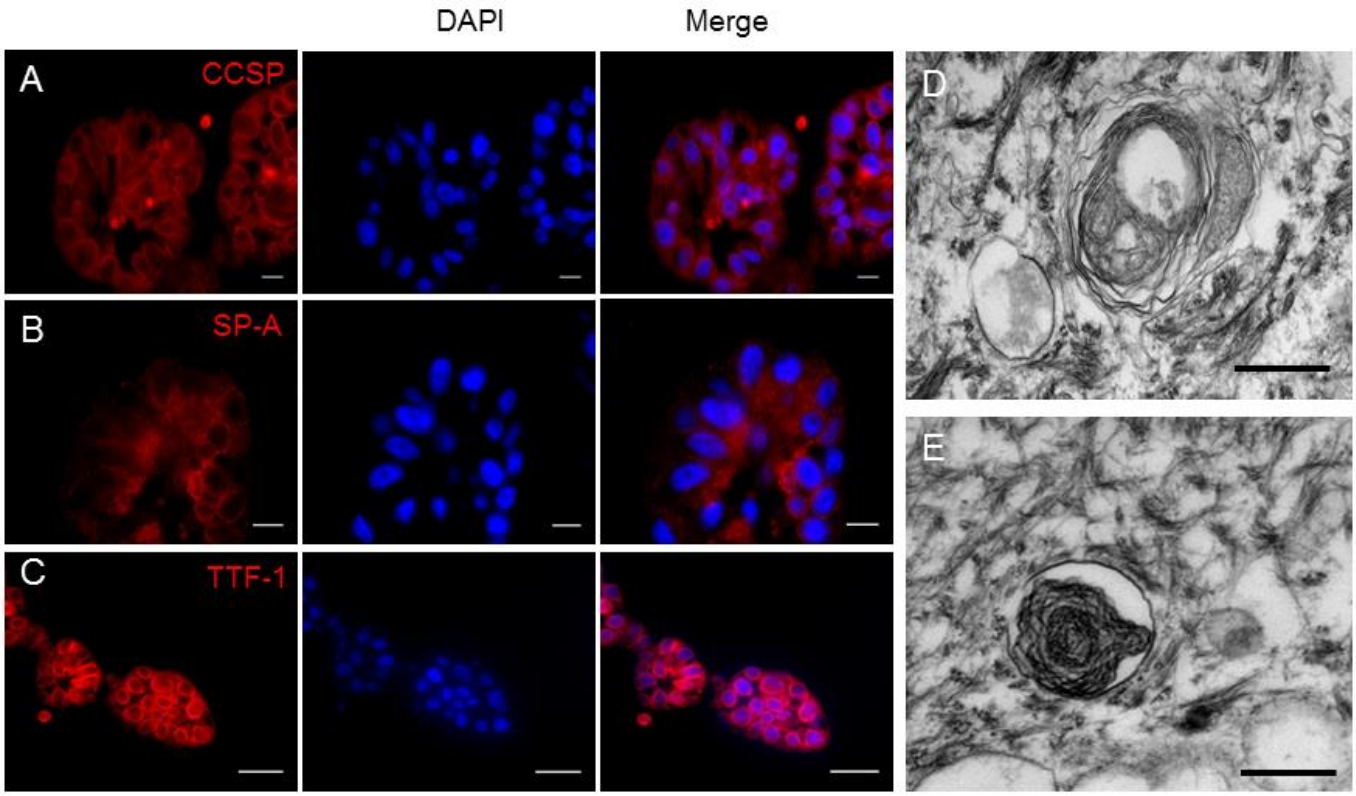

Figure 2.9: HBEC3 KTs express markers of distal lung lineages when cultured on Matrigel®

HBEC 3KT cells cultured on Matrigel® were immunostained for markers of cell types present in the distal lung (Day 8). (A) Nuclear stain with DAPI is shown in blue. CCSP (red) is expressed in HBEC3 KTs in 3D culture. The protein is localized within the cytoplasm of the cells in the branching structure. (B) Immunostaining with antibody against SP-A (red), a marker for type II pneumocytes cells. The expression of the protein is localized towards the apical side of the buds of the branching structures. (C) TTF1 is expressed in HBEC3 KTs cultured on top of Matrigel®. The TTF1 protein is expressed in the cytoplasm in a majority of the cells with weak nuclear expression within a few cells. Scale bar 10µm (A-C). (D-E) Transmission EM analysis on branching structures after 8 days in culture show the presence of lamellar-like bodies within the HBEC3 KT cells in 3D culture. Scale bar 0.5µm (D-E).

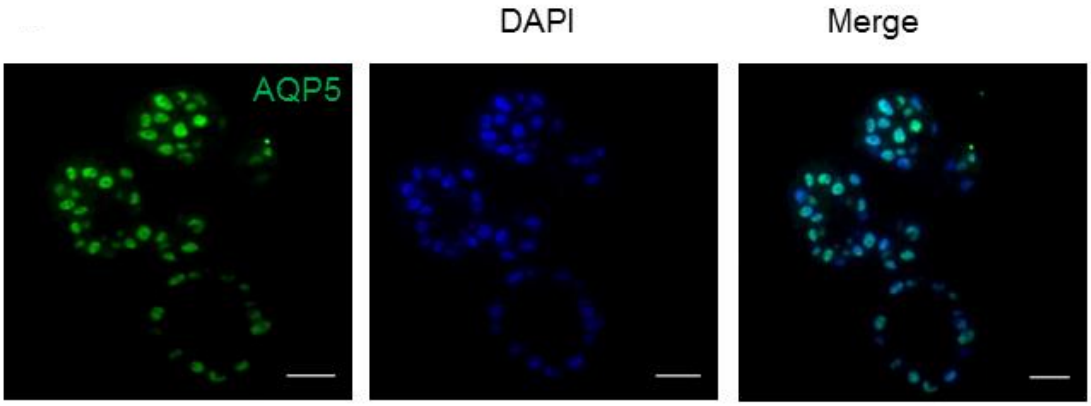

Figure 2.10: HBEC3 KTs express type I cell markers in 3D culture.

AQP5 (green) is expressed by HBEC3 KT cells in 3D culture. DAPI (blue); Scale bar 10 µm

2.3.4 Analyzing Partially/Fully Transformed HBEC3 KTs and Other HBECs in 3D Culture Model

To investigate if other HBEC cell lines can recapitulate the phenotype of HBEC3 KTs in 3D, we cultured another normal HBEC immortalized cell line (HBEC13 KT) on Matrigel®. Similar to HBEC3 KTs, HBEC13 KTs form a monolayer with cobblestone appearance under 2D conditions **(Figure 2.11 A)**. When cultured on top of Matrigel®, HBEC13 KTs reproduces the branching phenotype observed in HBEC3 KTs **(Figure 2.11 B)**. In the absence of IMR90 as a feeder layer under the 3D culture, HBEC13 KTs also fail to form complex branching structures (data not shown). This observation suggests that the 3D culture system can be used to study multiple HBEC cell lines and that the phenotype observed is not limited to HBEC3 KTs. The importance of signaling from the stroma during branching process is also confirmed in HBEC13 KTs.

To evaluate if the HBEC 3D model could be utilized to study lung cancer progression we cultured partially or completely transformed HBEC3 KTs on Matrigel®. HBEC3 KTs with ectopic expression of mutant K-ras v12 **(Figure 2.11 C)** or HBEC3 KTs with ectopic expression of mutant K-rasv12 and shRNA TP53 stably knocked down **(Figure 2.11 E)** exhibit normal HBEC phenotype in 2D. These cell lines also produce branching structures similar to normal HBEC3 KTs when cultured in 3D with IMR90s **(Figure 2.11 D, F)**. The observations suggest that introduction of oncogenic K-ras v12 and significant down regulation of the tumor suppressor TP53 is not sufficient to cause loss of branching phenotype in 3D. HBEC3 KT cells with over-expression of K-ras v12, c-myc and knocked down TP53 are completely transformed and do not

display normal HBEC cell morphology in 2D **(Figure 2.11 G)**. The cells do not display a cobblestone epithelial appearance; rather the cells convert to a mesenchymal phenotype in 2D. When cultured on Matrigel®, the cells aggregate and form tubular structures after day 1 but fail to progress into branching structures **(Figure 2.11 H)**. Instead, the cells form invasive structures within the Matrigel® (indicated by the arrows in **Figure 2.11 H**) correlating to their phenotype in 2D. These results demonstrate how this *in vitro* 3D system can be utilized in studying lung cancer progression.

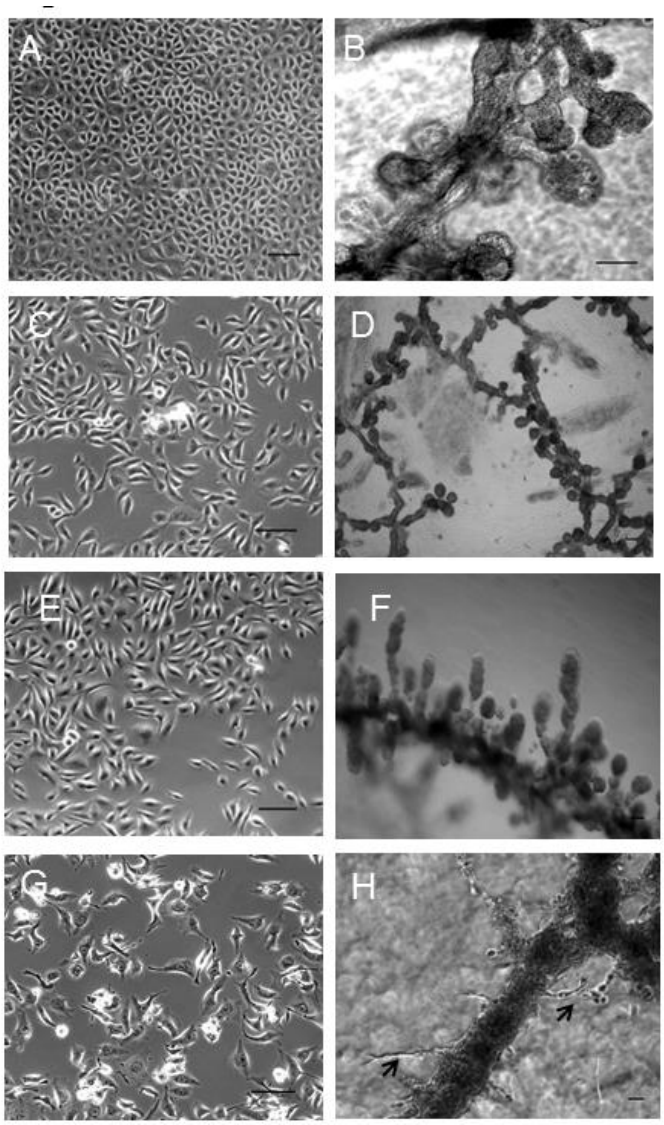

Figure 2.11: The *in vitro* 3D culture system can be utilized for understanding lung cancer progression.

The 3D system can be used to understand different respiratory diseases by analyzing the branching phenotype on Matrigel®. The branching characteristic that HBEC 3KTs demonstrate on Matrigel® can be recapitulated by other HBECs. (A) HBEC13 KTs exhibit cobblestone monolayer appearance in 2D. (B) When cultured on top of Matrigel® in the presence of IMR90s, HBEC13 KTs forms complex branching structures. (C) Mutant K-rasv12 or (E) both K-rasv12 and stable TP53 knockdown HBECs retain normal epithelial morphology in 2D. (D, F) These partially transformed cells also form branching structures when cultured on Matrigel®. (G) HBEC3 KTs expressing K-rasv12, c-myc and knockdown TP53 display a mesenchymal morphology in 2D culture. (H) These HBECs fail to form branching structures when cultured on top of Matrigel®. The cells
invade through the reconstituted basement membrane (pointed by the arrows). Scale bar 100µm

2.4 Discussion

Development of human cell culture models is an important complement to animal models in understanding basic developmental, differentiation, and disease processes. In the present study, we have described a novel *in vitro* lung epithelial cell culture system that is reminiscent in part to the process of lung branching morphogenesis during development. In our model, we also discovered that interaction between fibroblasts and the HBECs were critical to reproduce the branching phenotype *in vitro.* This is analogous to human lung development where critical signaling from the mesenchyme leads to the branching and differentiation of the airway epithelia. Developmental processes such as branching morphogenesis of the lung have primarily been studied using embryonic human or mouse tissue extracts (Miura and Shiota, 2000; Weaver et al., 2000). This model allows the use of immortalized HBECs to study such process *in vitro* and also recapitulates important stromal epithelial interactions. While our understanding of the lung epithelium homeostasis, repair and regeneration has been greatly enhanced by the use of mouse models, translating them to the human lung has been hindered due to the inherent anatomical differences between the two species (Rackley and Stripp, 2012; Rock and Hogan, 2011; Warburton et al., 2010). The present study demonstrates a new cell-based model to understand these processes within the human lung.

A critical role in organogenesis and tissue maintenance is performed through the crosstalk between the epithelial and mesenchymal cells. This signaling is critical for many tissues including mammary glands and prostate (Cunha, 2008; Kimura and Deutsch, 2007; Ronnov-Jessen and Bissell, 2009). The initial lung emerges from the ventral foregut endoderm and requires a coordinated sequence of processes to develop (Kimura and Deutsch, 2007). The

mesenchyme originates from the mesoderm which includes fibroblasts, endothelial cells and other connective tissue and these cell types progress in parallel to the surrounding developing airways. Induction of transcription factors and growth-factor signaling in a temporal-spatial manner orchestrate migration and branching of the lung airway epithelium (Kimura and Deutsch, 2007). The signaling also plays a role in specification of cell fate once the airway has developed (Boggaram, 2009; Maeda et al., 2007; Rock and Hogan, 2011). While several reports have described the formation of spheroid structures when human or mouse airway epithelial cells are cultured in Matrigel®, these models do not account for the epithelial-mesenchymal interactions (McQualter et al., 2010; Rock et al., 2009; Wu et al., 2011). The lack of such interaction may explain why HBECs in these models do not differentiate into cells associated with the distal airway. Interaction between stromal components such as fibroblasts and endothelial cells is much more intimate in the distal airway. Septation of terminal sacs in the branching lung epithelia involves interactions between airway epithelial cells, myofibroblasts and endothelial cells (Warburton et al., 2010). Fibroblast growth factor (FGF) signaling in particular FGF-10 from the mesenchyme also plays a critical role in differentiation and branching in the developing distal lung (Nyeng et al., 2008). Furthermore, fibroblasts adjacent to Type II pneumocytes in adult human tissue are responsible for maintaining communication between epithelia and migrating leukocytes (Sirianni et al., 2003). Branching morphology of HBECs in our 3D model support the notion that co-culturing mesenchymal and epithelial cells may be required to differentiate HBECs into cells enriched in the distal airways.

Most prior studies involving cell culture models have also failed to recapitulate the branching phenotype *in vitro* using immortalized HBECs. Branching morphogenesis of HBECs

in 3D culture was recently described (Franzdottir et al., 2010). There are distinct differences under which cells are cultured in our versus the Franzdottir et al (2010) studies. Franzdottir and co-workers embedded HBECs immortalized with E6/E7 viral oncogenes in Matrigel®. The HBECs were co-cultured with human umbilical vein endothelial cells (HUVECs) resulting in the formation of branching structures (Asgrimsson et al., 2006). In our model, HBECs immortalized with CDK4 and TERT are not embedded but overlaid on top of Matrigel® with fetal lung fibroblasts below the Matrigel as a monolayer. Under these conditions the HBECs aggregated to form budding and branching structures. When HBEC3 KTs are cultured on Matrigel® with HUVECs seeded as the feeder layer, HBEC 3KTs did not form any tubule-like structures after day 1 but aggregated and formed cyst-like structures **(Figure 2.12 A)**. When HUVECs are used a branching phenotype was rarely observed, while the vast majority of structures failed to demonstrate branching phenotypes by day 10 **(Figure 2.12 B)**. Interestingly, the endothelial cells seeded under the Matrigel® formed tubule-like structures **(Figure 2.12 C)**. The results demonstrate that while signaling from multiple stromal components may be required for development and differentiation of the lung epithelium, factors secreted from fibroblasts are crucial in our 3D cell culture system for HBEC3 KTs. Although HBECs grown with endothelial cells or fibroblasts under certain conditions may have similar phenotypes, the effects of different immortalization processes on differentiation are also not completely understood and certain subtle variations may exist between different HBEC lines.

HBEC3 KTs encompass multipotent capacity *in vitro* as described in the current study and by us previously (Delgado et al., 2011). The cells were derived from the central airway of the lung but in 2D culture, express markers of both central and distal lung. The cells express

basal cell markers p63 and keratin 14 (central) while also expressing Surfactant protein A, C, D and CCSP (distal). When placed in different 3D culture conditions, HBEC3 KTs demonstrate the capacity to differentiate into both central and distal lineages of the human airways (Delgado et al., 2011; Vaughan et al., 2006). These observations support the suggestion that there may be a human lung stem-like cell type capable of multipotent differentiation. When cultured on top of Matrigel® HBEC3 KTs form branching structures that retain these markers from multiple cell lineages. Immunofluorescence analysis of the branching structures demonstrates that HBEC3 KTs during branching continue to express basal cell, Clara cell and Type II pneumocytes cell markers. This indicates that signaling from other cell types beside fibroblasts or further changes in the microenvironment may be necessary to entirely differentiate the HBEC3 KTs into distal airway. TTF-1 a transcription factor which regulates surfactant proteins and CCSP expression in the distal lung was also expressed in 3D (Maeda et al., 2007). Expression of TTF-1 in HBEC3 KTs is variable in 2D, but TTF-1 is constituently expressed evenly in the cytoplasm of HBEC3 KTs in the branching structures. This indicates that HBEC3 KTs in the branching structures are primed to differentiate into distal lineages but additional signaling from the stroma may be required.

We also tested the utility of this novel 3D model to analyze lung cancer progression. HBEC3 KTs have previously been utilized to understand lung cancer progression. Partially transformed HBEC3 KTs with the addition of oncogenic mutant K-ras v12, knockdown of TP53 or both do not form xenograft tumors in immuno-compromised mice at a high frequency (Sato et al., 2006). Our 3D branching model was able to predict this *in vitro*, as these cells were able to branch and bud and appeared similar to unprogressed HBEC3 KTs. Fully transformed HBEC3

KTs with oncogenic K-ras v12, c-myc and knocked down TP53 are able to form tumors in mice at a higher frequency compared to partially transformed HBEC3 KTs (Sato et al., 2013) and when cultured in 3D on top of Matrigel® failed to branch and bud. The cells formed invasive structures in Matrigel® indicating their malignant transformation and their capacity to invade the basement membrane. The 3D model was able to distinguish between partial and fully transformed cell lines *in vitro* and predict their behavior *in vivo*. Therefore, the culture system may provide a physiologically relevant system that may help predict tumorigenic behavior *in vivo*. Loss of differentiation is a critical event in cancer progression and *in vitro* models such as the one described in the present studies may assist in understanding certain aspects of lung cancer progression and may be a useful system for testing therapeutic regimens. The 3D model can also help understand the epithelial-mesenchymal interactions in lung cancer progression.

Overall, our results characterize a novel model of branching morphogenesis using hTERT and Cdk4 immortalized human bronchial epithelial cells. We demonstrate that signaling from mesenchymal cells is critical for HBEC3 KTs to branch and bud when cultured on top of Matrigel®. The current model can also be extended further to recapitulate complex signaling between epithelium and stroma by including other stromal factors. Conversely, the model can also be simplified to understand the role of individual factors in lung development and diseases.

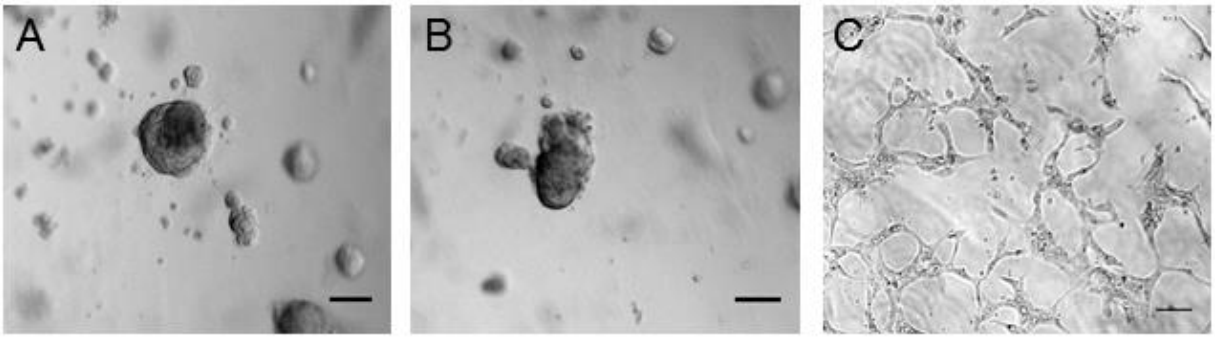

Figure 2.12: HBEC3 KTs do not recapitulate the 3D phenotype on top of Matrigel® when the IMR90 feeder layer is replaced with HUVECs.

(A) HBEC3 KTs aggregate and form cyst like structures when cultured on top of Matrigel® with HUVECs as the feeder layer.(B) A very few colonies, demonstrate a branching phenotype by day 10. (C) HUVECs seeded under the Matrigel® formed tubule- like structures. Scale bar 100 µm

2.5 Future Directions:

Ongoing studies using the described HBEC model focus on understanding how cells irradiated in a more physiologically relevant setting (3D) differ in their response in contrast to cells in 2D conditions. Irradiating HBECs using the organotypic 3D culture model may better mimic response of cells *in vivo.* Previous studies have indicated that HBECs irradiated in 3D culture conditions experience longer persistent DNA damage in contrast to cells under 2D conditions (Asaithamby et al., 2011). DNA damage repair pathways in HBECs irradiated in 3D

culture are also down-regulated. However it is not clear how this persistent damage impacts lung carcinogenesis. Ongoing studies involve irradiating HBECs in 2D and 3D conditions with space and terrestrial radiation and analyzing how different culture conditions affect HBECs transformation. Future studies will focus on understating the role of cell microenvironment on radiation induced carcinogenesis. Important signaling from the microenvironment dictates epithelial cell behavior during carcinogenesis and it not well understood how these signaling pathways are altered after radiation exposure.

Chapter Three:

Understanding Radiation Induced Invasive Carcinoma in LA1 K-Ras Mouse Model

3.1 Introduction

Although various physiological health risks caused by altered gravity are a major concern for astronauts on long-term space missions, radiation induced carcinogenesis is considered the main hindrance. This increase in cancer risk is attributed to the type of radiation originating in space. Unlike terrestrial radiation which primarily comprises of low- linear energy transfer (LET) radiations such as X-rays, β and γ-rays, space radiation includes high LET radiation fields. Astronauts in space are exposed to galactic cosmic radiation (GCR) comprising of high-energy protons and high charge and energy (HZE) nuclei, as well as medium energy protons that are trapped within the earth's magnetic belt. In addition, solar particle events (SPE) with higher energies and doses can occur in unpredicted intervals (Blot et al., 2011; Michaels and Hunt, 1978). Both GCR and SPE contain highly ionizing ions that have the capacity to penetrate shielding and human tissue. These differences between terrestrial and space radiation also

translate into different modes of energy deposition and cellular damage. In contrast to sparsely ionizing low-LET radiation such as X-rays, HZE and protons deposited their energy densely along well-defines linear tracks. HZE particles and protons also directly ionize their DNA target in contrast to low-LET radiation which ionizes the target with the aid of intermediary molecules such as water (Hall and Giaccia, 2006). Secondary radiation events along the tracks of HZE particle and proton radiation are also specific to space radiation (Li et al., 2014). These secondary radiation events are caused by δ-rays and can extend to cells not directly traversed by the primary particle and thus have important biological consequences.

Due to these differences in physical characteristics and cellular effects of terrestrial and space radiation our understanding of carcinogenesis due to low-LET radiation such as X-rays and γ-rays cannot be extrapolated to space radiation. Epidemiological data from atomic bomb survivors, miners exposed to radiation and radiotherapy patients cannot be extended without introducing uncertainties to predict risk for astronauts (Blot et al., 2011). Based on the recommendations from National Council of Radiation Protection and Measurement (NCRP), National Aeronautic and Space Association (NASA) limits lifetime risk of astronauts to 3% increased risk of radiation induced death (REID). These limitations require the need to establish new *in vitro* and *in vivo* model systems to better determine the risk of space radiation induced cancer compared to terrestrial radiation (Neyman and Puri, 1976). Since there is clear evidence that exposure to radiation poses significant health risk in particular carcinogenesis this study focuses on understanding lung cancer risk associated with radiation exposure.

Lung cancer is the second most common cancer in the US accounting for an estimate 224,210 new cases each year. More people in the US die of lung cancer than of colon, breast and prostate cancer combined. An estimated 159,260 deaths from lung cancer will account for 27% of all cancer deaths in 2014 (ACA, 2014). Activation of oncogenic pathways as a result of cells acquiring mutations drives the carcinogenesis process. On such pathway in lung cancer is the RAS/RAF pathway which is activated most commonly by mutation in the *K-ras* gene and occurs in about 20% of cancers (Sun et al., 2007). The importance of K-ras activation in lung cancer has been extensively studied using both cellular and murine models. While *in vitro* models have greatly enhanced our understanding of the signaling intricacies of the Ras pathway, these models cannot phenocopy the systemic effects of lung cancer such as the microenvironmental and the inflammatory system (Larsen and Minna, 2011). Using transgenic mouse models to understand lung cancer also helps analyze effects on the tumor microenvironment, gender and strain background specific effects on lung cancer progression. The LA1 K-ras mouse model was engineered to have a latent G12D allele (glycine to aspartic acid integrated mutation in codon 12) integration into the endogenous *KRAS* locus. The activation of the latent G12D allele occurs spontaneously, initiating during the development period of the mice. The expression of oncogenic K-ras (G12D) results in development of pre-malignant lesions within the lungs of LA1 K-ras mice (Raju et al., 1978). The tumors associated with LA1 K-ras mice originate from the type II pneumocytes lineage resembling the adenocarcinoma subtype of non-small cell lung cancer (NSCLSs) in patients. With the activation of oncogenic K-ras, the life span of the LA1 mice significantly decrease compared to their wildtype littermates; most LA1 K-ras mice are dead by the age of 500 days in contrast to wildtype mic which can survive over 800 days **(Figure 3.1 A)**. This decrease in lifespan is most likely due to the significant tumor burden

sustained by the lungs of LA1 K-ras mice **(Figure 3.1 B)** even though the direct cause of death may be due to pneumonia or bronchial extensions.

The integration of oncogenic *KRAS* allele results in the development of hyperplastic lesions within alveolar airways **(Figure 3.1 C, D)**. These hyperplastic lesions eventually progress to adenomas in all LA1 K-ras mice **(Figure 3.1 E)**. Only a certain fraction of the LA1 K-as population has tumor progression to atypic adenomas or invasive carcinomas stages (**Figure 3.1 F, G)**. Approximately 14% of LA1 K-ras mice develop invasive carcinomas which have the potential to metastasize. Most studies assessing the risk of radiation induced cancer focus only on cancer initiation. The LA1 K-ras mouse model can be used to determine not only an increase in cancer initiation but also progression after exposure to radiation. In this study, we analyzed the effects of SPE and HZE particle radiation on induction of invasive lung adenocarcinoma using the LA1 K-ras mice. Mice were irradiated between the ages of 5-15 weeks to analyze if irradiation provides an additional genetic or epigenetic insult during the early stages of tumor progression, eventually leading to an increase in the incidence of invasive carcinoma.

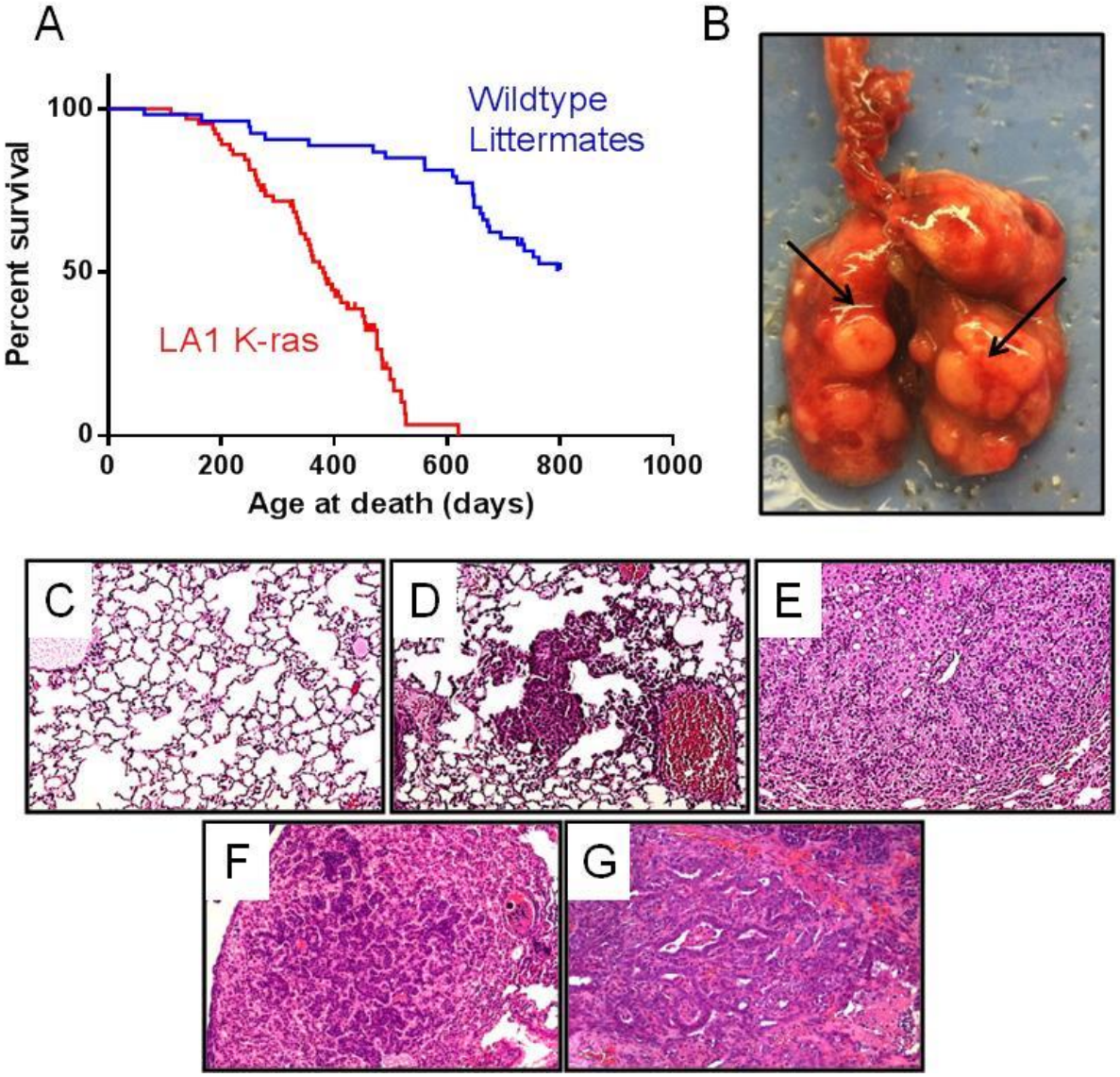

Figure 3.1: Tumor progression in LA1 K-ras mouse model.
(A) Expression of mutant *KRAS* (G12D) allele results in significant decrease in lifespan of LA1 K-ras mice in comparison to wildtype littermates ($P < 0.0001$). (B) A significant increase is also observed in LA1 K-ras as indicated by a lung from 300 day old mouse; lesions are pointed by the arrows. Tumor progression in LA1 K-ras mice mimics progression observed in humans. Lesions in LA1 K-ras mice begin to appear in the open alveolar airways (C) eventually progressing into hyperplastic lesions (D). All LA1 K-ras mice develop adenomas (E) from initial hyperplastic lesions with a small subset advancing to atypic adenoma (F). Tumors in approximately 14% of LA1 K-ras mice progress to invasive carcinoma (G).

3.2 Materials and Methods

3.2.1 LA1 K-ras Mice:

The LA1 K-ras mouse used to analyze the effect of radiation on lung cancer progression were backcrossed into C57/B6 and 129sv mouse backgrounds as previously described (Raju et al., 1978). All animal experiments were reviewed and approved by the Institutional Animal Care and Use Committee (IACUC) at University of Texas Southwestern Medical Center (Dallas, TX) and Brookhaven National Laboratory (Upton, NY).129sv LA1 K-ras mice were obtained from Dr. Jonathan Kurie (MD Anderson Cancer Center, Houston) and B6.129sv LA1 K-ras mice from the National Cancer Institute (NCI) Mouse Models of Human Cancer Consortium. Animals were housed and bred in automated ventilated cages at UTSW in specific pathogen free (SPF) facility. Heterozygote LA1 K-ras mice were crossed with wild-type mice of the same background.

3.2.2 Study Design:

To evaluate the impact of radiation on lung cancer progression, LA1 K-ras mice were transported to Brookhaven National Laboratory where they were irradiated with simulated SPE, Silicon (Si-) and Iron (^{56}Fe-) particles at the NASA space radiation laboratory (NSRL). Initial SPE studies comprised of a whole body 2.0 Gy dose of radiation which is considered to be a non-lethal tolerable dose. LA1 K-ras mice from both B6.129sv and 129sv backgrounds were irradiated to parse out strain specific effects of SPE on LA1 K-ras mice. Subsequent experiments

were designed to dissect the impact of SPE radiation by altering dose rates and energies. To understand the impact of other ion species on lung cancer progression, LA1 K-ras mice were irradiated with a fractionated dose and corresponding acute dose of silicon and Iron charged particles. At completion of radiation, mice were shipped back to the SPF animal facility at UTSW and monitored twice daily until death or euthanasia. Animals were randomly assigned to all experimental cohorts, irradiated and monitored until death or euthanization due to health concerns. Euthanized animals were censored from survival analysis. LA1 K-ras mice were also irradiated with X-ray to analyze the effects of terrestrial radiation and contrast it with HZE particle studies. The X-ray studies are also used to calculate relative biological effectiveness (RBE) for HZE particle radiation studies.

3.2.3 Irradiation:

For simulated SPE experiments, LA1 K-as mice between the age of 5 weeks and 15 weeks were shipped to Brookhaven National Laboratory. Animals were irradiated with a whole body dose of 2.0 Gy comprising of protons over 2 hours (dose rate of 1.0 Gy/hr). The simulation deposited the dose at energies ranging from 50 to 150 MeV/n. This SPE simulation was based on the 1972 solar particle event. The table below **(Table 3.1)** demonstrates the percentage of dose delivered at varying energies within the range. For acute radiation schemes, a whole body dose of 2.0 Gy of proton at either 50 or at 150 MeV/n was delivered at a dose rate of 0.2 Gy/min. For X-ray irradiation, LA1 K-ras mice between the ages of 5 weeks to 15 weeks, were irradiated with 250-kV X-rays using an X-RAD 320 irradiator (Precision Xray, Inc., North Branford, CT) at UTSW at a dose rate of approximately 0.2 Gy/min. The animals were irradiated with a whole

body dose of 2.0 Gy and were also monitored twice daily in the UTSW SPF facility until death or euthanasia. The dosimetry for all experiments was provided by the Medical Physics Division of the Department of Radiation Oncology at UTSW as part of their routine calibration and dosimetry responsibilities and by physicists at BNL

Iron (^{56}Fe-) and Silicon (Si-) studies were either single acute doses or dose equivalent given in fractionated doses. LA1 K-ras mice were irradiated with a whole body Si- dose of 0.4 Gy over five days (600 MeV/n). Corresponding acute doses at 0.4 Gy and 2.0 Gy (600 MeV/n) were also delivered to analyze the effects of fractionated/chronic irradiation on lung cancer progression in LA1 K-ras mice. ^{56}Fe- studies consist of delivering a whole body dose of 0.2 Gy a day (1 GeV/n) over five days for a total of 1.0 Gy. Single acute doses of 0.2 Gy and 1.0 Gy (1 GeV/n) were delivered as acute to compare to fractionated dose **(Figure 3.2)**.

Energy (MeV/n)	Dose Fraction (%)
50	91.661
60	2.929
70	2.033
80	1.508
90	1.059
100	0.81
110	0.55
120	0.367
130	0.278
140	0.195
150	0.14

Table 3.1: Percentage of dose fractions delivered at various energies to simulate SPE. LA1 K-ras mice are irradiated with protons varying in energy from 50-150 MeV/n in energy to mimic SPE in space.

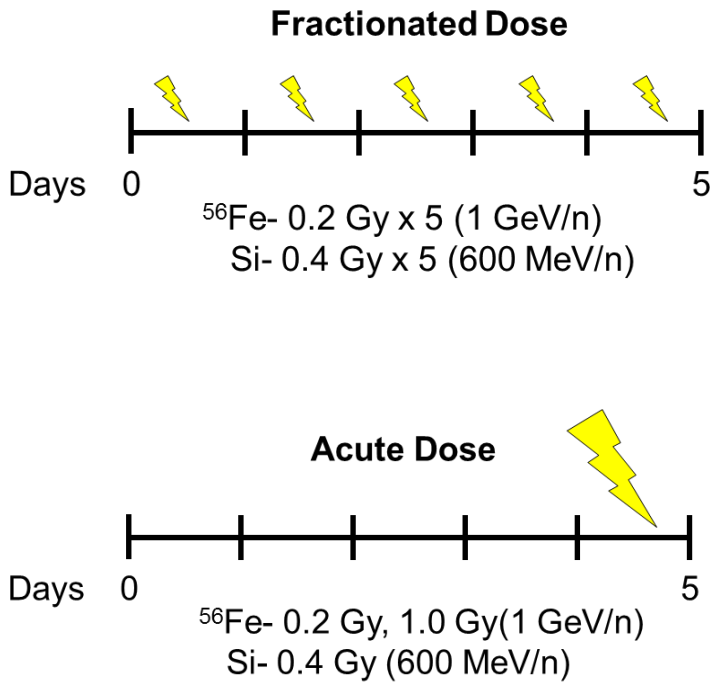

Figure 3.2: Irradiation scheme for LA1 K-ras mice.
LA1 K-ras mice were irradiated with either a fractionated dose (split over five days) or an acute dose.

3.2.4 Lung Tumor Histopathology:

At death, the carcasses were necropsied; lungs were removed and inflated via intra-tracheal infusion with 10% neutral buffer formalin (NBF). The lungs were then clamped at the trachea and the entire tissue was immersed in 10% NBF overnight. Other tissue types including kidney, liver and spleen, were also extracted and fixed overnight in 10% NBF. Tissues were processed, paraffin-embedded, cut into 5 µm thick sections and stained with hematoxylin and

eosin (H&E) for histopathological assessment. To analyze tumor grade and quantify lesions, two sections were cut 50 µm apart per animal. The stained sections were then analyzed; tumor grade and other histopathological features were scored and confirmed by pathologist Dr. James Richardson (UTSW). Axiovision software v4.6.3 on Axioskop 2 plus microscope mounted with AxioCamHR color camera (Carl Zeiss Microscopy) was used to further quantify lesion number and size. Measurements were performed using the ImageJ software.

3.2.5 Lung Tissue and Blood Collection for Analysis:

Age matched LA1 K-ras mice irradiated with a simulated SPE whole body dose of 2.0 Gy and unirradiated controls were sacrificed at various time points. Mice were sacrificed at forty, seventy and one hundred days post-irradiation. Animals were anesthetized with an intraperitoneal injection of Ketamine, Xylazine, and Acepromazine cocktail (Dosage: 100 mg/kg, 10 mg/kg, and 2 mg/kg, respectively). Cardiac puncture was performed immediately after anesthetization followed by cervical dislocation. Lung and other desired tissues were then extracted and flash frozen in liquid nitrogen.

3.2.6 Protein Extraction and Western Blot Analysis:

Age-matched 129sv LA-1 K-ras mice were shipped to BNL and irradiated with a simulated SPE whole body dose of 2.0 Gy or left unirradiated. Seventy days after irradiation, the lungs were extracted and flash frozen in liquid nitrogen. Frozen tissues were then homogenized on ice in cold lysis buffer (50 mmol/L Tris-HCl, pH 7.5; 120 mmol/L NaCl; and 1 mmol/L

EDTA) supplemented with PhosStop phosphatase inhibitor and cOmplete protease inhibitor cocktail tablets (Roche). Triton X-100 (1% final concentration; Sigma-Adrich) was then added to the tissue samples after homogenization and the samples were incubated for 20 minutes on ice. Lysates were centrifuged (at 13,000 rpm for 20 minutes) and supernatants were transferred to new tubes. Centrifugation was repeated twice to ensure the lysates were free from all tissue debris. Protein concentration was calculated using Bradford assay (Bio-Rad) and 15 mg of protein was loaded on gradient gels (4% to 15% Criterion TGX gels; Bio-Rad). Gels were transferred onto nitrocellulose membranes (Bio-Rad) using the Trans-Blot Turbo Transfer System (Bio-Rad) and blocked with 5% milk (1 hour at room temperature). Blots were incubated with primary antibodies, diluted in 1X PBST, overnight at 4°C. The following antibodies were used for western blot analysis MAPK14 Cat# 9212, phospho-p38MAPKCat# 9211,JUNCat# 9165, phospho-JUN Cat# 3270, phospho-STAT3 Y705 Cat# 9145, and phospho-STAT3 S727 Cat# 9134 (Cell Signaling Technology); STAT3 Cat# 06-596 (Millipore)]; c-Met Sampler Kit Cat# 3019 (Cell Signaling Technology).

After three washes with 1X PBST the next day, blots were incubated with secondary antibody (horseradish peroxidase–conjugated AffiniPure goat anti-mouse IgG or goat anti-rabbit IgG) diluted in 5% skim milk for 1 hour at room temperature. The blots were then washed again with 1X PBST. Blots were exposed with SuperSignal West Femto Chemiluminescent Subtrate diluted in 1X PBST (Thermo Fisher Scientific). Images were processed with GeneSnap software (Syngene) on the G: BOX Chemisystem (Syngene) and quantified using GeneTools software (Syngene).

3.2.9 Statistical Analysis:

Survival analysis of Kaplan-Meier curves were performed using the log rank test. Statistical analyses for histopathological studies and tumors lesions quantification were performed using two-tailed chi-square tests.

3.3 Results

3.3.1 Effects of Simulated Solar Particle Event on LA1 K-ras Mice.

LA1 K-ras mice were irradiated with a whole body dose of 2.0 Gy of proton (as a simulated SPE) or X-rays. The simulated SPE was delivered at energies ranging from 50 to 150 MeV/nucleon with a majority of the dose being delivered at the lower range while the X-ray irradiation was delivered at 250-kV energy. Animals were exposed to SPE for two hours (dose rate of 1.0 Gy/hour) and exposed to X-rays for ten minutes (dose rate of 0.2Gy/minute) to deliver the total dose. The survival of LA1 K-ras mice was significantly decreased upon irradiation with simulated SPE **(Figure 3.3 A)**. A significant decrease in survival was observed in LA1 K-ras mice exposed to SPE after 300 days compared to unirradiated control cohort of mice. Irradiation to X-rays also decreased the lifespan of LA1 K-ras mice **(Figure 3.3 B)** although this decrease in survival was not as substantial as SPE irradiation. All LA1 K-ras mice were irradiated between the ages of 5 and 15 weeks. During this age interval LA1 K-ras mice only e a few hyperplastic lesions are observed on the lungs of LA1 K-ras mice.

To analyze whether irradiation influences the progression of lung cancer in LA1 K-ras mice, histopathological analysis were performed at the end of animal's lifespan. Incidence of invasive carcinoma in particular was analyzed to determine the effects of radiation on tumor progression. Invasive carcinoma is characterized as a tumor that has a potential to metastasize.

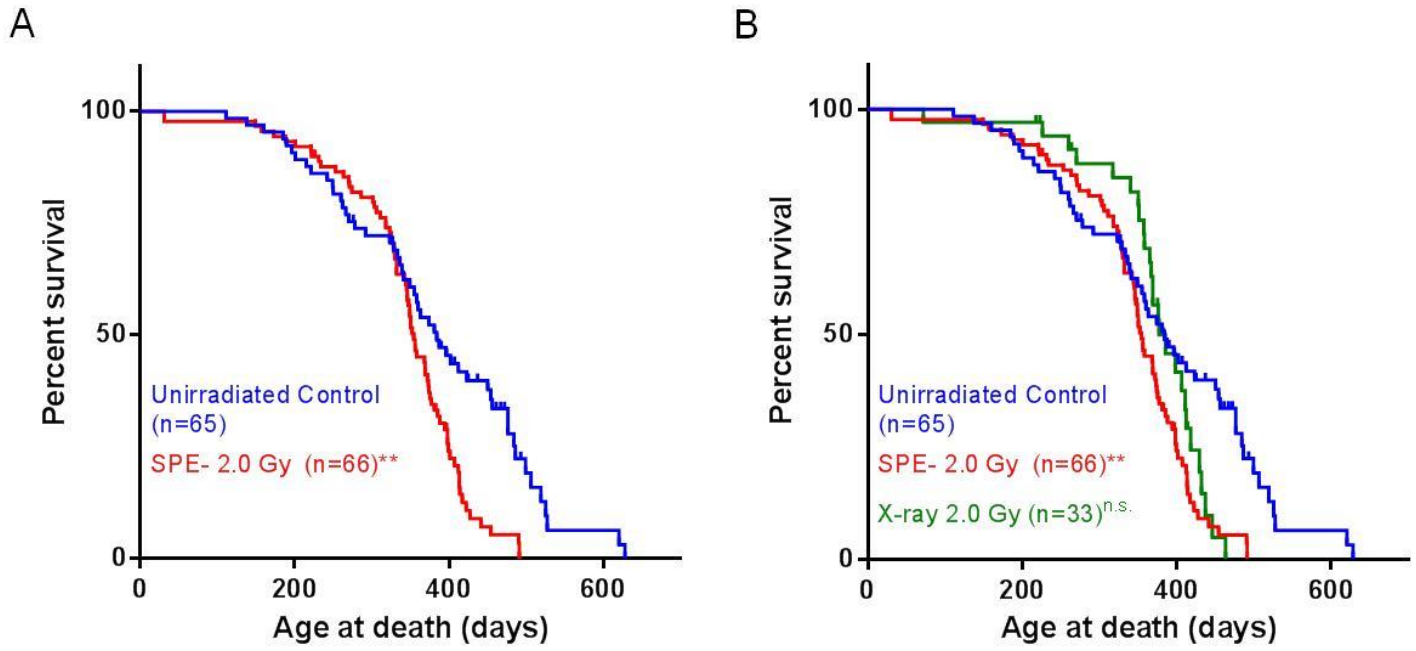

Figure 3.3: 2.0 Gy dose of whole body irradiation with simulated SPE significantly reduces lifespan of LA1 K-ras mice.
LA1 K-ras mice were irradiated a 2.0 Gy dose of either simulated SPE or X-rays. Survival of LA1 K-ras mice was monitored post irradiation. (A) Kaplan-Meier survival curves of LA1 K-ras mice irradiated with 2.0 Gy compared to unirradiated control cohort. There was significant decrease in lifespan of irradiated mice in comparison to unirradiated mice. (B) A decrease in lifespan was also observed in LA1 K-ras mice irradiated with X-rays in contrast to unirradiated cohorts. Although the shortening of lifespan was more significant in mice irradiated with SPE compared to X-rays. (** indicates $p \leq 0.01$, log rank test).

The tumor cells in an invasive carcinoma present high nuclear to cytoplasmic ratio, nuclear pleomorphism, loss of basement membrane and invasion into the surrounding activated stroma. The tumor cells also present undifferentiated characteristics with loss of resemblance to the normal airway epithelium cell types. Since radiation considerably decreased the overall survival of LA1 K-ras mice, the analysis was performed with an age cutoff corresponding to the maximum life span of these cohorts (500 days). About 14% of LA1 K-ras mice demonstrated disease progression to the invasive carcinoma stage without any irradiation. The incidence of invasive carcinoma significantly increased in mice irradiated with simulated SPE to 41% **(Table 3.2)**. Conversely, only 19% of LA1 K-ras mice irradiated with X-rays demonstrated invasive lung adenocarcinoma.

Radiation Type	Energy	Total Dose (Gy)	Carcinoma incidence
Control	0	0	14% (n=54)
SPE 2.0 Gy	50 – 150 (MeV/n)	2	41% (n=70)**
X- 2.0 Gy	250-kV	2	19% (n=27)n.s.

Table 3.2: Incidence of invasive carcinoma in unirradiated LA1 K-ras mice and mice irradiated with 2.0 Gy total dose of X-rays or SPE.
A significant increase in invasive carcinoma was observed in LA1 K-ras mice irradiated with SPE in comparison to unirradiated cohorts (** indicates $p \leq 0.01$ compared to unirradiated control).

Hematological disorders such as lymphoma and leukemia are known to have impact on the health of mice after radiation exposure (Hall and Giaccia, 2006). In order to parse out the effects hematological malignancies from lung cancer progression, analyses were performed by adjusting carcinoma incidence for leukemia and lymphoma. The incidence of invasive cancer was altered minimally in unirradiated control LA1 K-ras mice form 14% to 17% after the adjustment **(Table 3.3)**. There was also no significant increase in incidence observed in mice irradiated with SPE (an increase of 5%) or X-rays (an increase of 3%) indicating that hematological malignancies had little impact on the health of LA1 K-ras mice.

Radiation Type	Energy	Total Dose (Gy)	Carcinoma incidence
Control	0	0	17 % (n=45)
SPE 2.0 Gy	50 – 150 (MeV/n)	2	46% (n=63)**
X-2.0 Gy	250-kV	2	22% (n=23) n.s.

Table 3.3: Lymphoma and leukemia adjusted incidence of invasive carcinoma in unirradiated LA1 K-ras mice and mice irradiated with 2.0 Gy total dose of X-rays or SPE. There was no significant increase in the incidence of carcinoma in unirradiated LA1 K-ras or mice irradiated with 2.0 Gy of SPE or X-rays after leukemia and lymphoma adjustment cohorts (** indicates $p \leq 0.01$ compared to unirradiated control).

To determine mouse strain related effects on the incidence of invasive carcinoma, LA1 K-ras mice with a B6.129sv and 129sv background were used for simulated SPE studies **(Table 3.4)**. The B6.129sv strain had a higher susceptibility to invasive carcinoma without any irradiation at 24% compared to 9% in 129sv strain. Even though the background rates vary between the two strains, the overall percent increases in invasive carcinoma were similar. Both strains demonstrated an estimated 3-fold increase in invasive carcinoma after irradiation with simulated SPE. This observation demonstrates that strain differences in LA1 K-ras mice do not alter the increase in invasive carcinoma after SPE irradiation.

Radiation Type	Strain		Overall
	129sv	B6.129sv	
Control	9% (n=33)	24% (n=21)	14% (n=54)
SPE 2.0 Gy	30% (n=47)	65% (n=23)	41% (n=70)**

Table 3.4: Incidence of invasive carcinoma in different strains of LA1 K-ras unirradiated mice and mice irradiated with 2.0 Gy dose of SPE.
Although LA1 K-ras B6.129sv mice were more susceptible to invasive carcinoma in contrast to LA1 K-ras 129sv mice, the fold increase (~3) in carcinoma observed after SPE irradiation is similar in both backgrounds (** indicates $p \leq 0.01$ compared to unirradiated control).

To examine other variables besides tumor burden that might explain the shortened lifespan of irradiated mice, additional histopathological features were characterized. The incidence of pneumonia, bronchial extensions, atypic adenomas, leukemia and lymphoma were

investigated. Pulmonary pneumonia is defined as an inflammatory condition affecting the alveolar sacs. It can be identified by observing the infiltration of alveolar macrophages into the open alveolar airways. Small populations of alveolar macrophages are always present in the alveoli as a host defense mechanism, but these numbers exponentially increase in an inflammatory condition such as pneumonia. About 48% of unirradiated LA1 K-ras mice were susceptible to pneumonia in contrast to 54% of mice irradiated with SPE and 81% irradiated with X-rays **(Figure 3.4 A)**. Bronchial extension is defined by the aggressive growth of tumors in the larger airways of the lung. This aggressive growth in the larger airways may account for one of the factors responsible for shortened lifespan of irradiated LA1 K-ras mice. Approximately 31% of unirradiated mice displayed tumors with bronchial extension into the larger airways compared to 68% of mice irradiated with SPE and 63% with X-rays **(Figure 3.4 B)**. This may be one of the possible explanations for the shortened lifespan of the irradiated mice but does not explain the large differences in invasive cancers between SPE and X-rays irradiated mice. Atypic adenoma is described as an advanced stage adenoma with a higher probability of transitioning into an invasive carcinoma. Atypic adenomas are characterized by pleomorphic nuclei and high nuclear to cytoplasmic ratio, but no activation of surrounding stroma. There is a significant increase in atypic adenomas in LA1 K-ras irradiated with SPE (78%) and X-rays (77%) compared to unirradiated LA1 K-ras mice (50%) **(Figure 3.4 C)**. There was no significant increase in either leukemia or lymphomas in LA1 K-ras mice irradiated with SPE or X-rays in contrast to unirradiated control mice. This observation demonstrated that hematological disorders were not responsible for the shortened lifespan of irradiated LA1 K-ras mice **(Figure 3.4 D, E)**.

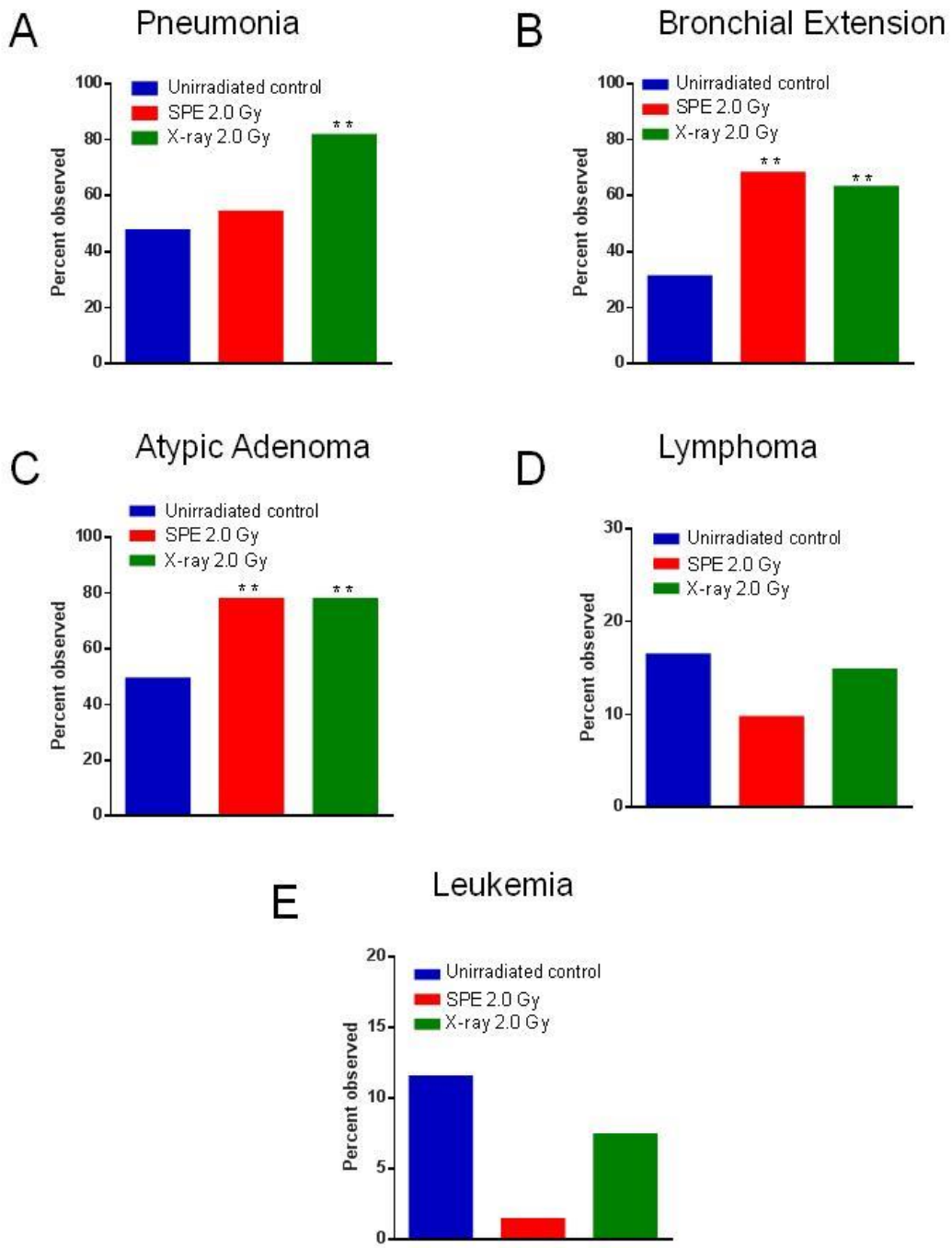

Figure 3.4: Incidence of several histopathological features observed in LA1 K-ras mice irradiated with 2.0 Gy dose of SPE or X-rays in comparison to unirradiated cohorts
Percent of pneumonia (A), bronchial extension (B), atypic adenoma (C), lymphoma (D), and leukemia (E) observed in irradiated and unirradiated LA1 K-ras mice (** indicates $p \leq 0.01$ compared to unirradiated control, two-tailed chi-square test).

3.3.2 Analyzing Potential Molecular Mechanisms Responsible for Increased Incidence of Invasive Carcinoma in LA1 K-ras Mice Irradiated with Simulated SPE.

Lung tissue was collected from LA1 K-ras mice irradiated with SPE and their unirradiated counterparts 40, 70 and 100 days after irradiation. The rationale for collecting tissue at these time points was based on tumor progression and recovery time from irradiation effects in mice. The 40 to 100 day time points allowed the LA1 K-ras mice to recover from the acute radiation damage while the time point was brief enough that the lungs from all cohorts remain histologically identical. At these time points (40-100 days post irradiation), no atypic adenomas or carcinomas were observed in either control or irradiated mice and hematological malignancies (leukemia and lymphoma) and inflammatory conditions (pneumonia) are negligible. Therefore these time point allowed the analysis of underlying molecular changes that may be responsible for the increase in incidence of lung adenocarcinoma.

A significant increase in number of hyperplastic lesions **(Figure 3.5 A)** was observed in LA1 K-ras mice irradiated with simulated SPE at 40, 70 and 100 days post-irradiation in contrast to unirradiated cohorts **(Figure 3.5 B)**. The higher number of lesions at each time point could be interpreted to indicate that exposure to simulated SPE results in a higher number of initiated lesions. However, there was no difference between the size and grade of the hyperplastic lesions between the two cohorts **(Figure 3.5 C)**. There was also a significant increase in the number of adenomas **(Figure 3.5 D)** observed 100 days after irradiation with SPE **(Figure 3.5 E)**. No adenoma differences are observed at the 40 or 70 day timepoints. The sizes of adenomas were also significantly higher in LA1 K-ras mice irradiated with SPE at the 100 day timepoint **(Figure**

3.5 F). These differences observed between the two groups demonstrate that tumor initiation and progression are altered after SPE irradiation although there is no difference observed in the tumor grade.

To determine potential mechanisms responsible for the increase in invasive carcinoma in LA1 K-ras mice irradiated with SPE, western blot analyses were performed. Tissue lysates from SPE irradiated lungs were collected (70 day post-irradiation) although no tumor micro-dissections were performed. Previously it has been shown that inflammatory signaling may play a role in radiation induced carcinogenesis (Delgado et al., 2014) therefore we analyzed protein expression of known inflammatory pathways. There was a significant difference in expression of phosphor-NFkB observed between unirradiated and SPE irradiated mice **(Figure 3.6)**. LA1 K-ras mice irradiated with SPE have lower expression of phosphor-NFkB, in comparison to unirradiated controls while no differences are observed in total NFkB expression. LA1 K-ras mice irradiated with SPE also demonstrated higher expression of phospho-Gab1 (GRB2-Associated-Binding Protein 1) and phospho-met in contrast to unirradiated mice. No differences were observed in total expression of Gab1 and c-met.

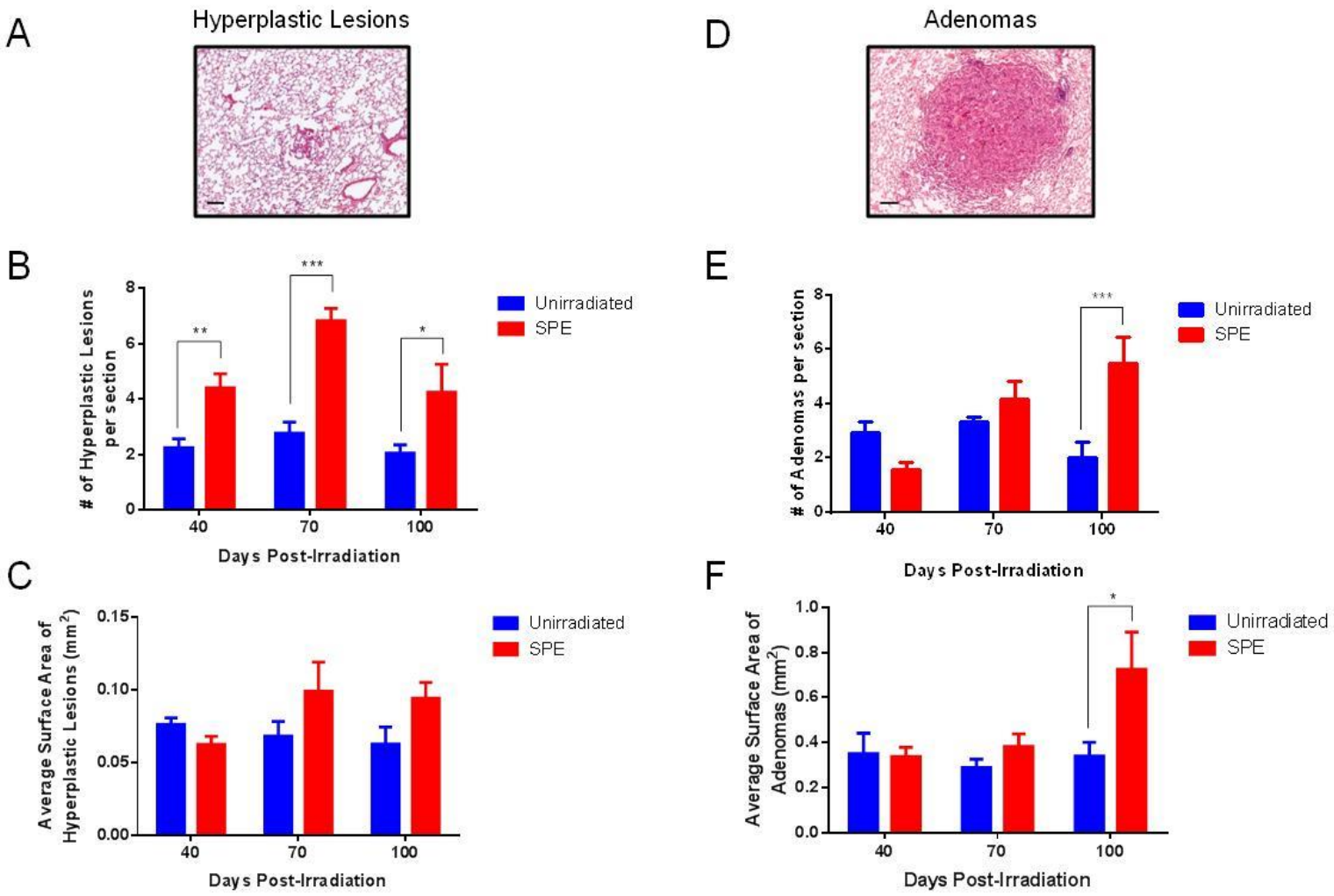

Figure 3.5: Tumor burden was higher in LA1 K-ras mice irradiated with SPE in contrast to unirradiated controls 40, 70 and 100 days post-irradiation.
Numbers and sizes of hyperplastic lesions (A) and adenomas (D) were determined in LA1 K-ras mice 40, 70 and 100 days after irradiation with SPE. (B) An increase in the number of benign hyperplasias was observed in LA1 K-ras mice irradiated with SPE 40, 70 and 100 days after irradiation in comparison to unirradiated mice. (C) No significant difference in the size of hyperplasias was observed between the two groups. An increase in number (E) and size (F) of adenomas was observe 100 days post-irradiation in LA1 K-ras mice irradiated with SPE in contrast to unirradiated controls. (N= 4-6 mice per timepoint. Scale bars denote 100 µm and mean± SEM is plotted on the graphs. (* $p \leq 0.05$, ** $p \leq 0.01$, *** $p \leq 0.001$; two-way ANOVA test)

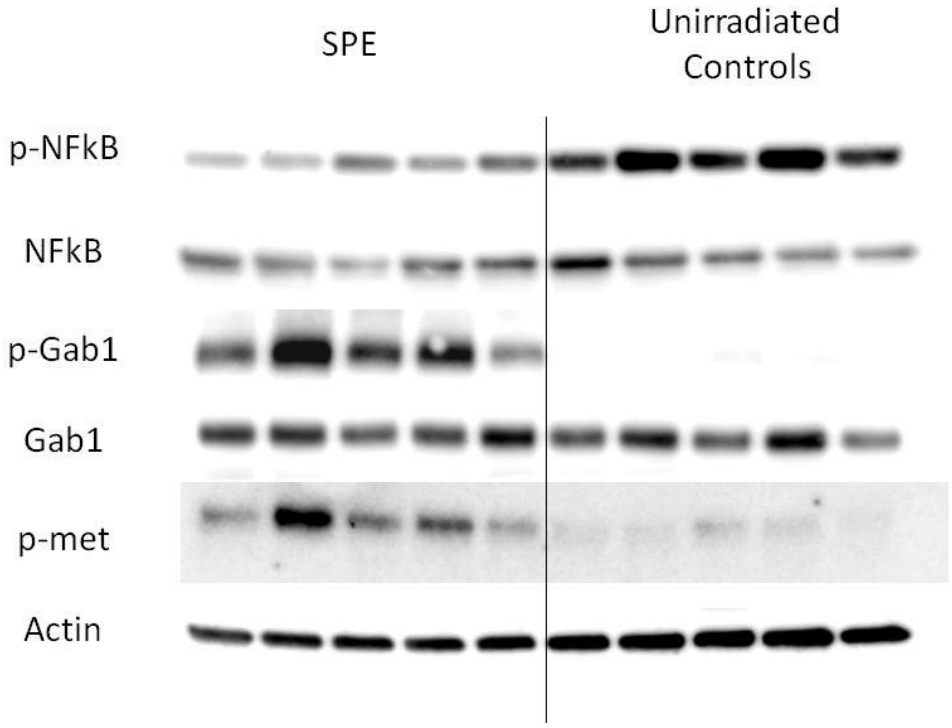

Figure 3.6: Analyzing protein expression in SPE irradiated LA1 K-ras mice 70 days post-irradiation.
A difference in the expression of p-NFkB, p-Gab1 and p-met was observed between LA1 K-ras mice irradiated with SPE and unirradiated cohorts.

3.3.3 Effects on LA1 K-ras Mice Irradiated by Protons as an Acute Dose in Contrast to Simulated SPE.

LA1 K-ras mice were irradiated with a whole body dose of acute 2.0 Gy protons at two different energies; 50 or 150 MeV/n. The rationale for irradiating mice with these two energies was to understand the impact of various energies on lung carcinogenesis. Since simulated SPE irradiation comprised of doses ranging in energy from 50 to 150 MeV/n, LA1 K-ras mice were irradiated at the two energy extremes. Different energies of particle radiation have defined depths as to how far they traverse through matter. This difference also translates into particles having different Bragg peaks and may affect lung carcinogenesis differently in LA1 K-ras mice. The acute irradiation dose was also delivered at a dose rate of 0.2 Gy/min in contrast to SPE which was delivered over two hours.

LA1-Kras mice irradiated with acute proton dose of 50 or 150 MeV/n have shortened lifespan compared to unirradiated control mice. This decrease in lifespan was even greater than what is observed in mice irradiated with simulated SPE **(Figure 3.7 A, B)**. This observation suggests that a change in dose rate compared to SPE significantly impacts the lifespan of LA1 K-ras mice regardless of the energy. LA1 K-ras mice irradiated with a dose of 2.0 Gy protons at 50 MeV/n also demonstrated a significant increase in the incidence of carcinoma in contrast to unirradiated mice. This increase in incidence of lung carcinoma was comparable to what was observed in mice irradiated with simulated SPE **(Table 3.5)**. This suggests that the different dose rate between acute and SPE radiation do not impact the incidence of carcinoma. Analysis of LA1 Kras mice irradiated with 150 MeV/n is still in progress.

Radiation Type	Energy	Total Dose (Gy)	Carcinoma incidence
Control (129sv Only)	0	0	9% (n=33)
SPE 2.0 Gy	50 – 150 (MeV/n)	2	30% (n=47)**
Acute 2.0 Gy (50 MeV/n)	50 (MeV/n)	2	28% (n=32)*
X- 2.0 Gy	250-kV	2	19% (n=27)$^{n.s.}$

Table 3.5: Incidence of invasive carcinoma in unirradiated LA1 K-ras mice and mice irradiated with 2.0 Gy total dose of acute proton or SPE.
A significant increase in invasive carcinoma was observed in LA1 K-ras mice irradiated with SPE and acute proton (50 MeV/n) in comparison to unirradiated cohorts. No significant increase in incidence of invasive carcinoma was observed in mice irradiated with X-rays (** indicates $p \leq 0.01$, * $p \leq 0.05$ compared to unirradiated control).

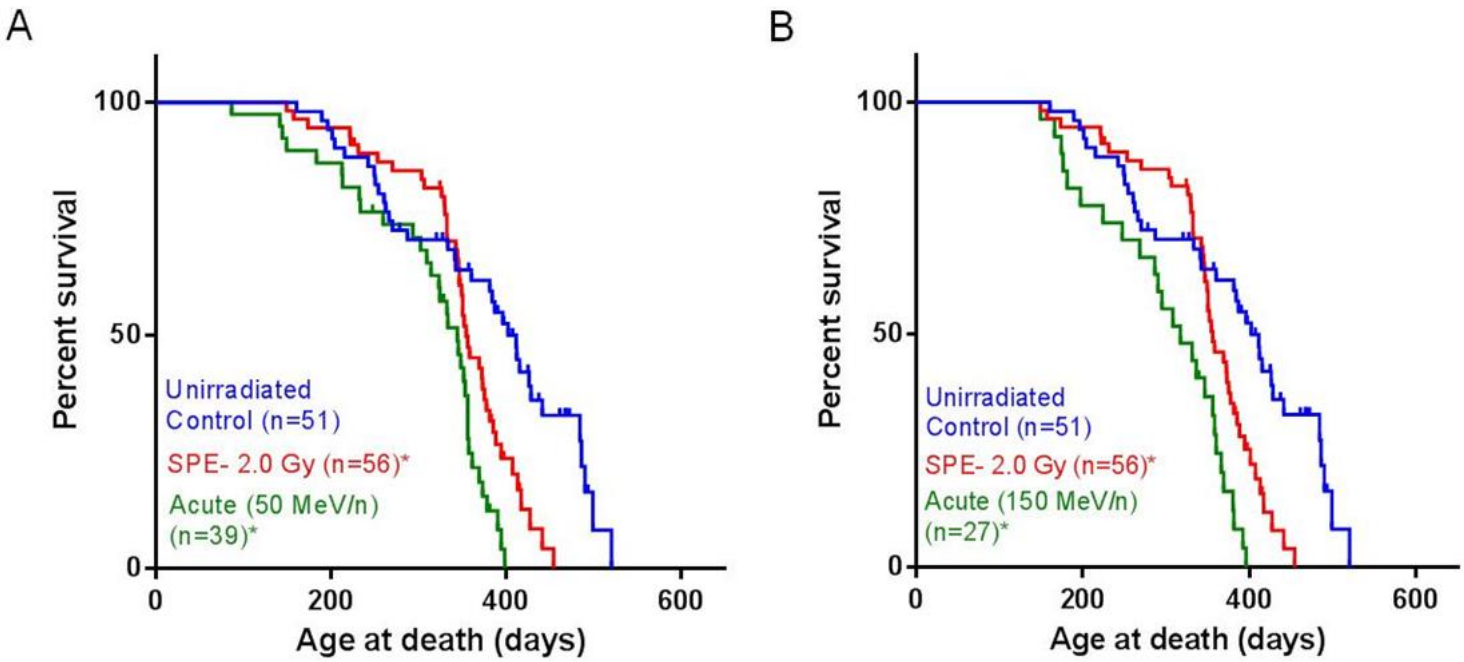

Figure 3.7: 2.0 Gy proton irradiation delivered as an acute dose significantly decreased the lifespan of LA1 K-ras mice

LA1 K-ras mice were irradiated a 2.0 Gy dose of proton as an acute dose at either 50 or 150 MeV/n. Survival of LA1 K-ras mice was monitored post irradiation.(A) Kaplan-Meier survival curves of LA1 K-ras mice irradiated with 2.0 Gy dose of acute proton (50 MeV/n) or SPE in contrast to unirradiated controls. (B) Survival curves of LA1 K-ras mice irradiated with 2.0 Gy dose of acute proton (150 MeV/n) or SPE in contrast to unirradiated controls. A significant decrease in survival was observed in mice irradiated with acute (50 and 150 MeV/n) and SPE in contrast to unirradiated cohort. (* indicates $p \leq 0.05$, log rank test).

3.3.4 Impact of Fractionated Irradiation Compared to Acute Particle Irradiation on Lung Carcinogenesis in LA1 K-ras Mice.

Previously, it has been demonstrated that irradiation with fractionated but not acute dose of ^{56}Fe- leads to a significant increase in the incidence of invasive carcinoma in LA1 K-ras mice (Delgado et al., 2014). Therefore, we tested to see if this observation held true for other HZE particles beside ^{56}Fe-. To analyze this, LA1 K-ras were exposed to a whole body dose of 2.0 Gy or 1.0 Gy of Si- (600 MeV/n). The irradiation was delivered either as an acute or fractionated dose delivered over multiple days (0.33 Gy x 3 days or 0.4 Gy x 5). Irrespective of fractionated or acute dose, irradiation with 2.0 and 1.0 Gy of Si- significantly decreased the lifespan of LA1 K-ras mice in comparison to unirradiated cohorts. Differences in lifespan were observed between LA1 K-ras mice irradiated with fractionated or acute dose of 2.0 Gy of Si-. Mice irradiated with fractionated 2.0 Gy dose had a substantially decreased life span, when compared to the acute dose **(Figure 3.8 A)**. Even though both the fractionated and acute cohorts had significantly shortened lifespans in contrast to unirradiated controls, mice irradiated with a fractionated dose had poorer outcomes. The notion that fractionated doses of irradiation are sparing is not supported by irradiation with 2.0 Gy of Si-. In contrast, there is no difference observed between the lifespan of LA1 K-ras mice irradiated with fractionated or acute 1.0 Gy dose of Si- **(Figure 3.8 B)**. The overall survival for both fractionated and acute irradiated mice decrease in contrast to unirradiated control, but no differences were observed between the two irradiation schemes.

Histopathological examination of irradiated LA1 K-ras mice was performed in order to analyze the incidence of invasive carcinoma. There was a significant increase in incidence of

carcinoma in mice irradiated with a fractionated dose of 2.0 Gy Si- compared to unirradiated control (42% vs 9%). This large (> 4-fold) increase in incidence was not observed in LA1 K-ras mice irradiated with an acute dose of 2.0 Gy (15% vs 9%) **(Table 3.6)**. Even though the irradiation with acute dose of Si- decreased the life span of LA1 K-ras mice, only a 2-fold increase in incidence of carcinoma was observed. These results are analogous to what is observed in LA1 K-ras mice irradiated with ^{56}Fe- where an increase in the incidence of invasive carcinoma was significantly increased in mice irradiated with a fractionated dose compared to single (1 Gy) doses . Additional analyses of invasive carcinoma in LA1 K-ras mice irradiated with a total dose of 1.0 Gy Si- as either an acute or fractionated dose are ongoing.

Radiation Type	Energy (MeV/n)	Total Dose (Gy)	Carcinoma incidence
Control (129sv Only)	0	0	9% (n=33)
Si- 0.4 Gy x 5	600	2	42% (n=31)**
Si- 2.0 Gy	600	2	15% (n=33) n.s
^{56}Fe- 0.2 Gy x 5	1000	1	34% (n=32)**
^{56}Fe- 1.0 Gy	1000	1	17% (n=29) n.s

Table 3.6: Incidence of invasive carcinoma in LA1 K-ras mice irradiated with a fractionated or acute doe of ^{56}Fe- or Si-.
A significant increase in invasive carcinoma was observed in LA1 K-ras mice irradiated with fractionated dose of Si- and ^{56}Fe or in comparison to unirradiated controls. This increase was not observed in mice irradiated with an acute dose. (** indicates $p \leq 0.01$, compared to unirradiated control).

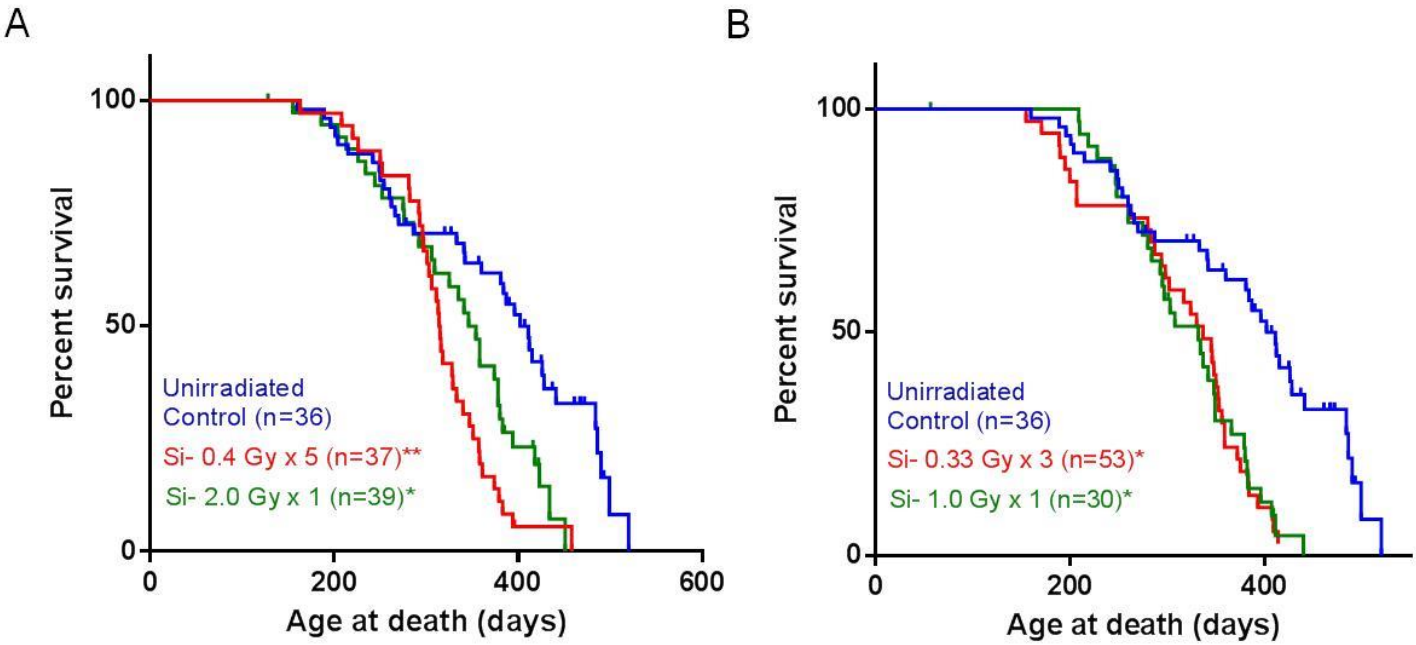

Figure 3.8: Fractionated irradiation with silicon shortens lifespan of LA1 K-ras mice. LA1 K-ras mice were irradiated a 2.0 Gy or 1.0 Gy dose of Si- as acute or fractionate dose. Survival of LA1 K-ras mice was monitored post irradiation. (A) Kaplan-Meier survival curves of LA1 K-ras mice irradiated with 2.0 Gy Si- (fractionated and acute) in comparison to unirradiated mice. A significant decrease in lifespan was observed in irradiated mice although the decrease is more significant in mice receiving fractionated doses. (B) A decrease in lifespan was also observed in LA1 K-ras mice irradiated 1.0 Gy Si- (fractionated and acute) in comparison to unirradiated mice. No differences were observed in lifespans of mice receiving either fractionated or acute dose (** indicates $p \leq 0.01$, * $p \leq 0.05$ log rank test).

3.4 Discussion

Understanding how space radiation affects the carcinogenesis process is critical to assess the risk for astronauts on long term missions. Differences between terrestrial and space radiation don't allow the extrapolation of our understanding of risks and mechanisms from X-rays and γ-rays to HZE particle radiations and SPEs. In the present study, we analyzed how the incidence of carcinoma is altered upon exposure to space radiation. The LA1 K-ras mouse model mimics cancer progression in humans by expression of oncogenic K-ras. The expression of mutant *KRAS* allele results in initiation and progression of lesions within the lungs mimicking lung cancer progression in humans.

In order to determine the effects of SPE on lung cancer progression, LA1 K-ras mice were irradiated with a whole body dose of 2.0 Gy protons over 2 hrs. The dose was delivered at energies ranging from 50-150 MeV/n simulating a SPE. Irradiation with SPE resulted in a significant shortening of life span in LA1 K-ras mice in contrast to unirradiated cohorts. Although irradiation with a whole body dose of 2.0 Gy of X-rays also decreased the lifespan of LA1 K-ras mice in comparison to unirradiated mice, this decrease was not as significant as SPE. Animals irradiated with SPE demonstrated a significant increase in invasive lung carcinoma. Approximately 41% of LA1 K-ras mice irradiated with SPE develop invasive carcinomas in contrast to 14% of unirradiated controls (age adjusted to 500 day). This increase in incidence of carcinoma was not observed in mice irradiated with terrestrial X-ray irradiation of equivalent dose. X-ray irradiation was not delivered at the same dose rate as SPE therefore it cannot be concluded if this difference in dose rates has an effect on cancer progression. Differences in the

method of energy deposition and LET between X-rays and SPE might explain the disparity in carcinoma incidence. These observations suggest that irradiation with simulated SPE is detrimental resulting in a decreased lifespan and an increase in carcinoma incidence in LA1 K-ras mice. There was also no strain specific differences observed in LA1 K-ras; both 129sv and B6.129sv strains of LA1 K-ras mice had a similar decrease in lifespan and a similar fold increase in invasive carcinoma.

The LA1 K-ras mice irradiated with acute protons (50 and 150 MeV/n) demonstrated a significant decrease in lifespan in contrast to unirradiated mice. This decrease in lifespan was even more significant than SPE irradiated mice and could be in part due to systemic effects on the mice associated with acute radiation. Fractionated doses or lower dose rates are known to have a sparing effect with terrestrial radiation in comparison to acute radiation; this may be the cause of decrease in lifespan of acute irradiated mice (Hall and Giaccia, 2006). Interestingly, acute proton irradiation (50 MeV/n) also resulted in a significant increase in incidence of invasive carcinoma (28%), similar to SPE (30%). This observation suggests that the low dose rate of simulated SPE is not responsible for the increase in invasive carcinoma. Experiments analyzing carcinoma incidence with acute proton (150 MeV/n) are ongoing.

To analyze potential mechanisms responsible for the increase in invasive carcinoma observed in mice irradiated with SPE, lungs from LA1 K-ras mice were collected 40, 70 and 100 days post-irradiation. A higher number of hyperplasias and adenomas were observed in SPE irradiated mice in contrast to unirradiated controls. Although SPE irradiated mice during this timepoint demonstrate an increase in initiation, there were no differences observed at the end of

their lifespan. The number of initiated lesions between SPE irradiated and unirradiated mice were similar with the only difference being the grade of tumors. Previously, we have shown that inflammatory signaling may play a crucial part in radiation induced carcinogenesis (Delgado et al., 2014). Therefore, we tested the expression on commonly deregulated inflammatory pathways in lung cancer. A significant difference was only observed in the expression of NFkB. SPE irradiated LA1 K-ras mice had a lower expression of phospho-NFkB in contrast to unirradiated controls. No differences in total NFkB expression were observed. Although NFkB is known to be mutated or deregulated in cancers serving as an oncogene, there is evidence that NFkB may have a dual role in carcinogenesis. Recent studies have demonstrated that during early cancer progression, NFkB may act as a tumor suppressor before switching to its oncogenic role. (Chen and Castranova, 2007). It is likely that at 70 days post-irradiation, NFkB is acting as a tumor suppressor in LA1 K-ras mice although analyses of downstream regulators from this pathway are need to confirm this claim. Significant difference in protein expression of phospho-Gab1 and phospho-Met were also observed in LA1 K-ras mice. Animals irradiated with SPE demonstrated a higher expression of both phosphorylated Gab1 and Met. Met receptor in lung cancer is known to up-regulated epithelial-mesenchymal pathways (Gherardi et al., 2012). Upon binding of a ligand (HGF), c-Met receptor signals downstream through the adaptor protein Gab1. It is likely that this upregulation of HGF pathway may be liable for the increase in invasive carcinoma observed in SPE irradiated mice, although further analyses of downstream pathways are needed. Analyses of lungs irradiated with X-rays are currently in progress.

Previously we have demonstrated that fractioned but not acute irradiation with HZE (^{56}Fe-) resulted in a significant increase in invasive carcinoma in LA1 K-ras mice (Delgado et

al., 2014). To extend this idea to other HZE particles, LA1 K-ras mice were irradiated with 2.0 and 1.0 Gy doses of fractionated Si-. Although fractionated radiation is considered sparing, mice irradiated with a 2.0 Gy fractionated dose experienced a significant decrease in lifespan compared to unirradiated controls. LA1 K-ras mice irradiated with acute Si- dose also had a shortened lifespan, but the decrease was not as significant as the fractionated dose. Similar to ^{56}Fe- studies, LA1 K-ras irradiated with fractionated dose of 2.0 Gy Si- demonstrated a significant increase in incidence of invasive carcinoma compared to unirradiated controls. This increase in carcinoma was not observed in mice irradiated with an acute dose. The adult lung has a slow-turnover rate with no specialized stem cell population. Unlike fast-turnover tissues such as colon and blood, the stem cells in the adult lung do not originate in a particular niche and do not give rise to transient amplifying cells. Upon acute irradiation, the stem cells in different lung compartments divide and trans-differentiate (a transformation of well differentiated cell type into another well-defined type) to repopulate the epithelial cell lining. Conversely, during fractionated irradiation where dose is delivered over multiple days, it is conceivable that stem-cells during the process of repopulating the epithelial lining are damaged. DNA damage caused to these stem like cells responsible for maintenance of specific lung compartments may result in the increase incidence of invasive carcinoma.

Overall, we have demonstrated that lung is highly susceptible to carcinogenesis as a result of radiation exposure. Differences between terrestrial and space radiation translate into biological effects observed in LA1 K-ras mice. Irradiation with SPE and HZE particles causes a significant shortening of lifespan and increase in invasive carcinoma. These outcomes are not observed in mice irradiated with X-rays. Pre-cancerous lesions can be driven to malignancy by

exposure to space radiation and further analyses of signaling pathways responsible for this phenotype are required to understand this progression and eventually assess the risk in astronauts.

2.5 Future Directions:

Ongoing studies focus on analyzing how inflammation affects carcinogenesis in SPE irradiated LA1 K-ras mice. Western blot analyses from 70 day post-irradiated tissue demonstrate down-regulation of NFkB although, it is not known how expression of proteins downstream of NFkB are altered. Therefore we are currently testing the expression of downstream regulators of NFkB pathway. Immunohistochemistry analyses are also being performed to determine if the NFkB pathway is altered in the tumor or the tumor microenvironment. The expression of proteins downstream of c-met and Gab1 is also being analyzed since they are differentially expressed between irradiated and unirradiated mice. Proteins playing a part in epithelial to mesenchymal transition will also be analyzed since c-met expression is known to be upregulated during this process. Future irradiation studies will focus on LA1 K-ras mice exposed to lower total doses, dose rates and energies. Different dose rates and energies may have varying effects on lung carcinogenesis. These lower doses and energies are also more relevant to the characteristic of radiation in space.

Chapter Four:

Using Bardoxolone (CDDO-EA), a Synthetic Triterpenoid as a Potential Radio-Protector Against Heavy Ion Radiation

4.1 Introduction

Radiation induced carcinogenesis risk is one of the major obstacles for long-term space missions. HZE and SPE radiations originating in space are highly ionizing in comparison to terrestrial radiation. While terrestrial radiation is sparsely ionizing, HZE and SPE are densely ionizing and capable of producing secondary radiations known as δ-rays. The secondary radiation can affect cells that are not traversed by the primary particle and can have important biological consequences. While shielding is effective against terrestrial radiation, it cannot protect against high-LET space radiation where particles can penetrate through the shielding (Blot et al., 2011). For this reason, effective countermeasures and radio-protective agents are needed to reduce the biological damage produced by the highly ionizing radiation found in space. Such countermeasures can also have important implications for therapeutic radiation oncology where the risk of secondary malignancies arising as a result of therapy is high

(Newhauser and Durante, 2011). Currently, amifostine is one of the only compounds approved as a radio-protective agent in many countries, however it has significant side effects. Therefore, there is need for effective radio-protective agents that are non-toxic and have minimal side effects.

Synthetic oleanane triterpenoids are non-cytotoxic compounds originally derived from plants that have anti-inflammatory and anti-tumor properties (Liby et al., 2007). CDDO (also known as bardoxolone) is a synthetic triterpenoid with highly multifunctional applications and a wide array of dose dependent biological responses. At lower concentrations, CDDO induces anti-inflammatory and anti-oxidant responses while at higher concentrations, CDDO can induce growth arrest and cellular apoptosis (Liby et al., 2007). At higher concentrations CDDO has been utilized as a chemotherapeutic agent against a variety of *in vivo* and *in vitro* cancer models (Liby et al., 2009; Yu and Kensler, 2005). At lower concentrations, antioxidant properties of CDDO are associated with transcription factor nuclear factor-erythroid 2–related factor 2 (Nrf2). CDDO is proposed to stabilize Nrf2 by interacting with its negative regulator Kelch-like ECH-associated protein 1 (Keap1). After Nrf2 is dissociated from Keap1, it translocates into the nucleus upon phosphorylation and activates antioxidant response elements (ARE) **(Figure 4.1)** (Kobayashi and Yamamoto, 2006).

Previously it has been demonstrated that CDDO-Me (bardoxolone-methyl) protects human colonic and bronchial epithelial cells against radiation induced damage by activating Nrf2 (Eskiocak et al., 2010; Kim et al., 2013). The compound is radio-protective against both terrestrial and space radiation *in vitro*. In a recent study, CDDO-EA (bardoxolone-ethylamide)

used as a countermeasure agent, protected wildtype mice against exposure to lethal dose irradiation. Mice on CDDO-EA diet were able to repair their DNA damage more quickly as opposed to mice on control diet (Kim et al., 2012). CDDO-EA also protected the mice from acute gastrointestinal toxicity resulting in improved overall survival **(Figure 4.2)**. Based upon these observations, we hypothesize that LA1 K-ras mice treated with CDDO during irradiation may experience a lower incidence of invasive carcinoma.

In the present study, LA1 K-ras mice were treated with CDDO-EA three days prior to irradiation. The compound was administered orally by integration into the animal chow. Animals were taken off the diet the day after irradiation and the incidence of invasive carcinoma was analyzed at the end of the animal's lifespan. LA1 K-ras mice for this study were irradiated with fractionated ^{56}Fe- and simulated SPE since these types of irradiation result in the highest increase in the incidence of invasive carcinoma.

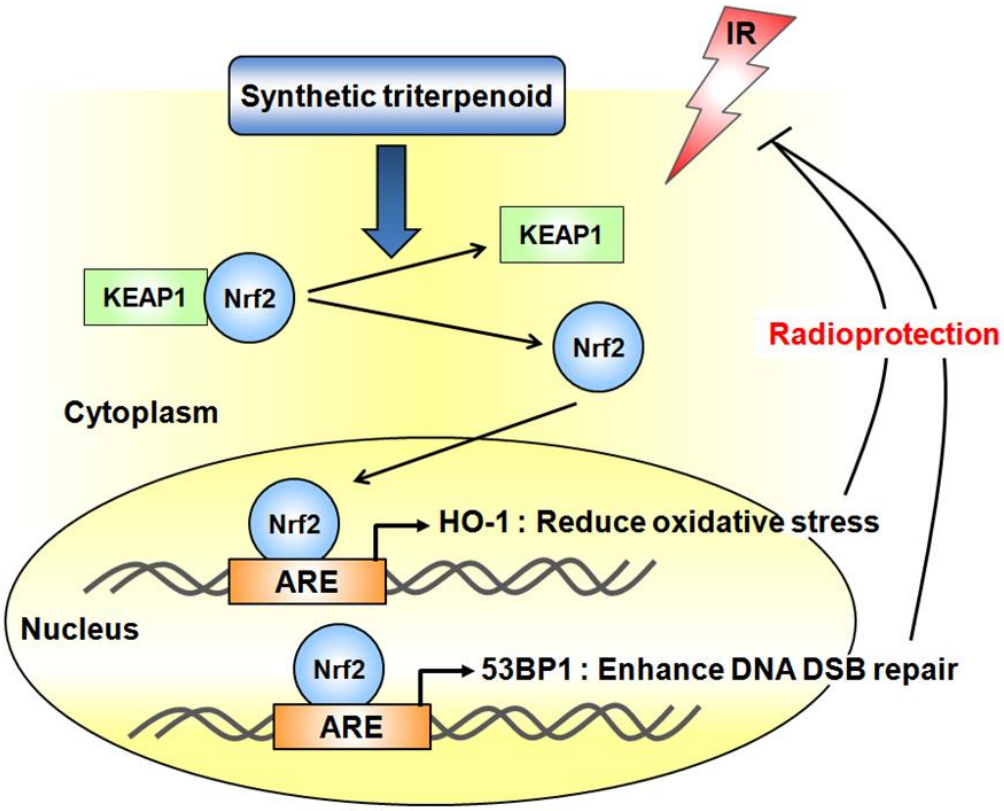

Figure 4.1: CDDO allows Nrf2 translocation into the nucleus.
At lower concentrations CDDO allows Nrf2 translocation into the nucleus where it binds to ARE elements helping reduce oxidative stress.

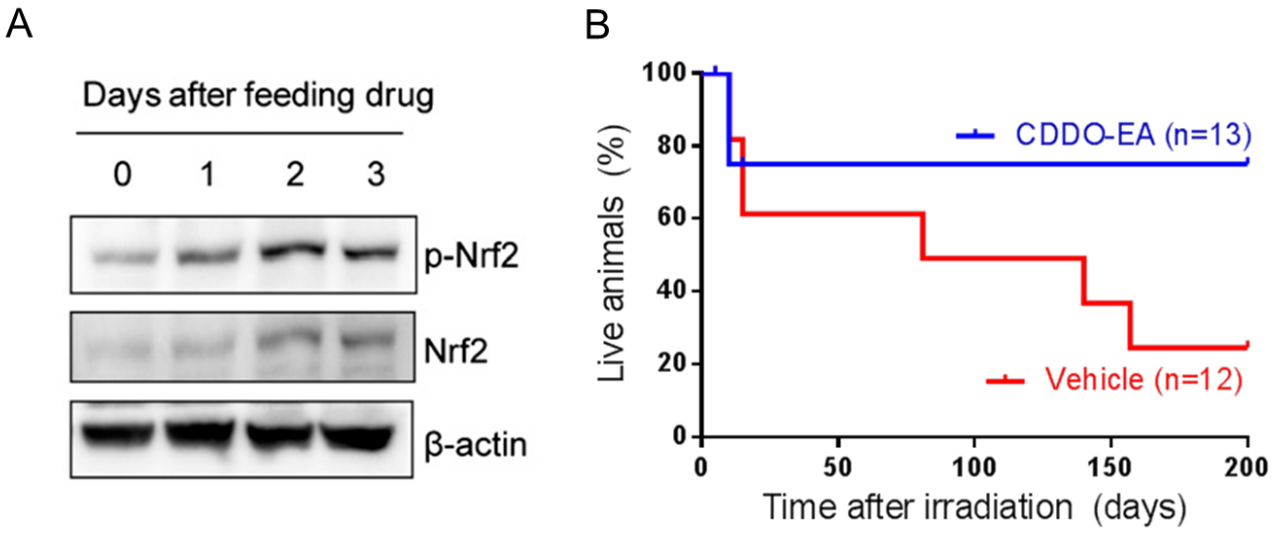

Figure 4.2: CDDO increases survival of wildtype mice after lethal doses of irradiation. CDDO used as countermeasure agent against lethal dose of X-ray radiation. (A) CDDO was administered orally through the diet three days prior to irradiation. An upregulation in phosphor-Nrf2 was observed as a result of CDDO treatment. (B) Mice fed CDDO countermeasure diet had an increased survival in comparison to control mice (Data from Dr. Sang Kim).

4.2 Materials and Methods

4.2.1 LA1 K-ras Mice:

The LA1 K-ras mice used to analyze the efficacy of CDDO-EA as a potential radio-protector again HZE radiation were backcrossed into 129sv mouse backgrounds only (Raju et al., 1978). All animal experiments were reviewed and approved by the Institutional Animal Care and Use Committee (IACUC) at University of Texas Southwestern Medical Center (Dallas, TX) and Brookhaven National Laboratory (Upton, NY). Animals were housed and bred in automated ventilated cages at UTSW in a specific pathogen free (SPF) facility. Heterozygote LA1 K-ras mice were crossed with wild-type mice of the same background.

4.2.2 Study Design for CDDO-EA Countermeasure Experiments:

To evaluate the impact of CDDO-EA as a potential countermeasure against HZE radiation, 129sv LA1 K-ras mice were fed chow containing CDDO-EA or control. The concentration of CDDO-EA in the diet was 400mg/kg (provided by Reata Pharmaceuticals and Michael Sporn, Dartmouth Medical School, Hanover, NH) and prepared into chow pellets by Purina Mills). Animal diet was changed three days prior to the radiation scheme to either chow containing CDDO-EA or control. Mice were taken of the diet after the last day of the radiation scheme. Animals were randomly assigned to all experimental cohorts, irradiated and monitored until death or euthanization due to health concerns.

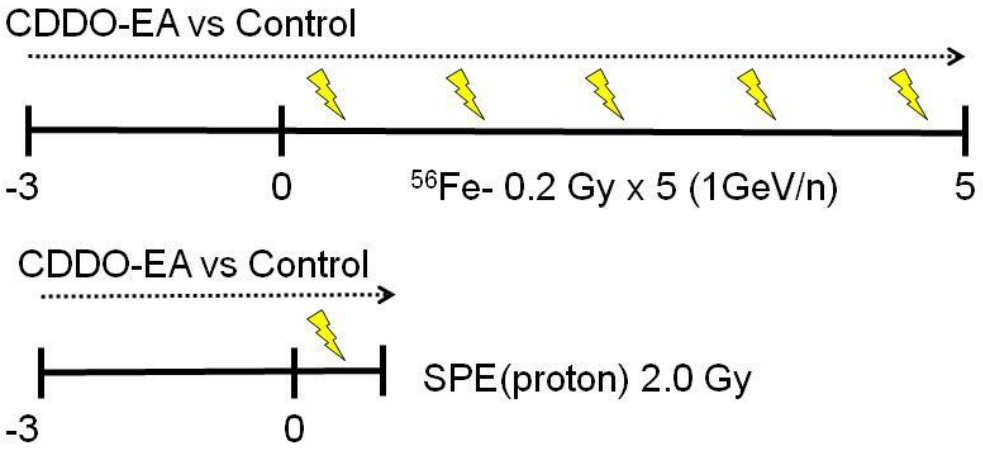

Figure 4.3: Irradiation scheme with CDDO-EA utilized as a countermeasure in LA1 K-ras mice
LA1 K-ras mice were placed on countermeasure CDDO-EA diet three days prior to irradiation. The mice were irradiated with a fractionated dose of 1.0 Gy of ^{56}Fe- or 2.0 Gy simulated SPE.

4.2.3 Irradiation:

LA1 K-ras (129sv background only) were irradiated with simulated SPE or a fractionated dose of ^{56}Fe- to analyze CDDO-EA's potential as radio-protector. The rationale for using these irradiation schemes was the high incidence of lung adenocarcinoma observed in LA1 K-ras mice after exposure to them. A total body dose of 2.0 Gy comprised of protons over 2 hours (dose rate of 1.0 Gy/hr) was delivered to LA1 K-ras mice. The simulation deposited the dose at energies ranging from 50 to 150 MeV/n. Whole body dose of 1.0 Gy (1 GeV/n) ^{56}Fe- was delivered as a fraction over five days (0.2 Gy/day). The animals irradiated ranged between the age of 5 and 15 weeks.

4.2.4 Statistical Analysis:

Survival analysis of Kaplan-Meier curves were performed using long rank test. Statistical analysis for histopathological studies was performed using two-tailed chi square test.

4.3 Results

4.3.1 Effects of CDDO-EA diet on Tumor Progression in LA1 K-ras mice

To investigate how CDDO-EA affects tumor progression, 50 day old LA1 K-ras mice were placed on either CDDO-EA or control diets **(Figure 4.1 A)**. Mice at this age only present small hyperplastic lesions in the lung and adenomas are rare. LA1 K-ras mice on CDDO-EA diet (400mg/kg) did not show any toxicity or adverse health effects. To analyze tumor progression, LA1 K-ras mice were necropsied after 50 days of continuous diet containing CDDO-EA. Mice on control diet showed significant numbers of lesions at 100 days of age **(Figure 4.2 B)**. This rate of progression was consistent with what was observed in LA1 K-ras mice on regular chow. In contrast, LA1 K-ras mice fed CDDO-EA demonstrated a significantly fewer number of lesions **(Figure 4.2 C)**. The lesions were also smaller in size and the majority of them had not progressed pass the hyperplastic stage. These observations demonstrate that treatment with CDDO-EA reduces the onset of tumors in LA1 K-ras mice. CDDO-EA treatment of LA1 K-ras mice with significant tumor burden (greater than 250 days) did not result in regression of tumors within the lungs (data not shown). These observations indicate that CDDO-EA is effective in delaying the onset of tumors in LA1 K-ras mice.

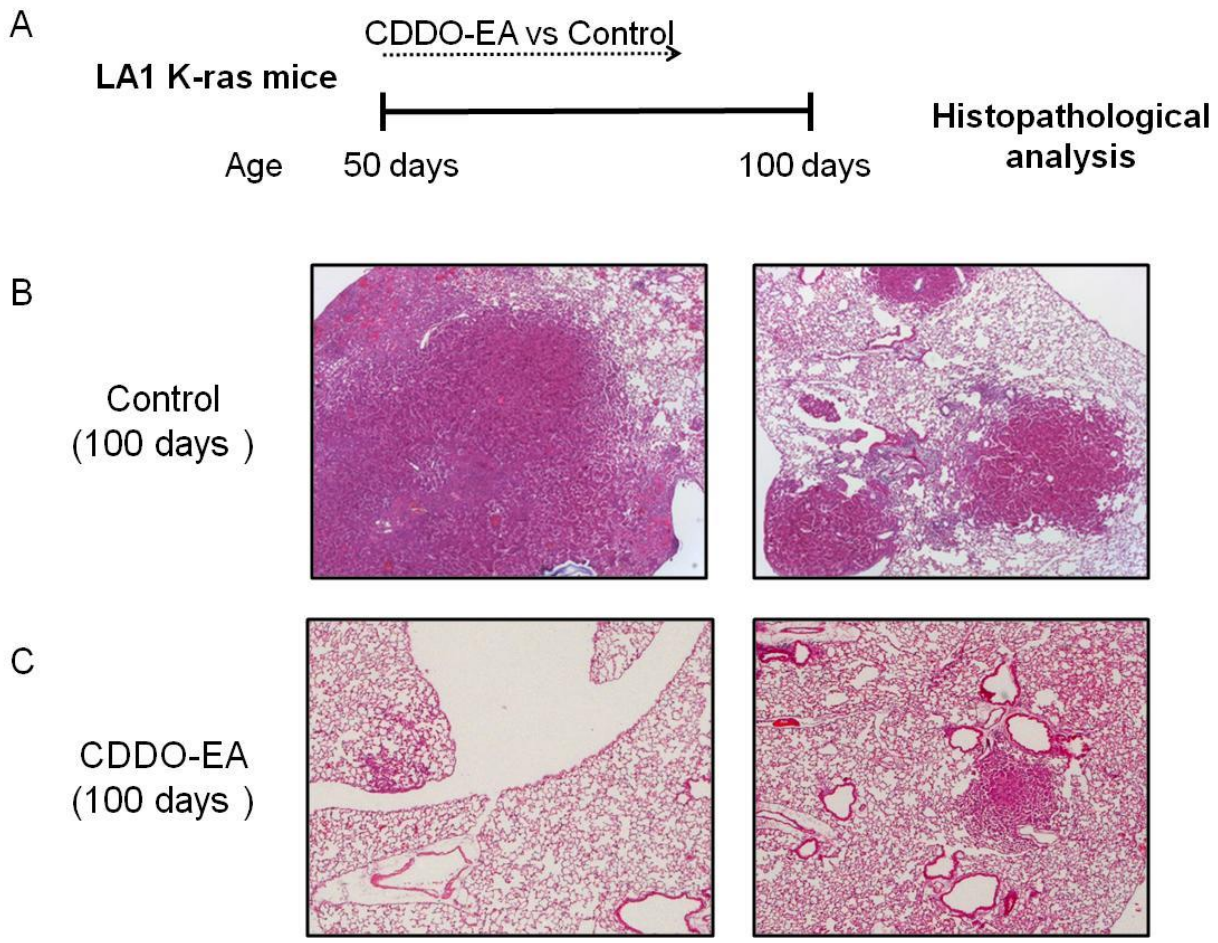

Figure 4.4: CDDO-EA diet reduces the onset of tumors in LA1 K-ras mice
To analyze the effects of CDDO-EA on LA1 K-ras mice, (A) 50 day old LA1 K-ras mice given a diet containing CDDO-EA or a control diet. Histopathological analyses were performed after 50 days of continuous treatment with the compound. (B) Mice on control diet demonstrated initiation and progression of tumors akin to what was observed in 100 day old LA1 K-ras mice. (C) Mice on CDDO-EA diet demonstrated a significantly lower number of tumors in contrast to animals on the control diet.

4.3.2 Analyzing the Potential of CDDO-EA as Radio-protector After Irradiation with SPE and HZE Particles.

LA1 K-ras mice irradiated with SPE or fractionated ^{56}Fe-demonstrate the highest increase in incidence of carcinoma. Therefore these irradiation schemes were chosen to analyze the potential of CDDO-EA as a radio-protector. The objective of this experiment was to observe if treatment with a countermeasure diet containing CDDO-EA can reduce the incidence of invasive carcinoma in irradiated LA1 K-ras mice. LA1 K-ras mice were fed CDDO-EA or control chow three days prior to irradiation. Mice were kept on the CDDO-EA or control diet through the last day of irradiation. This experimental setup helped assess CDDO-EAs potential as a countermeasure in particular. LA1 K-ras mice (129sv strain) are susceptible to lung carcinoma and approximately 9% of mice demonstrate disease progression to the invasive carcinoma stage. A significant decrease in the incidence of invasive carcinoma was observed in mice treated with CDDO-EA countermeasure diet. For fractionated ^{56}Fe- irradiation, LA1 K-ras mice were irradiated with a total dose of 1.0 Gy split over 5 days (0.2 Gy/day). Approximately 17% of LA1 K-ras mice on CDDO-EA diet during the irradiation had invasive carcinoma in contrast to 34% in mice on control diet **(Table 4.2)**. A similar decrease in the incidence of invasive carcinoma was also observed in LA1 K-ras mice of CDDO-EA diet during SPE irradiation. Only 19% of animals on CDDO-EA diet demonstrated disease progression to carcinoma stage in comparison to 30% of animals on control diet. These observations demonstrate that CDDO-EA can be used as a potential countermeasure against HZE and SPE radiations.

Irradiation Group	Total Dose	Overall Carcinoma Incidence
Control (129sv Only)	0.0	9% (n=33)
^{56}Fe- 0.2 Gy x 5	1.0	34% (n=32)**
^{56}Fe- 0.2 Gy x 5 (CDDO-EA)	1.0	17% (n=41) n.s.
SPE- 2.0 Gy	2.0	30% (n=47)**
SPE- 2.0 Gy (CDDO-EA)	2.0	19% (N=47) n.s.

Table 4.1: Incidence of invasive carcinoma in unirradiated LA1 K-ras mice and mice irradiated with CDDO-EA countermeasure diet.
A significant increase in invasive carcinoma was observed in LA1 K-ras mice irradiated with SPE and fractionated ^{56}Fe- in comparison to unirradiated cohorts. No significant increase in incidence of invasive carcinoma was observed in mice irradiated with SPE and fractionated ^{56}Fe- on countermeasure CDDO-EA diet (** indicates $p \leq 0.01$, compared to unirradiated control).

4.4 Discussion

Discovery of novel radio-protective compounds in essential since space radiation cannot be successfully shielded like terrestrial radiation. In this study, we analyzed the potential of CDDO-EA as a radio-protector against HZE and SPE radiation. Before testing CDDO-EA for countermeasure studies, we analyzed the effects of CDDO-EA on tumor progression. Previously it has been demonstrated that CDDO-EA can suppress the growth of chemically induce lung tumors therefore we tested if the compound could also regress K-ras driven tumors (Liby et al., 2007). Continuous treatment of 50 day old LA1-Kras mice significantly prolonged the onset of tumors. Mice on CDDO-EA diet had fewer and smaller lesions in comparison to control mice. However CDDO-EA was not able to reduce tumors in mice with significant tumor burden (over 250 day old mice). These observations indicate that CDDO-EA is able to suppress the initiation of tumors in LA1 K-ras however once significant tumor burden is established, it loses it chemotherapeutic potential. Oxidative and inflammatory stress plays a critical role in tumor progression and treatment with CDDO-EA likely reduces these stresses resulting in delayed onset of tumors in LA1 K-ras mice. Tumors during progression can tip the balance between pro- and anti-inflammatory factors in their favor resulting in the immune system aiding carcinogenesis (Elinav et al., 2013).

LA1 K-ras mice irradiated with fractionated ^{56}Fe- and simulated SPE were treated with CDDO-EA countermeasure diet three days prior to radiation. There was a significant decrease in incidence of invasive carcinoma observed in LA1 K-ras mice placed on countermeasure diet compared to control animals. However, there were no survival differences observed between the

two groups. A similar decrease in lifespan was observed in mice on CDDO-EA or control diets even though the mice on CDDO-EA demonstrated a significant reduction in carcinoma. Secondary health concerns beside tumor burden may be responsible for the shortening of lifespan and therefore no differences were observed between the two groups. The decrease in invasive carcinoma in irradiated LA1 K-ras mice can be attributed to the antioxidant properties of CDDO-EA (Liby et al., 2007). Most cells traversed by the primary radiation particle do not survive due to the high level of energy deposited, however cells exposed to low-LET δ-rays may survive. Oxidative stress and inefficient DNA repair in these surviving cells leads to mutations or genomic instability eventually resulting in carcinogenesis (Li et al., 2014). It is probable that CDDO-EA helps reduce oxidative stress in cells exposed to secondary radiation resulting in a smaller probability of cells acquiring mutations as a result of free-radical damage. Further experiments are required to analyze DNA repair in irradiated mice on countermeasure diet.

Overall we have demonstrated that CDDO-EA is a potent radio-protector against HZE and SPE radiations. Further studies are required to analyze DNA repair kinetics and oxidative stress in irradiated tissues. Countermeasure agents such as CDDO-EA can potentially help protect astronauts against space radiation. With the increasing use of particle radiation in cancer therapy, it may also help protect patients against secondary malignancies.

2.5 Future Directions:

Ongoing studies focus on analyzing DNA repair kinetics and oxidative stress in irradiated LA1-Kras mice on CDDO-EA diet. In particular, lung tissue at short time-points (up to 96 hours) after irradiation will be analyzed to assess if CDDO-EA reduces oxidative stress after irradiation and accelerates DNA repair. Nrf2 upregulation after treatment with CDDO-EA may help scavenge free-radical species resulting in lower over DNA damage. CDDO-EA will also be used as mitigator for future studies where LA1 K-ras mice will be fed CDDO-EA diet after irradiation.

Bibliography:

Alison, M.R., Vig, P., Russo, F., Bigger, B.W., Amofah, E., Themis, M., Forbes, S., 2004. Hepatic stem cells: from inside and outside the liver? Cell proliferation 37, 1-21.

Asaithamby, A., Chen, D.J., 2011. Mechanism of cluster DNA damage repair in response to high-atomic number and energy particles radiation. Mutation research 711, 87-99.

Asaithamby, A., Hu, B., Delgado, O., Ding, L.H., Story, M.D., Minna, J.D., Shay, J.W., Chen, D.J., 2011. Irreparable complex DNA double-strand breaks induce chromosome breakage in organotypic three-dimensional human lung epithelial cell culture. Nucleic acids research 39, 5474-5488.

Asgrimsson, V., Gudjonsson, T., Gudmundsson, G.H., Baldursson, O., 2006. Novel effects of azithromycin on tight junction proteins in human airway epithelia. Antimicrobial agents and chemotherapy 50, 1805-1812.

Bals, R., Beisswenger, C., Blouquit, S., Chinet, T., 2004. Isolation and air-liquid interface culture of human large airway and bronchiolar epithelial cells. Journal of cystic fibrosis : official journal of the European Cystic Fibrosis Society 3 Suppl 2, 49-51.

Blenkinsopp, W.K., 1967. Proliferation of respiratory tract epithelium in the rat. Experimental cell research 46, 144-154.

Blot, W.J., Cohen, S.S., Aldrich, M., McLaughlin, J.K., Hargreaves, M.K., Signorello, L.B., 2011. Lung cancer risk among smokers of menthol cigarettes. Journal of the National Cancer Institute 103, 810-816.

Boers, J.E., Ambergen, A.W., Thunnissen, F.B., 1998. Number and proliferation of basal and parabasal cells in normal human airway epithelium. American journal of respiratory and critical care medicine 157, 2000-2006.

Boers, J.E., Ambergen, A.W., Thunnissen, F.B., 1999. Number and proliferation of clara cells in normal human airway epithelium. American journal of respiratory and critical care medicine 159, 1585-1591.

Boggaram, V., 2009. Thyroid transcription factor-1 (TTF-1/Nkx2.1/TITF1) gene regulation in the lung. Clin Sci (Lond) 116, 27-35.

Borthwick, D.W., Shahbazian, M., Krantz, Q.T., Dorin, J.R., Randell, S.H., 2001. Evidence for stem-cell niches in the tracheal epithelium. American journal of respiratory cell and molecular biology 24, 662-670.

Bowden, D.H., Davies, E., Wyatt, J.P., 1968. Cytodynamics of pulmonary alveolar cells in the mouse. Archives of pathology 86, 667-670.

Brambilla, E., Travis, W.D., Colby, T.V., Corrin, B., Shimosato, Y., 2001. The new World Health Organization classification of lung tumours. The European respiratory journal : official journal of the European Society for Clinical Respiratory Physiology 18, 1059-1068.

Breuer, R., Zajicek, G., Christensen, T.G., Lucey, E.C., Snider, G.L., 1990. Cell kinetics of normal adult hamster bronchial epithelium in the steady state. American journal of respiratory cell and molecular biology 2, 51-58.

Breuer, R.H., Postmus, P.E., Smit, E.F., 2005. Molecular pathology of non-small-cell lung cancer. Respiration; international review of thoracic diseases 72, 313-330.

Brownson, R.C., Alavanja, M.C., Caporaso, N., Simoes, E.J., Chang, J.C., 1998. Epidemiology and prevention of lung cancer in nonsmokers. Epidemiologic reviews 20, 218-236.

Cardoso, W.V., Lu, J., 2006. Regulation of early lung morphogenesis: questions, facts and controversies. Development 133, 1611-1624.

Chapman, H.A., Li, X., Alexander, J.P., Brumwell, A., Lorizio, W., Tan, K., Sonnenberg, A., Wei, Y., Vu, T.H., 2011. Integrin alpha6beta4 identifies an adult distal lung epithelial population with regenerative potential in mice. The Journal of clinical investigation 121, 2855-2862.

Chen, F., Castranova, V., 2007. Nuclear factor-kappaB, an unappreciated tumor suppressor. Cancer research 67, 11093-11098.

Cole, B.B., Smith, R.W., Jenkins, K.M., Graham, B.B., Reynolds, P.R., Reynolds, S.D., 2010. Tracheal Basal cells: a facultative progenitor cell pool. The American journal of pathology 177, 362-376.

Cucinotta, F.A., Nikjoo, H., Goodhead, D.T., 1998. The effects of delta rays on the number of particle-track traversals per cell in laboratory and space exposures. Radiation research 150, 115-119.

Cucinotta, F.A., Wilson, J.W., Shinn, J.L., Badavi, F.F., Badhwar, G.D., 1996. Effects of target fragmentation on evaluation of LET spectra from space radiations: implications for space radiation protection studies. Radiation measurements 26, 923-934.

Cunha, G.R., 2008. Mesenchymal-epithelial interactions: past, present, and future. Differentiation; research in biological diversity 76, 578-586.

Delgado, O., Batten, K.G., Richardson, J.A., Xie, X.J., Gazdar, A.F., Kaisani, A.A., Girard, L., Behrens, C., Suraokar, M., Fasciani, G., Wright, W.E., Story, M.D., Wistuba, II, Minna, J.D., Shay, J.W., 2014. Radiation-enhanced lung cancer progression in a transgenic mouse model of lung cancer is predictive of outcomes in human lung and breast cancer. Clinical cancer research : an official journal of the American Association for Cancer Research 20, 1610-1622.

Delgado, O., Kaisani, A.A., Spinola, M., Xie, X.J., Batten, K.G., Minna, J.D., Wright, W.E., Shay, J.W., 2011. Multipotent capacity of immortalized human bronchial epithelial cells. PloS one 6, e22023.

Dingfelder, M., 2012. Track-structure simulations for charged particles. Health physics 103, 590-595.

Domyan, E.T., Ferretti, E., Throckmorton, K., Mishina, Y., Nicolis, S.K., Sun, X., 2011. Signaling through BMP receptors promotes respiratory identity in the foregut via repression of Sox2. Development 138, 971-981.

Dor, Y., Brown, J., Martinez, O.I., Melton, D.A., 2004. Adult pancreatic beta-cells are formed by self-duplication rather than stem-cell differentiation. Nature 429, 41-46.

Downward, J., 2003. Targeting RAS signalling pathways in cancer therapy. Nature reviews. Cancer 3, 11-22.

Elinav, E., Nowarski, R., Thaiss, C.A., Hu, B., Jin, C., Flavell, R.A., 2013. Inflammation-induced cancer: crosstalk between tumours, immune cells and microorganisms. Nature reviews. Cancer 13, 759-771.

Engelhardt, J.F., Schlossberg, H., Yankaskas, J.R., Dudus, L., 1995. Progenitor cells of the adult human airway involved in submucosal gland development. Development 121, 2031-2046.

Eskiocak, U., Kim, S.B., Roig, A.I., Kitten, E., Batten, K., Cornelius, C., Zou, Y.S., Wright, W.E., Shay, J.W., 2010. CDDO-Me protects against space radiation-induced transformation of human colon epithelial cells. Radiation research 174, 27-36.

Evans, M.J., Shami, S.G., Cabral-Anderson, L.J., Dekker, N.P., 1986. Role of nonciliated cells in renewal of the bronchial epithelium of rats exposed to NO2. The American journal of pathology 123, 126-133.

Evans, M.J., Van Winkle, L.S., Fanucchi, M.V., Plopper, C.G., 2001. Cellular and molecular characteristics of basal cells in airway epithelium. Experimental lung research 27, 401-415.

Fehrenbach, H., 2001. Alveolar epithelial type II cell: defender of the alveolus revisited. Respiratory research 2, 33-46.

Fessart, D., Begueret, H., Delom, F., 2013. 3D culture model to distinguish normal from malignant human bronchial epithelial cells. The European respiratory journal : official journal of the European Society for Clinical Respiratory Physiology.

Finkel, T., Holbrook, N.J., 2000. Oxidants, oxidative stress and the biology of ageing. Nature 408, 239-247.

Franzdottir, S.R., Axelsson, I.T., Arason, A.J., Baldursson, O., Gudjonsson, T., Magnusson, M.K., 2010. Airway branching morphogenesis in three dimensional culture. Respiratory research 11, 162.

Fuchs, E., Tumbar, T., Guasch, G., 2004. Socializing with the neighbors: stem cells and their niche. Cell 116, 769-778.

Gadgeel, S.M., Ramalingam, S.S., Kalemkerian, G.P., 2012. Treatment of lung cancer. Radiologic clinics of North America 50, 961-974.

Gazdar, A.F., 2010. Should we continue to use the term non-small-cell lung cancer? Annals of oncology : official journal of the European Society for Medical Oncology / ESMO 21 Suppl 7, vii225-229.

Gherardi, E., Birchmeier, W., Birchmeier, C., Vande Woude, G., 2012. Targeting MET in cancer: rationale and progress. Nature reviews. Cancer 12, 89-103.

Giangreco, A., Reynolds, S.D., Stripp, B.R., 2002. Terminal bronchioles harbor a unique airway stem cell population that localizes to the bronchoalveolar duct junction. The American journal of pathology 161, 173-182.

Hackett, T.L., Shaheen, F., Johnson, A., Wadsworth, S., Pechkovsky, D.V., Jacoby, D.B., Kicic, A., Stick, S.M., Knight, D.A., 2008. Characterization of side population cells from human airway epithelium. Stem Cells 26, 2576-2585.

Hanahan, D., Weinberg, R.A., 2000. The hallmarks of cancer. Cell 100, 57-70.

Hanahan, D., Weinberg, R.A., 2011. Hallmarks of cancer: the next generation. Cell 144, 646-674.

Heine, U.I., Munoz, E.F., Flanders, K.C., Roberts, A.B., Sporn, M.B., 1990. Colocalization of TGF-beta 1 and collagen I and III, fibronectin and glycosaminoglycans during lung branching morphogenesis. Development 109, 29-36.

Herriges, M., Morrisey, E.E., 2014. Lung development: orchestrating the generation and regeneration of a complex organ. Development 141, 502-513.

Hirsch, F.R., Varella-Garcia, M., Bunn, P.A., Jr., Di Maria, M.V., Veve, R., Bremmes, R.M., Baron, A.E., Zeng, C., Franklin, W.A., 2003. Epidermal growth factor receptor in non-small-cell lung carcinomas: correlation between gene copy number and protein expression and impact on prognosis. Journal of clinical oncology : official journal of the American Society of Clinical Oncology 21, 3798-3807.

Hong, K.U., Reynolds, S.D., Giangreco, A., Hurley, C.M., Stripp, B.R., 2001. Clara cell secretory protein-expressing cells of the airway neuroepithelial body microenvironment include a label-retaining subset and are critical for epithelial renewal after progenitor cell depletion. American journal of respiratory cell and molecular biology 24, 671-681.

Hong, K.U., Reynolds, S.D., Watkins, S., Fuchs, E., Stripp, B.R., 2004a. Basal cells are a multipotent progenitor capable of renewing the bronchial epithelium. The American journal of pathology 164, 577-588.

.Hong, K.U., Reynolds, S.D., Watkins, S., Fuchs, E., Stripp, B.R., 2004b. In vivo differentiation potential of tracheal basal cells: evidence for multipotent and unipotent subpopulations. American journal of physiology. Lung cellular and molecular physiology 286, L643-649.

Ishihara, K., Hirano, T., 2002. Molecular basis of the cell specificity of cytokine action. Biochimica et biophysica acta 1592, 281-296.

Karnoub, A.E., Weinberg, R.A., 2008. Ras oncogenes: split personalities. Nature reviews. Molecular cell biology 9, 517-531.

Katz, R., Cucinotta, F.A., 1999. Tracks to therapy. Radiation measurements 31, 379-388.

Kauffman, S.L., 1980. Cell proliferation in the mammalian lung. International review of experimental pathology 22, 131-191.

Kim, C.F., Jackson, E.L., Woolfenden, A.E., Lawrence, S., Babar, I., Vogel, S., Crowley, D., Bronson, R.T., Jacks, T., 2005. Identification of bronchioalveolar stem cells in normal lung and lung cancer. Cell 121, 823-835.

Kim, S.B., Ly, P., Kaisani, A., Zhang, L., Wright, W.E., Shay, J.W., 2013. Mitigation of radiation-induced damage by targeting EGFR in noncancerous human epithelial cells. Radiation research 180, 259-267.

Kim, S.B., Pandita, R.K., Eskiocak, U., Ly, P., Kaisani, A., Kumar, R., Cornelius, C., Wright, W.E., Pandita, T.K., Shay, J.W., 2012. Targeting of Nrf2 induces DNA damage signaling and protects colonic epithelial cells from ionizing radiation. Proceedings of the National Academy of Sciences of the United States of America 109, E2949-2955.

Kimura, J., Deutsch, G.H., 2007. Key mechanisms of early lung development. Pediatric and developmental pathology : the official journal of the Society for Pediatric Pathology and the Paediatric Pathology Society 10, 335-347.

Kobayashi, M., Yamamoto, M., 2006. Nrf2-Keap1 regulation of cellular defense mechanisms against electrophiles and reactive oxygen species. Advances in enzyme regulation 46, 113-140.

Kosaka, T., Yatabe, Y., Endoh, H., Kuwano, H., Takahashi, T., Mitsudomi, T., 2004. Mutations of the epidermal growth factor receptor gene in lung cancer: biological and clinical implications. Cancer research 64, 8919-8923.

Krane, C.M., Fortner, C.N., Hand, A.R., McGraw, D.W., Lorenz, J.N., Wert, S.E., Towne, J.E., Paul, R.J., Whitsett, J.A., Menon, A.G., 2001. Aquaporin 5-deficient mouse lungs are hyperresponsive to cholinergic stimulation. Proceedings of the National Academy of Sciences of the United States of America 98, 14114-14119.

Kris, M.G., Natale, R.B., Herbst, R.S., Lynch, T.J., Jr., Prager, D., Belani, C.P., Schiller, J.H., Kelly, K., Spiridonidis, H., Sandler, A., Albain, K.S., Cella, D., Wolf, M.K., Averbuch, S.D., Ochs, J.J., Kay, A.C., 2003. Efficacy of gefitinib, an inhibitor of the epidermal growth factor receptor tyrosine kinase, in symptomatic patients with non-small cell lung cancer: a randomized trial. JAMA : the journal of the American Medical Association 290, 2149-2158.

.Larsen, J.E., Minna, J.D., 2011. Molecular biology of lung cancer: clinical implications. Clinics in chest medicine 32, 703-740.

Lawson, G.W., Van Winkle, L.S., Toskala, E., Senior, R.M., Parks, W.C., Plopper, C.G., 2002. Mouse strain modulates the role of the ciliated cell in acute tracheobronchial airway injury-distal airways. The American journal of pathology 160, 315-327.

Le Calvez, F., Mukeria, A., Hunt, J.D., Kelm, O., Hung, R.J., Taniere, P., Brennan, P., Boffetta, P., Zaridze, D.G., Hainaut, P., 2005. TP53 and KRAS mutation load and types in lung cancers in relation to tobacco smoke: distinct patterns in never, former, and current smokers. Cancer research 65, 5076-5083.

Leach, J.K., Van Tuyle, G., Lin, P.S., Schmidt-Ullrich, R., Mikkelsen, R.B., 2001. Ionizing radiation-induced, mitochondria-dependent generation of reactive oxygen/nitrogen. Cancer research 61, 3894-3901.

Lee, G.Y., Kenny, P.A., Lee, E.H., Bissell, M.J., 2007. Three-dimensional culture models of normal and malignant breast epithelial cells. Nature methods 4, 359-365.

Li, M., Gonon, G., Buonanno, M., Autsavapromporn, N., de Toledo, S.M., Pain, D., Azzam, E.I., 2014. Health risks of space exploration: targeted and nontargeted oxidative injury by high-charge and high-energy particles. Antioxidants & redox signaling 20, 1501-1523.

Liby, K., Risingsong, R., Royce, D.B., Williams, C.R., Ma, T., Yore, M.M., Sporn, M.B., 2009. Triterpenoids CDDO-methyl ester or CDDO-ethyl amide and rexinoids LG100268 or NRX194204 for prevention and treatment of lung cancer in mice. Cancer Prev Res (Phila) 2, 1050-1058.

Liby, K.T., Yore, M.M., Sporn, M.B., 2007. Triterpenoids and rexinoids as multifunctional agents for the prevention and treatment of cancer. Nature reviews. Cancer 7, 357-369.

Little, M.P., 2009. Cancer and non-cancer effects in Japanese atomic bomb survivors. Journal of radiological protection : official journal of the Society for Radiological Protection 29, A43-59.

Liu, J.Y., Nettesheim, P., Randell, S.H., 1994. Growth and differentiation of tracheal epithelial progenitor cells. The American journal of physiology 266, L296-307.

Lynch, T.J., Bell, D.W., Sordella, R., Gurubhagavatula, S., Okimoto, R.A., Brannigan, B.W., Harris, P.L., Haserlat, S.M., Supko, J.G., Haluska, F.G., Louis, D.N., Christiani, D.C., Settleman, J., Haber, D.A., 2004. Activating mutations in the epidermal growth factor receptor underlying responsiveness of non-small-cell lung cancer to gefitinib. The New England journal of medicine 350, 2129-2139.

Madri, J.A., Williams, S.K., 1983. Capillary endothelial cell cultures: phenotypic modulation by matrix components. The Journal of cell biology 97, 153-165.

Madsen, J., Tornoe, I., Nielsen, O., Koch, C., Steinhilber, W., Holmskov, U., 2003. Expression and localization of lung surfactant protein A in human tissues. American journal of respiratory cell and molecular biology 29, 591-597.

Maeda, Y., Dave, V., Whitsett, J.A., 2007. Transcriptional control of lung morphogenesis. Physiological reviews 87, 219-244.

Mahlapuu, M., Ormestad, M., Enerback, S., Carlsson, P., 2001. The forkhead transcription factor Foxf1 is required for differentiation of extra-embryonic and lateral plate mesoderm. Development 128, 155-166.

McQualter, J.L., Yuen, K., Williams, B., Bertoncello, I., 2010. Evidence of an epithelial stem/progenitor cell hierarchy in the adult mouse lung. Proceedings of the National Academy of Sciences of the United States of America 107, 1414-1419.

Merlino, G.T., Xu, Y.H., Ishii, S., Clark, A.J., Semba, K., Toyoshima, K., Yamamoto, T., Pastan, I., 1984. Amplification and enhanced expression of the epidermal growth factor receptor gene in A431 human carcinoma cells. Science 224, 417-419.

Michaels, H.B., Hunt, J.W., 1978. A model for radiation damage in cells by direct effect and by indirect effect: a radiation chemistry approach. Radiation research 74, 23-34.

Miura, T., Shiota, K., 2000. Time-lapse observation of branching morphogenesis of the lung bud epithelium in mesenchyme-free culture and its relationship with the localization of actin filaments. The International journal of developmental biology 44, 899-902.

Morrisey, E.E., Hogan, B.L., 2010. Preparing for the first breath: genetic and cellular mechanisms in lung development. Developmental cell 18, 8-23.

Mueller, M.M., Fusenig, N.E., 2004. Friends or foes - bipolar effects of the tumour stroma in cancer. Nature reviews. Cancer 4, 839-849.

Newhauser, W.D., Durante, M., 2011. Assessing the risk of second malignancies after modern radiotherapy. Nature reviews. Cancer 11, 438-448.

Neyman, J., Puri, P.S., 1976. A structural model of radiation effects in living cells. Proceedings of the National Academy of Sciences of the United States of America 73, 3360-3363.

Nyeng, P., Norgaard, G.A., Kobberup, S., Jensen, J., 2008. FGF10 maintains distal lung bud epithelium and excessive signaling leads to progenitor state arrest, distalization, and goblet cell metaplasia. BMC developmental biology 8, 2.

Odom, M.J., Snyder, J.M., Mendelson, C.R., 1987. Adenosine 3',5'-monophosphate analogs and beta-adrenergic agonists induce the synthesis of the major surfactant apoprotein in human fetal lung in vitro. Endocrinology 121, 1155-1163.

Ohuchi, H., Hori, Y., Yamasaki, M., Harada, H., Sekine, K., Kato, S., Itoh, N., 2000. FGF10 acts as a major ligand for FGF receptor 2 IIIb in mouse multi-organ development. Biochemical and biophysical research communications 277, 643-649.

Pageau, S.C., Sazonova, O.V., Wong, J.Y., Soto, A.M., Sonnenschein, C., 2011. The effect of stromal components on the modulation of the phenotype of human bronchial epithelial cells in 3D culture. Biomaterials 32, 7169-7180.

Pepicelli, C.V., Lewis, P.M., McMahon, A.P., 1998. Sonic hedgehog regulates branching morphogenesis in the mammalian lung. Current biology : CB 8, 1083-1086.

Perl, A.K., Riethmacher, D., Whitsett, J.A., 2011. Conditional depletion of airway progenitor cells induces peribronchiolar fibrosis. American journal of respiratory and critical care medicine 183, 511-521.

Pham, D., Kris, M.G., Riely, G.J., Sarkaria, I.S., McDonough, T., Chuai, S., Venkatraman, E.S., Miller, V.A., Ladanyi, M., Pao, W., Wilson, R.K., Singh, B., Rusch, V.W., 2006. Use of cigarette-smoking history to estimate the likelihood of mutations in epidermal growth factor receptor gene exons 19 and 21 in lung adenocarcinomas. Journal of clinical oncology : official journal of the American Society of Clinical Oncology 24, 1700-1704.

Plopper, C.G., Suverkropp, C., Morin, D., Nishio, S., Buckpitt, A., 1992. Relationship of cytochrome P-450 activity to Clara cell cytotoxicity. I. Histopathologic comparison of the respiratory tract of mice, rats and hamsters after parenteral administration of naphthalene. The Journal of pharmacology and experimental therapeutics 261, 353-363.

Preston, D.L., Ron, E., Tokuoka, S., Funamoto, S., Nishi, N., Soda, M., Mabuchi, K., Kodama, K., 2007. Solid cancer incidence in atomic bomb survivors: 1958-1998. Radiation research 168, 1-64.

Que, J., Choi, M., Ziel, J.W., Klingensmith, J., Hogan, B.L., 2006. Morphogenesis of the trachea and esophagus: current players and new roles for noggin and Bmps. Differentiation; research in biological diversity 74, 422-437.

Rackley, C.R., Stripp, B.R., 2012. Building and maintaining the epithelium of the lung. The Journal of clinical investigation 122, 2724-2730.

Raff, M., 2003. Adult stem cell plasticity: fact or artifact? Annual review of cell and developmental biology 19, 1-22.

Raju, M.R., Bain, E., Carpenter, S.G., Cox, R.A., Robertson, J.B., 1978. A heavy particle comparative study. Part II: cell survival versus depth. The British journal of radiology 51, 704-711.

Ramirez, R.D., Sheridan, S., Girard, L., Sato, M., Kim, Y., Pollack, J., Peyton, M., Zou, Y., Kurie, J.M., Dimaio, J.M., Milchgrub, S., Smith, A.L., Souza, R.F., Gilbey, L., Zhang, X., Gandia, K., Vaughan, M.B., Wright, W.E., Gazdar, A.F., Shay, J.W., Minna, J.D., 2004. Immortalization of human bronchial epithelial cells in the absence of viral oncoproteins. Cancer research 64, 9027-9034.

Randell, S.H., Comment, C.E., Ramaekers, F.C., Nettesheim, P., 1991. Properties of rat tracheal epithelial cells separated based on expression of cell surface alpha-galactosyl end groups. American journal of respiratory cell and molecular biology 4, 544-554.

Rawlins, E.L., Hogan, B.L., 2006. Epithelial stem cells of the lung: privileged few or opportunities for many? Development 133, 2455-2465.

Rawlins, E.L., Okubo, T., Xue, Y., Brass, D.M., Auten, R.L., Hasegawa, H., Wang, F., Hogan, B.L., 2009. The role of Scgb1a1+ Clara cells in the long-term maintenance and repair of lung airway, but not alveolar, epithelium. Cell stem cell 4, 525-534.

Rawlins, E.L., Ostrowski, L.E., Randell, S.H., Hogan, B.L., 2007. Lung development and repair: contribution of the ciliated lineage. Proceedings of the National Academy of Sciences of the United States of America 104, 410-417.

Reynolds, S.D., Giangreco, A., Power, J.H., Stripp, B.R., 2000. Neuroepithelial bodies of pulmonary airways serve as a reservoir of progenitor cells capable of epithelial regeneration. The American journal of pathology 156, 269-278.

Rock, J.R., Gao, X., Xue, Y., Randell, S.H., Kong, Y.Y., Hogan, B.L., 2011. Notch-dependent differentiation of adult airway basal stem cells. Cell stem cell 8, 639-648.

Rock, J.R., Hogan, B.L., 2011. Epithelial progenitor cells in lung development, maintenance, repair, and disease. Annual review of cell and developmental biology 27, 493-512.

Rock, J.R., Onaitis, M.W., Rawlins, E.L., Lu, Y., Clark, C.P., Xue, Y., Randell, S.H., Hogan, B.L., 2009. Basal cells as stem cells of the mouse trachea and human airway epithelium. Proceedings of the National Academy of Sciences of the United States of America 106, 12771-12775.

Rock, J.R., Randell, S.H., Hogan, B.L., 2010. Airway basal stem cells: a perspective on their roles in epithelial homeostasis and remodeling. Disease models & mechanisms 3, 545-556.

Ron, E., 2003. Cancer risks from medical radiation. Health physics 85, 47-59.

Ronnov-Jessen, L., Bissell, M.J., 2009. Breast cancer by proxy: can the microenvironment be both the cause and consequence? Trends in molecular medicine 15, 5-13.

Rydberg, B., Cooper, B., Cooper, P.K., Holley, W.R., Chatterjee, A., 2005. Dose-dependent misrejoining of radiation-induced DNA double-strand breaks in human fibroblasts: experimental and theoretical study for high- and low-LET radiation. Radiation research 163, 526-534.

Saccone, S.F., Hinrichs, A.L., Saccone, N.L., Chase, G.A., Konvicka, K., Madden, P.A., Breslau, N., Johnson, E.O., Hatsukami, D., Pomerleau, O., Swan, G.E., Goate, A.M., Rutter, J., Bertelsen, S., Fox, L., Fugman, D., Martin, N.G., Montgomery, G.W., Wang, J.C., Ballinger, D.G., Rice, J.P., Bierut, L.J., 2007. Cholinergic nicotinic receptor genes implicated in a nicotine dependence association study targeting 348 candidate genes with 3713 SNPs. Human molecular genetics 16, 36-49.

Sakai, T., Larsen, M., Yamada, K.M., 2003. Fibronectin requirement in branching morphogenesis. Nature 423, 876-881.

Sato, M., Larsen, J.E., Lee, W., Sun, H., Shames, D.S., Dalvi, M.P., Ramirez, R.D., Tang, H., Dimaio, J.M., Gao, B., Xie, Y., Wistuba, II, Gazdar, A.F., Shay, J.W., Minna, J.D., 2013. Human lung epithelial cells progressed to malignancy through specific oncogenic manipulations. Molecular cancer research : MCR.

Sato, M., Vaughan, M.B., Girard, L., Peyton, M., Lee, W., Shames, D.S., Ramirez, R.D., Sunaga, N., Gazdar, A.F., Shay, J.W., Minna, J.D., 2006. Multiple oncogenic changes (K-RAS(V12), p53 knockdown, mutant EGFRs, p16 bypass, telomerase) are not sufficient to confer a full malignant phenotype on human bronchial epithelial cells. Cancer research 66, 2116-2128.

Schoch, K.G., Lori, A., Burns, K.A., Eldred, T., Olsen, J.C., Randell, S.H., 2004. A subset of mouse tracheal epithelial basal cells generates large colonies in vitro. American journal of physiology. Lung cellular and molecular physiology 286, L631-642.

Sekine, K., Ohuchi, H., Fujiwara, M., Yamasaki, M., Yoshizawa, T., Sato, T., Yagishita, N., Matsui, D., Koga, Y., Itoh, N., Kato, S., 1999. Fgf10 is essential for limb and lung formation. Nature genetics 21, 138-141.

Shepherd, F.A., Rodrigues Pereira, J., Ciuleanu, T., Tan, E.H., Hirsh, V., Thongprasert, S., Campos, D., Maoleekoonpiroj, S., Smylie, M., Martins, R., van Kooten, M., Dediu, M., Findlay, B., Tu, D., Johnston, D., Bezjak, A., Clark, G., Santabarbara, P., Seymour, L., 2005. Erlotinib in previously treated non-small-cell lung cancer. The New England journal of medicine 353, 123-132.

Sirianni, F.E., Chu, F.S., Walker, D.C., 2003. Human alveolar wall fibroblasts directly link epithelial type 2 cells to capillary endothelium. American journal of respiratory and critical care medicine 168, 1532-1537.

Sun, S., Schiller, J.H., Gazdar, A.F., 2007. Lung cancer in never smokers--a different disease. Nature reviews. Cancer 7, 778-790.

Tefft, D., Lee, M., Smith, S., Crowe, D.L., Bellusci, S., Warburton, D., 2002. mSprouty2 inhibits FGF10-activated MAP kinase by differentially binding to upstream target proteins. American journal of physiology. Lung cellular and molecular physiology 283, L700-706.

Treuting, P.M., Dintzis, S.M., Frevert, C.W., Liggitt, H.D., Montine, K.S., 2012. Comparative anatomy and histology : a mouse and human atlas, 1st ed. Elsevier/Academic Press, Amsterdam ; Boston.

Vahakangas, K.H., Bennett, W.P., Castren, K., Welsh, J.A., Khan, M.A., Blomeke, B., Alavanja, M.C., Harris, C.C., 2001. p53 and K-ras mutations in lung cancers from former and never-smoking women. Cancer research 61, 4350-4356.

Van Lommel, A., 2001. Pulmonary neuroendocrine cells (PNEC) and neuroepithelial bodies (NEB): chemoreceptors and regulators of lung development. Paediatric respiratory reviews 2, 171-176.

Van Lommel, A., Lauweryns, J.M., Berthoud, H.R., 1998. Pulmonary neuroepithelial bodies are innervated by vagal afferent nerves: an investigation with in vivo anterograde DiI tracing and confocal microscopy. Anatomy and embryology 197, 325-330.

Vaughan, M.B., Ramirez, R.D., Wright, W.E., Minna, J.D., Shay, J.W., 2006. A three-dimensional model of differentiation of immortalized human bronchial epithelial cells. Differentiation; research in biological diversity 74, 141-148.

Wansleeben, C., Barkauskas, C.E., Rock, J.R., Hogan, B.L., 2013. Stem cells of the adult lung: their development and role in homeostasis, regeneration, and disease. Wiley interdisciplinary reviews. Developmental biology 2, 131-148.

Warburton, D., El-Hashash, A., Carraro, G., Tiozzo, C., Sala, F., Rogers, O., De Langhe, S., Kemp, P.J., Riccardi, D., Torday, J., Bellusci, S., Shi, W., Lubkin, S.R., Jesudason, E., 2010. Lung organogenesis. Current topics in developmental biology 90, 73-158.

Weaver, M., Dunn, N.R., Hogan, B.L., 2000. Bmp4 and Fgf10 play opposing roles during lung bud morphogenesis. Development 127, 2695-2704.

Weaver, M., Yingling, J.M., Dunn, N.R., Bellusci, S., Hogan, B.L., 1999. Bmp signaling regulates proximal-distal differentiation of endoderm in mouse lung development. Development 126, 4005-4015.

Wells, A.B., 1970. The kinetics of cell proliferation in the tracheobronchial epithelia of rats with and without chronic respiratory disease. Cell and tissue kinetics 3, 185-206.

Wu, X., Peters-Hall, J.R., Bose, S., Pena, M.T., Rose, M.C., 2011. Human bronchial epithelial cells differentiate to 3D glandular acini on basement membrane matrix. American journal of respiratory cell and molecular biology 44, 914-921.

Wuenschell, C.W., Sunday, M.E., Singh, G., Minoo, P., Slavkin, H.C., Warburton, D., 1996. Embryonic mouse lung epithelial progenitor cells co-express immunohistochemical markers of diverse mature cell lineages. The journal of histochemistry and cytochemistry : official journal of the Histochemistry Society 44, 113-123.

Yu, X., Kensler, T., 2005. Nrf2 as a target for cancer chemoprevention. Mutation research 591, 93-102.